SCIENTIFIC MINING JOURNAL

ISSN 2564-7024
e-ISSN 2587-2613
Vol: 63 *No:* 1 *March*
2024

The Publication of the Chamber of Mining Engineers of Türkiye

UCTEA CHAMBER OF MINING ENGINEERS

Scientific Mining Journal

Vol: 63, No: 1, March, *2024*

A peer-reviewed quarterly journal of the Chamber of Mining Engineers of Türkiye

AIMS AND SCOPE

Scientific Mining Journal, which is published in open access electronic environment and in printed, is a periodical scientific journal of Union of Chambers of Turkish Engineers and Architects Chamber of Mining Engineers. The name of the journal was "Mining" until June 2016 and it has been changed to "Scientific Mining Journal" since September 2016 because it can be confused with popular journals with similar names and the ISSN number has been updated from 0024-9416 to 2564-7024.

Scientific Mining Journal, published four times a year (March-June-September-December), aims to disseminate original scientific studies which are conducted according to the scientific norms and publication ethics at national and international scale, to scientists, mining engineers, the public; and thus to share scientific knowledge with society. The journal is in English.

The journal covers theoretical, experimental, and applied research articles, which reflects the findings and results of an original research in the field of mining engineering; review articles, which assess, evaluates, and interprets the findings of a comprehensive review of sufficient number of scientific articles and summarize them at present information and technology level; technical notes, which may be defined as a short article that describes a novel methodology or technique; a case studies, which are based on the theoretical or real professional practice and involves systematic data collection and analysis.

The journal gives priority to works that will enable the advancement of current available information necessary to serve humanity with nonrenewable mineral resources with the perspective of sustainable mining principles. In this context, mine exploration, mineral resource modeling, surveying, mine economics and feasibility, geostatistics, rock mechanics and geotechnics, diggability studies, underground and surface mining, mine design, support design in underground mines and tunnels, rock penetration and rock fragmentation, mine production planning and pit optimization, mine health and safety management, mine ventilation, methane emission and drainage in underground coal mines, mineral processing and beneficiation, process mineralogy, analytical techniques, mineral comminution, mineral classification and separation, flotation/flocculation, solid/liquid separation, physical enrichment methods, hydro and biometallurgy, production metallurgy, modeling and simulation, instrumentation and process control, recycling and waste processing, mining law, environmental health and management, transportation, machinery and equipment selection and planning, coal gasification, marble technology, industrial minerals, space mining, submarine mining and mechanization are included in the journal content.

Submitted manuscripts are evaluated by the editorial board and expert referees independently in accordance with the best practices in academic publishing. The publishing rights of the manuscripts, approved for publication at the end of the evaluation process, are transferred to the Chamber of Mining Engineers by the authors.

Scientific Mining Journal

Scientific Mining Journal is indexed or abstracted in:

SCOPUS

Google Scholar

ULAKBİM TR Dizin

GeoRef

OpenAIRE

Author Instructions, Editorial Advisory Board, the Peer Review Process and Reviewer Lists can be accessed from http://www.mining.org.tr

Publication Ethics

Complying with the research and publication ethics is considered an indisputable precondition to be published. Publication Ethics can be accessed from http://www.mining.org.tr

Scientific Mining Journal

Owner on behalf of the Chamber of Mining Engineers of Türkiye: Ayhan Yüksel

Responsible editing manager: Mehmet Erşat Akyazılı

Correspondence address:
Selanik Cad. No: 19/4 06650 Kızılay-Çankaya / Ankara Türkiye

Tel: +90 312 425 10 80 / +90 312 418 36 57 • Fax: +90 312 417 52 90

e-mail: smj@maden.org.tr
web: http://www.mining.org.tr

Publication type: Local periodical, quarterly

Design: Gülendem Gültekin

Printed at: Ziraat Gurup Matbaacılık Ambalaj San. ve Tic. A.Ş.

Printing date: 23.09.2024

Number of printed copy: 1500

SCIENTIFIC MINING JOURNAL

ISSN 2564-7024
e-ISSN 2587-2613
Vol: 63 *No:* 1 *March*
2024

The Publication of the Chamber of Mining Engineers of Türkiye

CONTENTS

ISSN 2564-7024
9 772564 702003

Madencilik - Mining, 2024, 63(1), 7-18

BİLİMSEL MADENCİLİK DERGİSİ
SCIENTIFIC MINING JOURNAL

TMMOB Maden Mühendisleri Odası Yayını / The Publication of the Chamber of Mining Engineers of Turkey

www.mining.org.tr

Original Research

Investigation of Surface Marble Quarry Enterprises in Marmara Island with Different Risk Methodologies in Terms of Occupational Health and Safety

Didem Kıray[a,*]

[a] *Çanakkale, TÜRKİYE*

Received: 16 November 2023 • Accepted: 26 March 2024

A B S T R A C T

Turkey is located on the Alpine-Himalayan orogenic belt, which has led to significant development in both surface and underground mining industries. Due to the growing mining sector, there has been an increase in raw material production and workforce, making occupational health and safety increasingly important. This study identifies 59 hazards and risks associated with 26 activity areas in the marble quarry operating areas on Marmara Island, the second largest island of Turkey in Balıkesir province. The geological structure of the area and the activities carried out in the quarry were taken into consideration. The hazards and risks were assessed using three quantitative risk methods: 5x5 L-type Matrix, Fine-Kinney, and Potential Failure Modes and Effects Analysis (FMEA). The 5x5 L-type Matrix identified 24 activity areas as high risk and two as medium risk. The Fine-Kinney method identified 16 areas as very high risk, 8 as high risk, and 2 in the important risk group. The FMEA method recommended 13 precautions based on RPN values. Among the identified risks, 11 require precautions while 2 do not. The Fine-Kinney method is considered suitable for marble quarry operations as it provides a detailed, comprehensive, and sensitive analysis of hazards and risks specific to environmental conditions, work areas, and employees, resulting in safer outcomes.

Keywords: *Marmara Island, Marble Quarry, 5x5 L Type Matrix, Fine-Kinney, FMEA.*

Introduction

Marble is a rock composed of carbonate, resulting from the metamorphism of limestone and dolomite, and bearing traces of this process. Commercially, according to the Mining Law, it is defined as a stone of sedimentary, magmatic, and metamorphic origin that can yield blocks in sizes in accordance with commercial standards, is cut and polished, and is suitable for use as a covering stone (DPT, 2001). Marble quarrying in our country is carried out using the surface mining method. This sector is economically important for the extraction and production of raw materials, but it is also one of the most hazardous in terms of occupational health and safety. The process of cleaning and stripping the ground cover in marble quarry operations involves drilling holes on the surface, dividing the surface into blocks with a cutting machine, demolishing the cut blocks, sizing the demolished blocks into small pieces with wire cutting machines, transporting them within the quarry, storing them in the stock area, and finally shipping them (Angotzi et al., 2005). Depending on the work areas and activities undertaken, there may be many potential dangers and high risks present. As the number of mines and enterprises increases, so do work-related accidents and occupational diseases. Therefore, it is essential to conduct a risk assessment to reduce hazards and risks to acceptable levels.

In recent years, researchers have evaluated occupational health and safety in marble quarries andenterprises. Konuk et al. (2009), identified hazards and risks in 15 marble quarries in Bilecik province using the Check-list method for risk analysis. Ağca (2010), conducted a risk analysis evaluation with the L-Type Matrix method in a private marble factory in Diyarbakır province. El Gammal et al. (2011), evaluated the health risks associated with marble. Eleren and Ersoy (2011), used the Failure Mode and Effects Analysis method to assess the risks of chain arm cutter and diamond wire cutting methods in natural quarry enterprises. de Melo Neto et al. (2012), conducted a Preliminary Risk Analysis in the Recife Metropolitan Region (RMR) of Brazil. They found that a quantitative study was necessary to determine the risks in the marble quarry. Göztepe et al. (2013), conducted a study on risk assessment and occupational health and safety nonconformance monitoring systems in marble production using a 3T method. The authors suggest that this method is easy to apply for those who are knowledgeable in the field and can help raise awareness. Özçelik (2013), conducted a risk analysis in a marble quarry using

* Corresponding author: dkiray17@gmail.com • https://orcid.org/0000-0002-4187-7285

https://doi.org/10.30797/madencilik.1391750

the Fine-Kinney methodology and proposed preventive measures. Çınar and Şensöğüt (2016), calculated risk scores for identified hazards in marble enterprises. The calculated risk scores helped to identify risky enterprises and sources of risk. Additionally, measures to eliminate high-risk sources or minimize risks were determined. Mikaeil et al. (2017), conducted a safety risk analysis using the FMEA method in Badeki marble quarries. The study identified wire saw tearing and rockfall as the primary safety concerns. The authors suggested that implementing preventive measures and making necessary changes can significantly reduce the initial risk in these mines, ensuring the safety of both personnel and equipment. Yilmaz (2018) conducted a survey on the 'Evaluation of Marble Production and Processing in Terms of Occupational Safety' among randomly selected employees from marble companies and quarries in the Bursa region. The survey aimed to measure workers' awareness of the risks in their work environment. Sarıkaya and Kasap (2019) identified existing hazards in a marble enterprise using the Failure Mode and Effects Analysis method and interpreted these hazards. Gür and Sezik (2020) conducted a focus group discussion to determine the working conditions of employees in a small-scale marble factory in Çorum province, with a focus on occupational health and safety. The questions for the study were prepared to cover working conditions, existing hazards and risks, occupational health and safety practices, occupational health and safety training, and precautions to be taken by the management. Esmailzadeh et al. (2022) conducted a study using the Failure Modes and Effects Analysis (FMEA) method to identify the most likely hazards in dimensional stone mines in West Azerbaijan. The study found that the top three hazards were diamond cutting wire breakage, rockfall, and car accidents, in that order. It was suggested that these hazards could be reduced by implementing preventive actions, such as timely replacement of the cutting wire, using an intelligent system for cutting tool control, providing necessary personal training, and considering protective measures. Gündüz (2023) identified the hazards present in all areas of activity of a marble enterprise in Bilecik and conducted a risk assessment using the Fine-Kinney risk analysis method. Hazards and risks in surface mining operations have been identified using various risk assessment methods

A comparison has been made between risk methodologies to determine which can provide better results for activities related to the operation and processing of marble quarries. In the study conducted by Özfırat et al. (2017), the L-matrix and ETA risk methods were applied in Afyon marble facilities, and three initiating events were identified: breaking of the lifting rope, breaking of the diamond wire, and electrical leakage caused by old systems. Dolmaz (2018) measured physical risk factors, including lighting, thermal comfort, noise, dust, and vibration, in a marble cutting and polishing facility. The data was analysed using L Matrix and Fine-Kinney risk analysis methods. The results showed that Fine-Kinney risk analysis is more advantageous than L Matrix analysis due to the frequency factor. In a study of a marble quarry, Gök (2018) employed the Fine-Kinney risk method with an L-type matrix for risk assessment. The study found that this method produced effective results due to its incorporation of multiple variables in risk scoring. However, the author suggested that the L matrix method should also be employed to support this approach. Demirel (2019) conducted separate risk assessments using FMEA and Fine-Kinney risk methods for machine-related risks in the mine and its facilities. They provided recommendations for reducing work accidents. Ersoy et al. (2019) identified potential accident types and effects in block production activities at a marble quarry. They performed risk analysis using the Fine-Kinney method and evaluated the data using the Grey Relational Analysis method. It was concluded that the GIA method can be integrated into the Fine-Kinney risk analysis method and used to solve problems and determine priorities for the improvement program.

In addition to mining, other sectors have also compared different risk methodologies to reveal similarities and differences. For instance, Erten and Utku (2017) compared the 5x5 Matrix, Fine Kinney, and FMEA risk methods in the pharmaceutical industry. They found that the 5x5 matrix was inadequate compared to the Fine Kinney method. When evaluating the FMEA method alongside the 5x5 L Matrix and Fine Kinney methods, it was found that the Fine Kinney method was more applicable and functional, and more comprehensive in terms of conditions. In their comparison of the Fine-Kinney and FMEA risk methods in the tea business, Durmuş et al. (2021) noted that while the FMEA method has advantages and disadvantages, it should be used to detect process errors and prevent them from occurring instantly. Kıray (2023) compared the hazards and risks of geothermal power plants using the 5x5 L Matrix and Fine Kinney methods. The study suggests that the Fine-Kinney Method should be preferred due to its classification as very hazardous and the need for a detailed analysis. Yorulmaz and Yeğin (2023) found that FMEA risk analysis is more effective than Fine-Kinney risk analysis in detecting the error that causes hazardous material handling activities in port enterprises. However, Fine-Kinney risk analysis provides more precise and detailed risk levels.

Marble quarrying is a crucial sector in the mining industry and has become a significant source of national income for producing countries due to its increasing importance. Our country has a substantial potential for marble resources with its geological and tectonic structure (Görgülü, 1994). Marmara Island, located in the Balıkesir province, has a significant resource of white dolomite stone and fulfils a significant portion of the marble demand. During the Paleozoic and Mesozoic Eras, Marmara island underwent sedimentation and was subjected to Alpine-Himalayan tectonic movements. As a result of orogeny, east-west faults were formed. Evidence of the island's exposure to the sea during the Quaternary period can be seen in the presence of marine terraces in its southern part. In the Halocene epoch, the Marmara island became separated from the other islands and the Kapıdağ Peninsula (Tunçdilek, 1987). The island's current appearance is the result of tectonic movements it has been exposed to (Aksoy, 1993).

Marmara Island is the largest island in the Marmara Sea and the second largest in Turkey. The study area is located on the Biga massif, which is surrounded by a complex tectonic mosaic of various tectono-stratigraphic layers and fault zones. The location was previously described by Ketin (1946) and Aksoy (1999). The Gündoğdu Metamorphics, the oldest unit of Marmara Island, were deposited on the edge of the continent and comprise mica schist, calcschist, and marble. The Erdek Complex is located on a unit with a tectonic contact and is mainly composed of metabasites, which are formed from oceanic crust, as well as smaller amounts of mica schist, calcschist, and marble blocks. It is overlaid by Marmara Marble, the most common rock type on the island, with an angular unconformity (Aksoy, 1993). The Saraylı Complex consists of exotic marble and metabasite blocks, as well as metapsammite, metapelite, and calcschist intercalations with metavolcanics (basic and intermediate). It is an intrusion that cuts through the calc-alkaline composition, WSW-ENE trending İlyasdağı Metagranodiorite, Marmara marble, and Erdek complex, and overlies the Marmara marble. Numerous aplites associated with this intrusion have cut along hot contacts with pegmatite and quartz veins (Tanyolu 1979; Aksoy 1993).

Based on previous studies have concluded that risk assessment is crucial in the mining industry as it directly impacts mining operations and production. The selection of the most effective risk methods should be based on their applicability to changing conditions, such as environmental or technological factors, and the measures taken to mitigate risks. It is important to continuously improve the selected risk assessment methodologies. The aim of

this study is to determine the most effective and reliable methodology for assessing the risks associated with marble quarrying. This will be achieved by comparing the hazards and risks of marble quarrying using commonly used 5 x 5 L-type matrix, Fine-Kinney, and FMEA.

Marble quarries on the Marmara Island (NW Kapıdağ Peninsula), which is the second largest island in Turkey and the largest island in the Marmara Sea and which gives its name to the sea, will be evaluated for the first time in terms of occupational health and safety with this study. In this study, a comparison of risk methods using 5x5 L Type Matrix, Fine-Kinney and Possible Failure Modes and Effects Analysis (FMEA) methods was made for the first time in determining the hazards and risks in these marble quarries.

1. Materials and Methods

The objective of this study was to identify the hazards and risks associated with a marble quarry. To achieve this, we compared the potential hazards and risks using three methods: the 5x5 L Type Matrix, Fine Kinney, and Possible Failure Modes and Effects (FMEA). The aim was to determine the most suitable risk assessment method for the quarry.

1.1. 5x5 L Type Matrix Method

The 5x5 L Type Matrix method is a widely used quantitative risk assessment technique. It was developed by the United States to meet the requirements of the system security program (MIL_STD_882-D Military Standard). The method calculates the risk score by multiplying the probability and severity parameters (Özkılıç, 2005). The risk score is obtained by multiplying the probability (Table 1) and severity (Table 2) parameters, as shown in Table 3. Table 4 outlines the acceptability and actions to be taken based on the risk score.

Table 1. The probability of an incident occurring(Özkılıç, 2005)

Likelihood	Rating for Likelihood of Occurrence
Very Small	Almost never
Small	Very rarely (once a year), only in abnormal cases
Medium	Less (a few times a year)
High	Frequency (once a Month)
Very High	Very often (once a week, every day), under normal operating conditions

Table 2. Severity of the incident outcome (Özkılıç, 2005)

Result	Rating
Very Light	No work hours lost, first aid required
Mild	No loss of working days, no permanent effects requiring outpatient first aid
Moderate	Minor injury, inpatient treatment
Serious	Serious injury, long-term treatment, occupational disease
Very Serious	Death, Permanent Disability

Table 3. Risk rating matrix (Özkılıç, 2005)

Likelihood	Severity				
	1	2	3	4	5
1	Acceptable 1	Low 2	Low 3	Low 4	Low 5
2	Low 2	Low 4	Low 6	Medium 8	Medium 10
3	Low 3	Düşük 6	Medium 9	Medium 12	High 15
4	Low 4	Medium 8	Medium 12	High 16	High 20
5	Low 5	Medium 10	High 15	High 20	Cannot Tolerate 25

Table 4. Acceptability values of the incident outcome (Özkılıç, 2005)

Result	Action
Intolerable Risks (25)	Activities should not commence until the identified risk has been reduced to an acceptable level. If activities are already underway, they must be halted immediately. If the risk level does not decrease despite the measures taken, the activity should be prevented.
High Level Risks (15,16,20)	Activities should not commence until the identified risk has been mitigated. If activities are already underway, they must be halted immediately. If the risk is related to the continuation of the work, urgent measures should be taken and a decision should be made on whether to proceed with the activity.
Moderate Risks (8,9,10,12)	Efforts are ongoing to decrease the identified risk levels. Mitigating risks may require a significant amount of time.
Low Level Risks (2,3,4,5,6)	The maintenance of existing controls and auditing of taken controls is recommended.
Acceptable Risks	Control to eliminate identified risks

1.2. Fine-Kinney Method

The Fine-Kinney method was developed in 1976 by Kinney and Wiruth as a quantitative risk assessment tool for controlling hazards. This method considers the risk value, consequences of an accident, and frequency and probability of occurrence of the hazard (Table 5, 6, and 7). The risk score is calculated by multiplying these three factors (Table 8, Fine, 1971).

Table 5. Probability of harm occurring (Kinney and Wiruth, 1976)

Value	Probability of Occurrence
10	Expected, sure
6	High / quite possible
3	Likely to happen
1	Rarely possible
0,5	Unexpected but possible
0,2	Not practically possible

Table 6. Severity of estimated damage to humans and the environment(Kinney ve Wiruth, 1976)

Value	Consequence
100	Multiple deaths - Environmental disaster
40	Fatal accidents - Serious environmental damage
15	Permanent damage, disability, need for internal first aid - Wide environmental impact
7	Significant damage, disability, external first aid – Environmental impact beyond land boundaries
3	Minor damage, injury, first aid – Environmental impact within land boundaries
1	Cheap bypass - No harm to the environment

Table 7. Repeated exposure to hazard (Kinney ve Wiruth, 1976)

Value	Frequency
10	Very often (Several times an hour)
6	Frequently (Once or several times a day)
3	Occasionally (Once or several times a week)
2	Not often (Once or a few times a month)
1	Rare (A few times a year)
0,5	Very rare (Once a year or less)

Table 8. Risk levels and acceptability values(Kinney ve Wiruth, 1976)

Risk Value	Risk Severity Level	Risk Control Measures
400<R	Very High Risk	Immediate action must be taken or work must be stopped to address the issue. It is imperative to take necessary precautions to prevent further occurrences.
200<R<400	High Risk	In the short term, it should be resolved within a few months.
70<R<200	Significant Risk	The improvement should be made within the year for long-term benefits.
20<R<70	Considerable Risk	Must be kept under surveillance.
R<20	Acceptable Risk	Priority is not to take immediate action.

1.3. Potential Failure Modes and Effects Analysis

The Failure Modes and Effects Analysis (FMEA) method was first introduced on November 9, 1949, as Military Procedure MIL-P-1629 by the United States Army. It is a reliable and straightforward method that can be easily applied by a risk assessment team with moderate experience, without requiring theoretical knowledge. FMEA is a systematic procedure used to analyse a system and identify potential failure modes, causes of failure, and their effects on system performance (Gandhi and Agrawal, 1992). The risk table is determined by analysing the frequency of error occurrence, the severity of impact, and detectability parameters (Table 9-11). Precautions are evaluated based on the risk priority numbers (Table 12).

Table 9. Likelihood of failure (Stamatis, 1995)

Likelihood	Occurrence	Degree
Very High:	more than 1/2	10
Unavoidable error	1/3	9
High:	1/8	8
Mistake over and over again	1/20	7
Middle:	1/80	6
Occasional error	1/400	5
Low:	1/2000	4
Relatively	1/15000	3
Few:	1/150000	2
Improbable error	1 less than 1/1500000	1

Table 10. Classification of the impact of consequence (Stamatis, 1995)

Effect	Effect of Severity	Level
Coming without warning High risk	There is a risk of catastrophic failure that could occur without warning.	10
Hazard that comes without warning	This text describes a potential error that could cause significant damage and mass casualties without warning.	9
Very high	This text describes a failure type that can cause complete damage to a system, resulting in catastrophic effects such as severe injuries, third-degree burns, acute burns, and even death.	8
Major	This failure type can cause severe damage to the equipment and result in fatalities, poisoning, third-degree burns, acute death, and other serious consequences.	7
Moderate	System failure can result in serious harm such as loss of limbs or organs, serious injury, or even cancer.	6
Low	Instances of failure may result in various injuries such as fractures, minor permanent disabilities, second-degree burns, concussions, and other similar injuries.	5
Very low	Injuries resulting in minor harm, such as bruises, minor cuts, abrasions, or crushing, may cause short-term discomfort.	4
Minor	System failure that causes a slowdown in operation.	3
Very minor	System failure that causes a slowdown in operation.	2
None	No effect	1

Table 11. Probability of occurrence of damage(Stamatis, 1995)

Noticeability	Probability of noticeability	Degree
Not detectable	Not possible to detect potential error	10
Not enough	Detectability of potential defect is too far away	9
Little	Detectability of potential defect is remote	8
Very low	Detectability of potential defect is very low	7
Low	Detectability of potential fault is low	6
Medium	Potential error detectability ismedium	5
High average	High average detectability of potential faults	4
High	High detectability of potential errors	3
Very high	Potential error detectability is very high	2
Almost certain	Detectability of potential error is almost certain	1

Table 12. Risk Priority Number(Stamatis, 1995)

Risk Priority Number Value	**Action**
RPN<40	No precautions need to be taken.
40<RPN<100	Precautions may be taken.
RPN>100	Precautions must be taken.

Precautions should be taken starting from the highest value of the risk priority number (RPN) coefficient as it causes the greatest damage (Özkılıç, 2005).

2. Results

Risk assessment studies were conducted to evaluate occupational health and safety in the marble quarries of Marmara Island. The risks associated with quarry activity areas and hazard situations were assessed using the 5x5 L Type Matrix, Fine-Kinney method, and FMEA risk assessment methods (Table 13).

Table 13. Comparison of Risk Assessment Methods: 5x5 L-Type Matrix, Fine-Kinney, and FMEA

	5x5 L Type Matrix			Fine-Kinney				FMEA			
HAZARD	Probability	Severity	Risk Score and Assessment	Probability	Severity	Frequency	Risk Score and Assessment	Probability	Severity	Detectability	Risk Score and Assessment
LEVEL The platform height and width of the platform, slope not suitable for the structure and durability of the ground, unsafe working on the platform and failure to take safety precautions.	3	5	15 High	6	40	2	480 Very High	5	7	1	35
DRAINAGE Lack of water drainage, improper installation	3	5	15 High	6	40	2	480 Very High	5	7	1	35
MİNE ROADS - TRANSPORT Lack of warning signs and markings, uncleaned benchs and roads, unsuitable road gradient, pedestrians using roads, speed limits exceeded.	3	5	15 High	6	40	2	480 Very High	6	7	3	126
BLOCK PRODUCTION Failure to drill holes properly, unsafe conditions in the diamond wire cutter, failure to take precautions during block cutter	3	5	15 High	6	40	2	480 Very High	6	7	2	84
BLOCK DESTRUCTION Failure to take safety precautions when breaking blocks can lead to block destruction.	3	5	15 High	6	40	2	480 Very High	6	7	2	84
LOADING Unsafe operation of trucks and construction equipment during loading	3	5	15 High	3	40	3	360 High	5	7	2	90

STOCK AREA Unsuitable ground, unsafe operation of lifting equipment, incorrect stacking of blocks, unauthorized persons.	3	5	15 High	3	40	2	240 High	5	7	3	105
EMERGENCIES Lack of designated assembly areas and escape routes in the quarry and in the building and its outbuildings, lack of drills, lack of emergency procedures, lack of employee training on the subject.	3	5	15 High	6		1	600 Very High	4	9	9	324
FIRE Lack of fire extinguishers, and the existing ones are not easily accessible, visible, or placed at a height of 90 cm, not regularly checked for functionality.	3	5	15 High	6		1	600 Very High	5	7	5	175
ELECTRIC Lack of leakage current relays in electrical panels, carelessness in the use of panels, lack of lightning conductors, failure to check electrical and earthing installations and lightning conductors, use of damaged cables.	3	5	15 High	6	40	2	480 Very High	9	8	2	144
CONSTRUCTION MACHINES Failure to check the equipment and machines to be used (such as hole drilling, diamond wire cutting, block cutter) before starting work, lack of operating instructions for the equipment and machines, lack of an emergency stop system, lack of metal body and equipment grounding,	3	5	15 High	6	40	1	240 High	5	7	2	70
WORK EQUIPMENT AND HAND TOOLS The misuse of work equipment and hand tools for purposes other than their intended use, as well as failure to wear protective visors while using work equipment.	3	5	15 High	6	40	1	240 High	5	7	3	105
PRESSURE VESSELS AND PRESSURE PIPES Lack of inspection of pressure vessels and cylinders, improper storage of cylinders, mobile compressors being close to employees	3	5	15 High	6	40	1	240 High	5	7	3	105
WELDING WORKS Welding work is not carried out by qualified personnel, check valves are not available, gas hoses are damaged, goggles/face shields are not used, flammable and combustible materials are in the welding area, fire extinguishers are not used while working.	3	5	15 High	6	40	1	240 High	4	7	4	112
MANUAL HANDLING AND ERGONOMICS The misuse of hand tools, absence of protective casing on rotating parts of electrical tools, and use of defective equipment	3	4	12 Medium	6	7	3	126 Significant	7	5	4	140

WORKING AT HEIGHT Failure to use personal protective equipment (parachute type seat belt etc.) when working at heights, working at heights not receiving proper training.	3	5	15 High	6	40	2	480 Very High	4	7	2	56
MAINTENANCE AND REPAIR Failure to obtain permission for work, failure to disconnect power from the machine/equipment, and failure to take safety precautions.	3	5	15 High	6	40	2	480 Very High	4	7	4	112
PHYSICAL RISK FACTORS Unsuitable working conditions and lack of environmental measurements.	5	4	20 High	6	15	6	540 Very High	9	6	5	270
CHEMICAL RISK FACTORS The use of hazardous chemicals without Material Safety Data Sheets (MSDS) and without working with a minimum number of employees, non-hazardous or less hazardous chemicals instead of hazardous chemicals.	3	5	15 High	6	40	3	720 Very High	8	6	2	96
BIOLOGICAL RISK FACTORS The exposure of workers to factors such as dust, humidity, heat, and other environmental hazards, as well as the lack of protective vaccinations	3	5	15 High	6	40	3	720 Very High	9	6	1	54
PSYCHOLOGICAL RISK FACTORS Events experienced by people and failure to find solutions to these events, lack of employment and periodic examinations	4	4	16 High	3	15	2	90 Significant	3	3	9	81
PERSONAL PROTECTIVE EQUIPMENT Failure to provide employees with appropriate personal protective equipment (PPE) for their work.	3	5	15 High	6	40	3	720 Very High	9	5	2	90
TRAINING The inadequate training of employees in areas such as occupational health and safety, vocational training, on-the-job training, emergency procedures, and first aid etc.	3	5	15 High	10	40	3	1200 Very High	8	8	2	128
HEALTH AND SAFETY SIGNS Inadequate or missing health and safety signs.	3	5	15 High	6	40	3	720 Very High	9	8	1	72
SAFETY The boundaries of the pit have not been determined. Additionally, third parties have been entering the site without permission due to the lack of cameras and inadequate lighting.	3	5	15 High	6	40	1	240 High	8	8	2	128
BUILDINGS AND EXTENSIONS The building and its outbuildings lack thermal comfort, hygiene, lighting, ventilation, and ergonomics.	3	4	12 Medium	3	40	2	240 High	5	7	2	70

2.1. Hazards Identified in Marble Quarries and Related Precautions

The risk analysis for the marble quarry operation was conducted using the L type (5x5) Matrix, Fine-Kinney, and FMEA methods. The analysis identified 59 hazards among 26 activities, and presented measures to reduce the risks to an acceptable level.

The bench height and slope angle of inclination should be appropriate to the specific characteristics of the rock being studied and the geological structure (Figure 1). The slope should be wide and flat for comfortable operation of work machines, trucks, and employees. Extensometers must be installed in designated locations within the marble quarry, and cracks should be regularly monitored during operation. To prevent slope slippage, measures such as reducing the slope angle, strengthening the ground, establishing a drainage system, and retaining walls should be taken. Employees should not stand or work under the face. Safety barriers must be installed in areas such as stages and casting areas (Official Newspaper, 2013; ÇSGB, 2018).

Figure 1. General view of the marble quarry

The determination of groundwater levels in quarries, which vary according to climatic, geological, and hydrogeological conditions, is necessary for the design and construction of appropriate drainage systems on site. Observations should be made after heavy rain and snowfall to detect any deformation in the water levels (ÇSGB, 2018).

At each level of work, there must be at least one functional path that is suitable for the vehicles being used. The path must be constructed in a manner that ensures safe movement of the vehicles. Vehicle paths and crossings should be clearly marked, and warning signs should be placed at the side of the road. The road must always be well-maintained, and benchs and road edges should be cleared of hazardous stones (Figure 2). The slope of the roads inside the mine should not be more than 10^0 and a safety distance of 1 meter should be maintained. The maximum speed limit on the quarry ramps and the roads inside the quarry should be 20 km/h. The quarry roads should be watered regularly to prevent dust exposure (ÇSGB, 2018).

Figure 2. Roads in marble quarry

Drilling (Figure 3) should only be carried out by individuals who possess a professional qualification certificate. It is important to exercise caution when handling, placing, adding, and removing rods. The use of appropriate equipment is necessary when adding and removing rods. Prior to drilling horizontal holes, it is essential to clear any shells that may fall from above. An adequate water supply should be provided and regularly checked. Work should not be conducted near the slope's edge to prevent workers from falling. To ensure worker safety when working close to the edge, it is necessary to provide secure anchor points and ensure that workers wear parachute-type safety harnesses. Additionally, safety barriers must be erected before work begins.

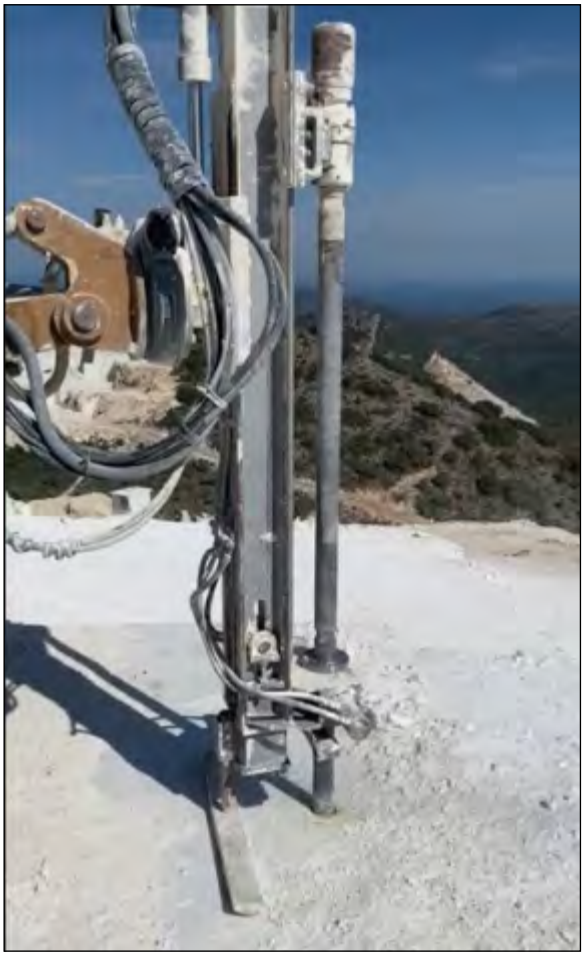

Figure 3. Image of drilling a vertical hole in a marble block

The ladders used must comply with health and safety regulations for work equipment. If possible, the diamond wire cutting machine should be at least 3 metres away from the face. The rails must be level. The machine should be securely placed on the rails. Before using the diamond wire, it is important to check its condition. Avoid applying excessive tension during cutting and ensure that the wire is run at an appropriate speed. The length of the wire inside the marble should not exceed the length of the wire outside. Constantly check for worn diamond wires and replace them as necessary. Water must be supplied during the cutting process. The machine should only be operated by competent individuals in accordance with the instruction manual. During vertical and horizontal cuts, it is important to ensure that no one is in line with the wire (Figure 4). The machine must be equipped with guards. For safety reasons, the operator should place the control panel at a higher level than the wire, as recommended by Urhan and Şişman (1993).

Figure 4. Vertical cutting and horizontal diamond wire cutting process

A specially designed water or air cushion should be used in the cutting gap to separate the block after cutting. After pushing the block, tilt the gap using a hydraulic jack. Before tipping the block, the area where it will be tipped should be cleared of all debris. Additionally, if an airbag is used instead of a water bag, care should be taken to prevent injuries due to explosions that may occur during inflation (MEGEP, 2011).

The process of block cutter (Figure 5) is identical to the precautions taken when cutting with diamond wire. The operations must be performed in safe areas, and the block sizing machine should be installed in a suitable location. Do not stand under or near the block, and do not enter the block until the process is complete. Take appropriate measures when climbing the block, and avoid keeping sharp hand tools near it. The blocks at the bottom of the stack should be well supported, with no gaps between them. If there is a gap, it should be filled with rubble to prevent the cover from falling. A portable screen should be placed behind the counters. Sufficient water flow should be used to prevent wire breakage. Wet cutting also prevents the release of dust into the environment (MEGEP, 2011).

Figure 5. Block cutter and sizing process

During block demolition, individuals other than the excavator operator and signalman should not be present in the area near the platforms. Additionally, it is important to inspect the platforms for any cracks following the demolition and remove them if found.

Loading should be carried out within the capacity of the trucks. Reversing signals must be installed on trucks and construction equipment and they should be ready for use at all times (Figure 6). In quarries, all signals and commands for the movements and manoeuvres of excavators, loaders, shovels, and other machinery must be given by a signalman. It is important to note that construction machinery should not be used for any purposes other than those for which it is intended, and only authorised personnel with an operator's certificate should operate it (ÇSGB, 2018).

Figure 6. Transport operations in a marble quarry

The storage area floor should be smooth, and no more than two blocks ought to be stacked on top of each other. It is important to follow regular and safe stacking practices, and access to the storage area should be restricted to authorized personnel only. Health and safety signs must be displayed in appropriate locations. It is crucial to avoid being underneath the trucks when lifting loads (Official Newspaper, 2022).

The risk of accidents should be reduced by taking precautions against the hazards identified in other areas of activity.

3. Conclusions and recommendations

The study identified 59 hazards in 26 areas of activity involved in operating surface marble quarries. The hazards and risks were compared using the 5x5 matrix and the Fine Kinney method, which are the most preferred risk assessment methods, and the FMEA method, which has become the preferred method in practice. Following the risk assessment, it was found that 24 of the hazards belong to the high-risk group, while only two belong to the medium-risk group, according to the 5x5 L-type matrix. Furthermore, the risk assessment identified 16 items as very high risk, 8 as high risk, and 2 as important risk. Based on the Fine Kinney method and RPN values, 13 precautions are required. The FMEA method identified 11 risks where precautions can be taken and 2 risks where no precautions are necessary. Appropriate measures have been determined to mitigate these risks. Table 14 presents the control measures for hazards identified in the risk assessment table.

Table 14. Comparison of 5x5 L-Type Matrix, Fine-Kinney and FMEA risk methods

Hazard	Risk Methodologies	Control Measures
Level, Drainage	5x5 L type matrix	Immediately take necessary precautions or stop the work
	Fine-Kinney	
	FMEA	No need to take precautions
Mine roads - transportation, emergencies, fire, electricity, maintenance and repair works, physical risk factors, training	5x5 L type matrix	Immediately take necessary precautions or stop the work
	Fine-Kinney	
	FMEA	
Block production, Block demolition, Loading, Working at height, Chemical risk factors, Biological risk factors, Personal protective equipment, Health and safety signs	5x5 L type matrix	Immediately take necessary precautions or stop the work
	Fine-Kinney	
	FMEA	Precautions can be taken
Stock area, Work equipment and hand tools, Pressure vessels and pressure tubes, Welding works, Security	5x5 L type matrix	Immediately take necessary precautions or stop the work
	Fine-Kinney	In the short term, it should improve within a few months
	FMEA	Precautions need to be taken
Construction Machines	5x5 L typematrix	Immediately take necessary precautions or stop the work
	Fine-Kinney	In the short term, it should improve within a few months .
	FMEA	Precautions can be taken
Manual handling and Ergonomics	5x5 L type matrix	Activities to reduce identified risk levels continue and response may take time.
	Fine-Kinney	In the long term, it should be improved year-round.
	FMEA	Precautions need to be taken
Psychological Risk Factors	5x5 L type matrix	Immediately take necessary precautions or stop the work
	Fine-Kinney	In the long term, it should be improved throughout the year.
	FMEA	Precautions can be taken
Buildings and Extensions	5x5 L type matrix	Activities to reduce identified risk levels continue and response may take time.
	Fine-Kinney	In the short term, it should improve within a few months
	FMEA	Precautions can be taken

The marble quarries on Marmara Island have various areas of activity, including stages, drainage, quarry roads for transportation, block production and demolition, loading, stock areas, emergencies, fire, electricity, work machines, work equipment and hand tools, pressure vessels, and pressure tubes. The following topics will be covered: welding works, manual handling and ergonomics, working at height, maintenance and repair works, physical risk factors, chemical risk factors, biological risk factors, psychological risk factors, personal protective equipment, training, health and safety signs, security, and building and its extensions. As the 5x5L type Matrix, Fine Kinney, and FMEA are the most commonly used risk assessment methods, the identified hazards and potential risks were evaluated using these three methods and their respective risk ratings compared.

After comparing these methods, it appears that the evaluations differ depending on the field experience and knowledge of those conducting the risk assessment study. It has been determined that the 5x5 L Type Matrix method is inadequate when compared to the Fine-Kinney and FMEA methods. In the 5x5 L type matrix method, high values are assigned to both probability and severity, resulting in urgent precautions being taken and the activity being continued. For the dangers caused by manual handling and ergonomics, the severity value should be 3 in the L-type matrix system. However, precautions were necessary, and the severity value was increased to 5.The Fine-Kinney method is unique in that it allows the frequency value to be multiplied by probability and severity. This enables a more detailed examination of hazards specific to work areas and employees, and provides quicker solutions. The FMEA method is deemed more appropriate for identifying mechanical risks in machine and system operation. However, it is not recommended for risks specific to the field of activity of the studies and employees. It is complex, difficult to apply and time consuming. The severity of the risks was determined by multiplying their detectability, probability, and severity values. Furthermore, it has been noted that assigning risk severity levels based on the need for precautions presents a significant challenge. In the FMEA method, events that require precautions should be assigned low detectability values. However, this approach poses a problem as there are limited measures that can be taken regardless of the risk severity. For example, in the FMEA method, there is no need to take precautions against the dangers that may occur in stage and drainage activities. However, other methods may require urgent precautions. The study suggests that selecting an appropriate risk assessment method for a given sector and work area is related to the severity of the risks involved and the effective implementation of control measures based on these levels.

Fine-Kinney risk method, taking into account the environmental conditions, areas of activity and results related to hazards and risks specific to employees in the operation of marble quarries,

- It is easy to implement, practical, effective and understandable;
- It produces safer outcomes by conducting a more detailed, comprehensive, and sensitive analysis of hazards and risks;
- Including the frequency value in the calculation of probability and severity enhances the clarity of risk classifications;
- It has quantitative results;
- The expertise and experience of the individual conducting the risk analysis are crucial.

Therefore, it is recommended to use this risk assessment method in the mining industry for a detailed and comprehensive study of occupational health and safety in mining activities.

Acknowledgments

I would like to thank all the referees who supported the study.

References

Ağca, E., 2010, Occupational Safety Risk Analysis in Marble Factories, Çukurova University, Institute of Science and Technology, Master's Thesis, Adana.

Angotzi, G., Bramanti, L., Tavarini, D., Gragnani, M., Cassiodoro, L., Moriconi, L., .Saccardi, P., Pinto, I., Stacchini, N., Bovenz, M. 2005. World at work: marble quarrying in Tuscany, Occupational Environmental Medicine, 62, 417-421. http://dx.doi.org/10.1136/oem.2004.018721

Aksoy, R.1993. Geology of Marmara Island and Kapıdağ peninsula. [doctoral thesis]. [Konya]: Selcuk University.

Aksoy, R. 1999. The relationship between progressive regional metamorphism and tectonic history in Marmara Island. Turkish Geological Bulletin, 42(1), 1-14.

Çınar İ., Şensöğüt, C. 2016. Risk assessment and application examples in Turkish marble quarries, 8th International Crushed Stone Symposium, Kütahya. 445-452.

ÇSGB. 2018. Occupational health and safety guide in underground and surface mining operations. İSGGM, 109-144. Ankara.

ÇSGB. 2018. Health surveillance guide in working life, İSGGM. 97-98. Ankara.

de Melo Neto, R. P., Kohlman Rabbani, E. R. 2012. Application of preliminary risk analysis at marble finishing plants in Recife's metropolitan area. Work, 41(Supplement 1), 5853-5855.

Demirel, Ş. A. 2019. Examination of machine-related risks in Şuhut Göcen mines and facilities with FMEA and Fine Kinney risk methodologies. [master's thesis]. [Istanbul]: Istanbul Yeni Yüzyıl University

DPT. 2001. Mining industrial raw materials (building materials), Special Expertise Report, Eighth Five-Year Development Plan, Ankara, p 9.

Dolmaz, O. 2018. Occupational health and safety measures and an example application in marble cutting and polishing facility [master's thesis]. [Manisa]: İnönü University

Durmuş, H., Yurtsever, Ö., Yalçın, B. 2021. Risk assessment in a tea factory with Fine-Kinney and FMEA methods. International Journal of Advances in Engineering and Pure Sciences, 33(2), 287-298.

Eleren, A., Ersoy, M. 2011. Application of the error mode effect analysis method in the comparison of diamond wire and sleeve cutter cutting technologies in marble quarries in terms of occupational safety. Turkish Science Research Foundation Journal, Volume: 4, Issue: 1, Page: 9-19.

El-Gammal, M. I., Ibrahim, M. S., Badr, E. A., Asker, S. A., El-Galad, N. M. 2011. Health risk assessment of marble dust at marble workshops. Nature and Science,9(11), 144-154.

Ersoy, M., Çelik, M. Y., Yeşilkaya, L., Çolak, O. 2019. Integration of Fine-Kinney and gia methods in solving occupational health and safety problems. Gazi University Faculty of Engineering and Architecture Journal, 34(2), 751-770.

Erten, B., Zafer, U. 2017. Comparison of risk assessments with 5x5 Matrix, Fine Kinney and FMEA methods by performing risk analysis in the pharmaceutical logistics sector: a company example. Anadolu Bil Vocational School Journal, 12(48), 1-14.

Esmaeilzadeh, A., Shaffiee Haghshenas, S., Mikaeil, R., Guido, G., Shirani Faradonbeh, R., Abbasi Azghan, R., Jafarpour, A., Taghizadeh, S. 2022. Risk assessment in quarries using failure modes and effects analysis method (Case study: West-Azerbaijan Mines). Journal of Mining and Environment, 13(3), 715-725.

Fine, W.T. 1971. Mathematical evaluations for controlling hazards (No. NOLTR-71- 31). Naval Ordnance Lab., White Oak Md.

Gandhi, O. P., Agrawal, V. P. 1992. FMEA-A diagram and matrix approach. Reliability Engineering & System Safety, 35(2), 147-158.Görgülü, K. 1994. Investigation of operating systems in some marble quarries (Isparta-Burdur-Sivas) and their association with primary rock material/ mass properties. [master's thesis]. [Sivas]:Cumhuriyet University.

Gür, B., Sezik, Y. 2020. Determination of Working Conditions of Employees in Marble Factories in Terms of Occupational Health and Safety: Çorum Province Example. OHS ACADEMY, 3(1), 47-52.

Gündüz, V. 2023. Analysis of marble quarry activities in terms of occupational health and safety: an example application. [master's thesis]. [Gümüşhane]: Gümüşhane University.

Gök, N. 2018. Occupational safety practice and risk assessment in Burdur Karaçal marble quarry. [master's thesis]. [Konya]: Konya Technical University.

Görgülü, K. 1994. Investigation of operating systems in some marble quarries (Isparta-Burdur-Sivas) and their association with primary rock material/mass properties. [master's thesis]. Institute of Science and Technology.

Göztepe, C., Erdim, B., Akyıldız, S. 2013. Risk assessment and heat non-conformity monitoring system in marble quarry and marble factory. Occupational Health and Safety Local Symposium and Exhibition, 15-16.

Kasap, Y., Subaşı E. 2011. Risk control in open pit mining with analytical hierarchy process. Occupational Health and Safety in Mining Symposium Proceedings Book, Zonguldak.

Ketin, İ. 1946. Geological research in Kapıdağ Peninsula and Marmara Islands: Journal of Istanbul University Institute of Science and Technology, Series B, Volume XI, issue 2, 69-81.

Kıray, D. 2023. Comparison of hazards and risks in geothermal power plants in the Tuzla region (Çanakkale, Biga Peninsula) with 5x5 L type matrix and Fine-Kinney risk methods. International Eastern Anatolia Science Engineering and Design Journal, 5(2), 227-247.

Kinney, G.F., Wiruth, A.D. 1976. Practical risk analysis for safety management, Naval Weapons Center, 1-20.Ketin, I. 1946. Geological investigations in the Marmara Island and the Kapıdağ Peninsula. İU Sci Fac Bull Serie B XI (2), 69-81.

Konuk, A., Kasap, Y., Aslan S. 2009. Risk analysis in Turkish marble quarries. Occupational Health and Safety in Mining Enterprises Symposium, Adana, 343.

MEGEP. 2011. Machine Technology. Block Separation and Sizing. MEB. 521MMI259. Ankara.

Mikaeil, R., Jafarpour, A., Hoboubeh, A. 2017. Safety risk analysis of dimensional stone quarried by diamond wire saws using FMEA method (Case study: Badeki marble quarry-Ghareh-Ziaeddin). Journal of Mineral Resources Engineering, 2(1), 75-84.

Özçelik, A. 2013. Risk management in occupational health and safety with the Fine-Kinney method, marble enterprise example, [master's thesis]. [Eskişehir]: Eskisehir Osmangazi University.

Özfirat, M. K., Özkan, E., Kahraman, B., Şengün, B., Yetkin, M. E. 2017. Integration of risk matrix and event tree analysis: a natural stone plant case. Sādhanā, 42, 1741-1749.

Özkılıç, Ö. 2005. Occupational health and safety, management systems and risk assessment methodologies. TİSK Publications, Ankara.

Official Newspaper. 2013. Regulation on Occupational Health and Safety in Mining Workplaces. https://www.resmigazete.gov.tr/eskiler/2013/09/20130919-3.htm [Access date: 6 November 2023].

Official Newspaper. 2022. Regulation on Amendments to the Regulation on Health and Safety Conditions in the Use of Work Equipment. https://www.resmigazete.gov.tr/eskiler/2022/02/20220218-1.htm [Access date: 6 November 2023].

Stamatis, D.H. 1995. FMEA from theory to execution. ASQ Publications, Milwaukee, Wisconsin, 49 p.

Tanyolu, E. 1979. Petrological studies of the Marmara Island metamorphic series. Zonguldak Engineering and Architecture Academy, Habiliation Thesis 108 pp (in Turkish).

Tunçdilek, N. 1987. Marmara archipelago (Today's land use potential). (No: 3471), Istanbul: Istanbul University Press.

Urhan, S., Şişman, A. N. 1993. The use of diamond wire cutting in block marble production, its application and optimization of cutting efficiency. Journal of Scientific Mining, 32(3-4), 23-30.

Yılmaz, S. 2018. Occupational health and safety in marble processing. [master's thesis]. [Istanbul]: Istanbul Gedik University

Yorulmaz, M., Yeğin, A. O. 2023. Risk analysis of hazardous material handling in port enterprises using Fine-Kinney and FMEA methods. R&S-Research Studies Anatolia Journal, 6(1), 1-37.

Madencilik - Mining, 2024, 63(1), 19-30

BİLİMSEL MADENCİLİK DERGİSİ
SCIENTIFIC MINING JOURNAL

TMMOB Maden Mühendisleri Odası Yayını / The Publication of the Chamber of Mining Engineers of Turkey

www.mining.org.tr

Original Research

Particulate matter emissions from open pit mines; measurement methodologies, instruments, and research undertaken

Zekeriya Duran[a,*], Tuğba Doğan[b,**], Bülent Erdem[c,***]

[a] *Sivas Technical Sciences Vocational School, Sivas Cumhuriyet University, Sivas, TÜRKİYE*
[b] *Industrial Engineering Department, Sivas Cumhuriyet University, Sivas, TÜRKİYE*
[c] *Geophysical Engineering Department, Sivas Cumhuriyet University, Sivas, TÜRKİYE*

Received: November 2023 • Accepted: 2024

A B S T R A C T

Particulate matter is one of the primary pollutants in open pit mining operations. Measurements must be taken to control particulate matter created during open pit mining activities and to compare them to the regulatory limits. Numerous studies have been undertaken to estimate particulate matter emissions produced by open pit mining. It was discovered that the research were largely conducted on coal mines (69.4%), with little study done in other mining types. Research studies on particulate matter estimation took into consideration mostly machine characteristics (loader bucket volume, truck capacity, number of truck wheels etc.) and atmospheric conditions (air temperature, wind speed, relative humidity etc.). This study emphasizes on particulate matter measurement methods along with other measuring parameters and equipment for particulate matter estimation (TSP, PM_{10}, PM_{4}, $PM_{2.5}$, and PM_{1}).

Keywords: Open pit mine, PM_{1}, $PM_{2.5}$, PM_{10}, TSP.

Introduction

Air pollution is a major health risk. Particulate matter (PM) is one element that contributes to air pollution (Choudhary and Garg 2013; Kim et al., 2015; Beloconi et al., 2018; THHP, 2019). There is a great deal of risk to people, other living things, and the environment because of the failure to manage air pollution. The mining industry is one of the pollutants that contributes to air pollution (Hendryx et al., 2020). Large amounts of dust released during both underground and surface mining activities exacerbate environmental problems (Kahraman and Erkayaoğlu, 2021). Dust and PM, which accumulate above the limit values in various places in and around mining areas, negatively affect the health of those working in mines and those living around them and can also cause serious damage to plants and other living things in the vicinity. For this reason, it is extremely important to measure and control dust and especially PMs that cause air pollution, especially in the mining industry. In this study, PM measurement methods are mentioned and at the same time, studies on PM measurement during open pit mining operations are compiled. The parameters used in these studies are examined. This compilation study also provides a perspective on which parameters are used in PM modeling in the open-pit mining industry.

1. Particulate matter concentration measurement methods

There are two ways in which PM concentration measuring devices operate. Under the first method, air quality measurement stations continuously record PM concentrations at predetermined intervals (e.g., seconds, minutes) and instantly monitor particulate matter content. These highly sensitive measurement devices can be controlled remotely via telemetry, or wireless transmission, and they can run for weeks or months once started with little or no operator involvement. However, high standards for calibration, quality control, and maintenance are necessary for accurate measurement. In addition to air quality monitoring stations, handheld or portable PM measuring devices with inexpensive optical sensors can also be used to record at specific intervals. However, devices operating on this principle are generally used to monitor dust exposures in workplaces due to their low sensitivity (NZG, 2009).

* Corresponding author: zduran@cumhuriyet.edu.tr • https://orcid.org/0000-0002-9327-8567
** tcamuzcu@cumhuriyet.edu.tr • https://orcid.org/0000-0002-2628-4238
*** bulent@cumhuriyet.edu.tr • https://orcid.org/0000-0002-1226-9248

https://doi.org/10.30797/madencilik.1396816

In the second method, PM concentrations are collected in filters and analyzed in laboratories at the end of the measurement period. Due to the laborious method of measuring PM concentration in ambient air and the complex nature of particulate matter, the chosen method can significantly affect the measurement result. Therefore, the choice of method is extremely important for accurate measurement of PM concentration. US Environmental Protection Agency (USEPA) particle monitoring methodologies are classified as reference or equivalent methods. Reference methods are referred to as gravimetric (such as measuring directly by mass), while equivalent methods are referred to as methods based on reference methods (NZG, 2009). Leading PM concentration measurement methods are given in Figure 1. The unit of measurement for PM concentrations is generally mg/m^3 or µm/m^3.

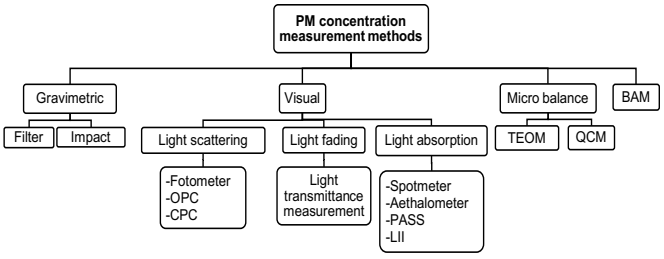

*Figure 1. PM concentration measurement methods (*modified from Amaral et al., 2015*)*

1.1. Gravimetric method

Gravimetric sampling and analysis methods are commonly used to quantify the amount of airborne particulate matter collected from workplace environments (O'Connor et al., 2014; Walley and Zandi, 2016). These measurements are frequently performed to estimate occupational exposure to airborne particles and/or to assess the efficacy of air pollution control technologies. Furthermore, gravimetric analysis of airborne particles is frequently supplemented by other analytical methods used to determine the concentrations of specific chemical agents in occupational environments (O'Connor et al., 2014). This method's main goal is to collect particulate matter in a filter. Air is drawn from a sampler at a certain flow rate with the help of a pump and collected in a pre-weighed filter. Then, the mass of PM is determined with the help of filters weighed under laboratory conditions, and the suspended PM concentration is determined by dividing the PM mass by the volume of air drawn through the filter by the pump. There are various types and manufacturers of samplers working on the gravimetric principle, from individual dosimeters to fully automatic units (Pfeiffer, 2005). With this principle, the average mass concentration for the sampling period is obtained. However, when measuring with this method, the flow rate of the device to be used and the laboratory conditions for weighing are extremely important. In addition, time-dependent concentration values are produced with the gravimetric method, and it is not possible to measure continuous values (minutes, hours, etc.) (Winkel et al., 2014; Walley and Zandi, 2016). With the gravimetric method, PM_{10} and $PM_{2.5}$ concentrations (Pfeiffer, 2005; Mojala et al., 2017) and TSP concentration are found using the equations 1-3 (Mojala et al., 2017). Here, the volume of air sampled for $PM_{2.5}$ (V) is calculated by the sampler's microprocessor, rather than manually as in high-volume PM_{10} analysis (Pfeiffer, 2005; EPA, 2008).

$$TSP = \left[\left(W_f - W_i\right) - \left(CW_f - CW_i\right)\right]/V \quad (1)$$

$$PM_{2.5\ \&\ 10} = \left(W_f - W_i\right) \cdot 10^3/V \quad (2)$$

$$V = Q_a \cdot t \quad (3)$$

where:

W_f : Mass of filter after sampling (mg)
W_i : Mass of the filter before sampling (mg)
CW_f : Mass of the powder cone after measurement (mg)
CW_i : Mass of the powder cone before measurement (mg)
V : Sampled air volume (m^3)
Q_a : Average air flow rate during the sampling period (m^3/min)
t : Sampling time (min)

i. Filter-based samplers are widely used because their cost is low, atmospheric particles can be easily stored, and the collected PM can be used later in simple and/or complex analyses (EPA, 2008). In this method, particles are collected in a pre-weighed filter. Filters are weighed before and after sampling ("loaded" and "unloaded" filters) under standard temperature and relative humidity conditions. The difference between both readings is equal to the mass of the PM (Baumann et al., 2006; Giechaskiel et al., 2014; Amaral et al., 2015; Walley and Zandi, 2016). Since filters are sensitive to environmental factors such as relative humidity, their selection is extremely important. Traditional filters are made of glass fiber and their surface is protected from chemical reactions by a special coating (such as Polytetrafluoroethylene, PTFE). For this reason, PTFE-coated glass fiber filters are widely used by EPA and European Union institutions (EPA, 2008; Walley and Zandi, 2016). The USA also recommends the use of PTFE type filters with legal regulations (Giechaskiel et al., 2014). On the other hand, it has been stated that quartz fiber filters should be used for PM_{10} measurement according to the EN 12341, and glass fiber, quartz fiber, PTFE or PTFE-coated glass fiber filters should be used for $PM_{2.5}$ measurement according to the EN 14907. It has also been stated that EN 12341 needs to be revised to be consistent with EN 14907, and that any of the four filters listed in EN 14907 can be used in both PM_{10} and $PM_{2.5}$ reference samplers (Harrison et al., 2006).

ii. Impactors are devices used to measure the size distribution in the mass with the gravimetric method, and some types have multiple holes (Amaral et al., 2015). In this measurement method, aerosols pass through sequential filter stages. At each stage, an air jet containing aerosol reaches the impinging plate and particles larger than the filter diameter are collected for the stage. While the smaller particles follow the gas flow surrounding the collection plate and are collected in the next stage where the holes are smaller and with higher air velocity conditions, this process continues until the smaller particles are cleared in the final filter (Vincent, 2007). Low-pressure cascade impactors (Andersen impactor, Dekati Low Pressure Impactor (DLPI), Berner Low Pressure impactor (BLPI), etc.) used for measurements of PM size distributions are generally suitable for size ranges ranging from 30 nm to 10-20 µm. Sampling can be done in lower size ranges with filters. Due to the sampling method, the particles obtained can also be used for additional analyses (Nussbaumer et al., 2008).

1.2. Optical method

Optical particle monitors utilize the interaction between airborne particles and visible, infrared or laser light (Pilling et al., 2005) for measurement. Optical Particle Counters (OPC) work on the principle of light scattering to detect the size and number of individual particles. OPCs are used in aerosol research in long-

term monitoring networks. The size of particles detectable with OPCs is approximately 0.05 to 50 µm, with general measurement ranges from 0.2 to 30 µm. Although size measurements with OPCs are very precise, their accuracy depends on particle composition and shape (EPA, 2008). Real-time monitoring of PM_{10} concentrations can be achieved using optical instruments (Walley and Zandi, 2016). In the optical measurement method, aerosol particles are illuminated with a beam of light. With the particles spreading in all directions, a part of the light beam is transformed into other forms of energy (absorption). The extinction of light is calculated by scattering and absorption (Giechaskiel et al., 2014). Optical instruments used to measure particle concentration in real time are based on the principles of scattering, absorption and light extinction (Giechaskiel et al., 2014; Amaral et al., 2015; Walley and Zandi, 2016).

i. Light scattering devices absorb sample air from a laser-illuminated chamber. A photodetector, which indicates the degree of light beam scattering, is used to classify airborne particles (Giechaskiel et al., 2014; Winkel et al., 2014; Amaral et al., 2015). The photodetector's signal converts the categorized particles into mass concentration by employing a calibration constant that is predetermined at the factory with a particular calibration aerosol (Winkel et al., 2014). Light scattering devices are generally portable, have an internal pump, are equipped with batteries and data storage, and can provide continuous data (Pilling et al., 2005; NZG, 2009; Winkel et al., 2014). Some devices can simultaneously determine several mass fractions (such as PM_{10}, $PM_{2.5}$, PM_1) or count the number of particles in a series of size channels. The main disadvantages of this method are that the optics inside the device can be contaminated with PM and the concentration readings can differ from the actual values because the particle size, shape, density and refractive index of the measured PM differ from the aerosol used to calibrate the device (Winkel et al., 2014). Nephalometers and/or transmissometers are widely used in the USA to determine visibility loss due to airborne particulate material, especially in national park areas (Pilling et al., 2005). Devices operating on this principle are generally used to monitor dust exposures in workplaces. Over the last few years, some of these devices have been adapted for environmental monitoring with varying degrees of success. In addition, they are more suitable for use in research or in low-level survey studies due to their measurement sensitivity and not being suitable for continuous monitoring (NZG, 2009).

ii. Light fading: The light transmitted from the exhaust can be measured with opacity meters. In addition, it has been stated that measurements based on light extinction depend on the particle concentration, shape and composition, as well as the path length and wavelength of the light (Giechaskiel et al., 2014).

iii. Light absorption: Measuring devices based on the principle of light absorption measure the concentration of black carbon that forms the aerosol in motor vehicles. Black carbon is a positive radiative substance that strongly absorbs light and therefore contributes to climate change, and due to this feature, it has been extensively used in atmospheric measurement studies (Giechaskiel et al., 2014; Amaral et al., 2015). Common techniques used to measure aerosol absorbance include (i) the difference method, where the absorbance is derived from the difference between extinction and scattering, (ii) filter-based methods, which measure light attenuation by PM collected on a filter, (iii) Photoacoustic spectroscopy, which measures black carbon through heat particles and (iv) laser-induced incandescence (LII). The last two methods measure black carbon by heating particulate matter and the particles absorb light (Giechaskiel et al., 2014).

1.3. Microbalance principle

There are two main measuring devices in the microbalance method: conical element oscillating microbalance (TEOM) and quartz crystal microbalance (QCM) (Amaral et al., 2015). Particulate matter monitoring devices using TEOM technology are "gravimetric" devices that draw ambient air through a filter by continuously heating it (50 °C) at a constant flow rate, continuously weigh the filter, and calculate particle concentrations in near real time (EPA, 2008; Winkel et al., 2014). Although these devices are used in the United States by many government agencies to obtain $PM_{2.5}$ and PM_{10} mass concentration data, they are only approved as an equivalent method for PM_{10} sampling (EPA, 2008). The TEOM measurement technique is based on a replaceable filter cartridge placed at the end of a hollow conical tube. The wider end of the pipe is fixed, particles accumulate as the air passes through the filter, and since the flow rate is constant throughout the sampling, the mass concentration can also be calculated (Baumann et al., 2006). The filtered air then passes through the conical tube to a flow controller. The conical pipe with the filter at the end is kept oscillating in clamp-free mode (Figure 2).

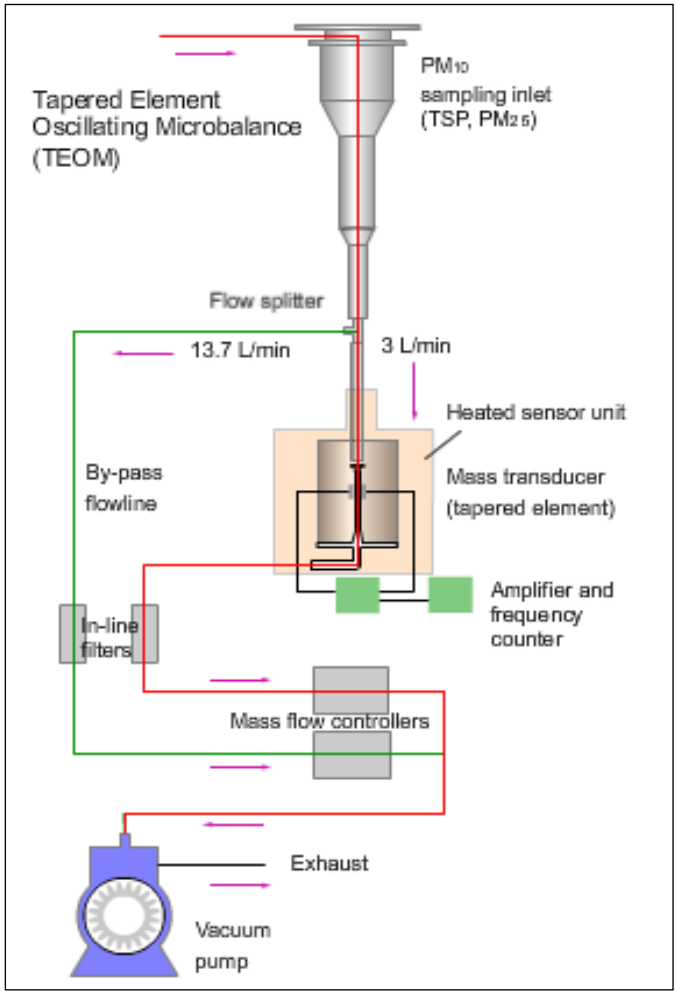

Figure 2. Working principle of conical element oscillating microbalance (TEOM) (Url-2, 2023)

The frequency of oscillation depends on the physical properties of the conical tube and the mass at its free end (Nosratabadi et al., 2019; Url-1, 2023). On the other hand, in this method, evaporation of PM material may occur due to sample flow heating, which may cause the actual PM concentration to be underestimated (Grim and Eatough, 2009; Winkel et al., 2014). PM concentration

changes collected in TEOM devices are affected by airflow, relative humidity, temperature, gaseous pollutants and particulate matter characteristics (Li et al., 2012). For this reason, it has been stated that the concentration value calculated during measurement with the TEOM device in England should be multiplied by a factor of 1.3 (Pilling et al., 2005; Harrison et al., 2006). TEOM monitors are currently used only for measuring PM_{10}, $PM_{2.5}$ or PM_{1} concentrations. However, airborne particle concentrations are normally low and therefore long sampling times or the use of high volume pumps are necessary to collect sufficient particles to perform an accurate gravimetric analysis and/or more specific chemical or biological analysis of the collected material (Nosratabadi et al., 2019) . Devices with TEOM analyzers are widely used both in the UK and the rest of the world (Pilling et al., 2005; Walley and Zandi, 2016). Quartz crystal microbalance (QCM) devices have piezoelectric properties that change the resonance frequency when a small mass is added to the quartz crystal surface. In these devices, particles are deposited by electrostatic precipitation in a thin quartz crystal resonator (EPA, 2008; Giechaskiel et al., 2014). On the other hand, QCM-based devices use the detection electrode of the quartz crystal as a collision plate. Particles in the air are sampled into the detection chamber and then deposited onto the crystal electrode via inertial force. However, it has been stated that these devices have significant disadvantages such as splashing of particulate matter due to poor adhesion, the need for frequent cleaning of the crystal electrode, and uneven distribution of collected particles (Ngo et al., 2019). Nevertheless, these devices can measure the mass concentration of 100 µg/m^3 aerosol in less than a minute (EPA, 2008).

1.4. Beta ray attenuation principle (BAM)

Beta-ray attenuation particle analyzers are the most widely used method for measuring ambient PM_{10} concentrations in national networks across Europe (Pilling et al., 2005). In addition, in Türkiye, measurements are made with devices working with this method at air quality stations in some provinces affiliated with the Ministry of Environment and Urbanization. The devices automatically measure and record airborne particulate matter concentrations (mg/m^3 or µg/m^3). Devices working with this principle collect the particulate matter in the air on the strip filter with the help of a pump. With the beta ray source coming from a radioactive source (Carbon-14 or Krypton 85), fixed high-energy electrons are emitted from the clean filter band to the particulate matter collected on the filter along a point, and these beta rays are detected and counted by a sensitive detector. The system automatically advances this band point to the sample spray system, where the vacuum pump then draws a measured and controlled amount of dust-laden air through the filter band and fills it with ambient dust. At the end of the sample hour, this dirty spot is placed back between the beta source (Carbon-14 or Krypton 85) and the detector, causing attenuation of the beta beam signal used to determine the mass and volumetric concentration of particulate matter on the filter band (Figure 3). This mass is used to calculate the volumetric concentration of particulate matter in the ambient air (Pilling et al., 2005; Baumann et al., 2006; EPA, 2008; Kamyotra, 2012; Url-3, 2023). Samplers working with the BAM principle are the only systems that continuously measure the mass concentration of particles by extraction and are not affected by chemical composition, size or color changes in the particles (Castellani et al., 2014). Although the filter material in the monitors of devices operating on this principle is generally not heated, in some analyzer configurations the inlet system can be heated to reduce the relative humidity in the sample, minimizing the water content of the particulate matter mass (Pilling et al., 2005; Winkel et al., 2014). Glass fiber filters are commonly used in particle analyzers that work on the beta attenuation principle. Additionally, while these monitors can produce half-hour average mass concentrations, a 24-hour averaging period is required for typical ambient concentrations to obtain sufficient particle accumulation for accurate estimation (EPA, 2008).

Comparison of PM_{10} and $PM_{2.5}$ concentration measurement methods is given in Table 1. According to this; filter-based gravimetric samplers are the PM_{10} reference measurement method according to EN 12341 and EPA 40 CFR PART 50 and EU directives, and chemical analyses of the measurement results are performed. However, this method is costly and measurement values are obtained from laboratory results. On the other hand, measurement results can be obtained in a short time (< 1 hour) with real-time monitoring techniques. Only PM_{10} sampling with the BAM method, one of the real-time monitoring techniques, complies with EU directives.

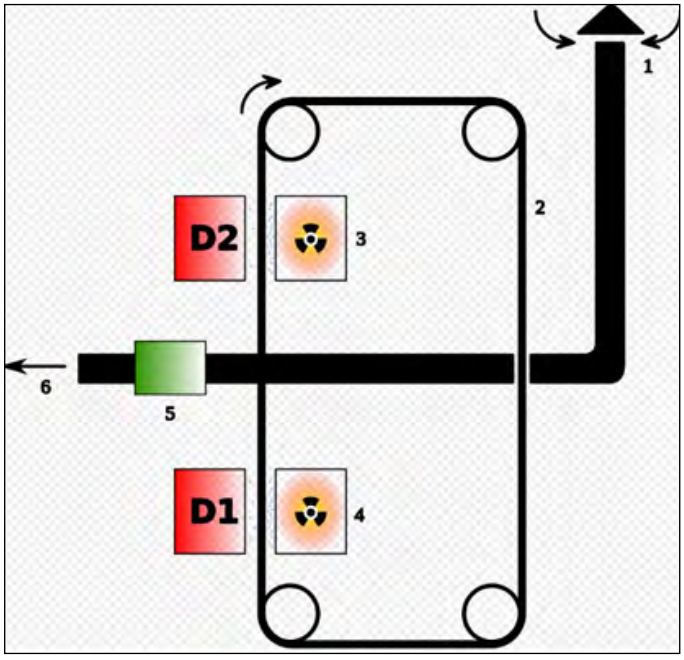

Figure 3. Working diagram of a BAM analyzer "1. "Air intake, 2. Bicycle lane, 3 and 4. Beta radiation source, D1 and D2 Beta radiation detectors, 5 air pumps, 6. Air exhaust" (Url-4, 2023)

1.5. PM related standards

Determination of PM_{10} mass concentration in ambient air is made in accordance with EN 12341 or EPA 40 CFR PART 50, $PM_{2.5}$ mass concentration in accordance with EN 14907. According to the European Union First Air Quality Directive (1999/30/EC), PM_{10} measurements should be made using the reference method as defined in the EN 12341 European Standard. This standard includes "very high volume sampler-WRAC", "high volume sampler-HVS" (PM_{10} sampler-1133.33 L/min) and "low volume sampler-LVS" (PM_{10} sampler-38.33 L/min). It recommends three sampling devices: very high volume samplers are often considered the 'primary standard' and are not suitable for placement in general work environments (Pilling et al., 2005). When the literature was examined, it was seen that low volume samplers were frequently used. According to this standard, the measurement period, the laboratory temperature for filter weighing and humidity should be 24 hours, 19-21 °C and 45-50% (TSE EN 12341, 2014; Url-5, 2023), respectively. In the EPA 40 CFR PART 50, the measurement period, the flow rate of the device to be used, the laboratory temperature for filter weighing and humidity should be 24 hours,16.67 L/min, 15-30 °C and 20-45% (EPA, 1999), respectively.

Table 1. Comparison of PM10 and PM2.5 particulate matter concentration measurement methods (Pilling et al., 2005; EPA, 2008; Environment Agency, 2011; Winkel et al., 2014; Amaral et al., 2015; Walley and Zandi, 2016)

Monitoring type	Measurement technique	Standard method	Advantages	Disadvantages	Measuring range and time	Measurement accuracy ($\mu g/m^3$)
Period-average sampling	Filter-based gravimetric samplers	i. EN 12341 ii. EPA 40 CFR PART 50	i. PM10 reference measurement method according to EU directives ii. Chemical analysis can be done as a result of the measurement	i. Measurement cost is high. ii. Measurement time is limited to 24 hours. iii. It does not meet the reporting requirements of EU directives. iv. The measurement result is obtained after the laboratory results.	Measuring time 24 hours and volumetric flow 16.67 l/min	± 2
Real-time monitoring	Conical element oscillating micro balance (TEOM)	i. Standard TEOM does not meet the equivalence criteria in the EU reference method for PM_{10} (EN12341) or $PM_{2.5}$ (EN14907). ii. Many government agencies in the USA have adopted the equivalent method for measuring PM_{10}.	i. Real-time data reading can be done for short periods of time (<1 hour), which users can easily see. ii. Measurement accuracy is better than the reference method.	i. The preheated airflow causes greater semivolatile loss compared to the reference method. ii. Measurement cost is high. iii. The expanded uncertainty in the limit value for PM_{10} and $PM_{2.5}$ exceeds 25%. iv. The filter should be replaced when the PM concentration is high. v. Filter life is 2 - 4 weeks.	0-5000 mg/m^3	± 0,5
Real-time monitoring	Beta ray attenuation (BAM)	i. Some models comply with EN12341 without correction factors, some with correction factors. ii. PM_{10} measurement complies with EU directives, $PM_{2.5}$ does not.	i. Real-time data reading can be done for short periods of time (<1 hour), which users can easily see. ii. Measurements are semi-continuous and provide hourly results, not instantaneous.	i. If heated inlet is used, some semi-volatile PMs may be lost. ii. Unheated samplers may have reduced flow due to the presence of water. iii. The analyzer contains a radioactive source.	0-1000 $\mu g/m^3$	± 3, but this value depends on the analyzer.
Real-time monitoring	Luminescent optical particle counter (Nephelometer)	i. It measures in accordance with some standards (CEN-TR 16013-3) in England. There are currently no CEN, ISO or BS standard methods covering this technique.	i. PM_{10}, $PM_{2.5}$ and PM_1 measurement can be done simultaneously. Stationary and portable versions are available. ii. The number of particles present in different size ranges is measured and mass concentrations can be derived mathematically using a density factor.	i. It is not suitable for the popular automated method of scanning surveys that consistently gives real-time results. ii. The PM magnitude during measurement is affected by shape, color and refractive index. iii. The accuracy rate is 30%. iv. The optics inside the meter may become contaminated with PM. v. Because the calibrated PM used to check the accuracy of the PM measurement differs from the measured PM, actual concentration readings may be seriously underestimated or overestimated.	Varies by analyzer. 0-6000 $\mu g/m^3$	Depends on analyzer type.

The European Standard EN 12341 is defined as the TSE EN 12341 in Türkiye as "*Ambient air - Standard gravimetric measurement method for the determination of PM_{10} or $PM_{2.5}$ mass concentrations of suspended particulate matter*". The original version of this standard (EN 12341: 2014) was prepared by the technical committee CEN/TC 264 "Air quality", whose secretariat is managed by DIN. This standard also replaces EN 12341:1998 and EN 14907:2005. This standard can also be used to calculate mass concentrations of other PM fractions such as PM_1. According to this standard, measurements are carried out with samplers operating at a nominal flow rate of 2.3 m^3/h during a nominal sampling period of 24 hours, with inlet designs as specified in Annex A of the standard, and measurement results are expressed in $\mu g/m^3$. The range of application of this European Standard is from approximately 1 $\mu g/m^3$ (i.e. the limit of observability of the standard measurement method expressed in terms of the uncertainty of the method) to 150 $\mu g/m^3$ for PM_{10} and 120 $\mu g/m^3$ for $PM_{2.5}$. Here, ambient air is passed at a constant flow rate through a known size selective inlet and the relevant PM fraction is collected in a strainer for a known period of nominal 24 hours. The mass of the PM material is determined by weighing it with a strainer at pre-specified constant conditions before and after collecting the particulate matter, hence the concentration in micrograms per cubic meter ($\mu g/m^3$) in the measured environment. It is then calculated by dividing the difference between sampled and unsampled filter masses by the sample volume found by multiplying the flow rate and sampling time as given in Equation 4.

$$c = (m_1 - m_u)/(Q_a * t) \quad (4)$$

Where;

c : Concentration per cubic meter ($\mu g/m^3$)

m_1 : Sampled strainer mass (μg)

m_u : Unsampled filter mass (μg)

Q_a : Flow rate at ambient conditions (m^3/h)

t : Sampling time (h)

When using sampling systems operating at flow rates other than 2.3 m^3/h, the strainer conditioning and weighing requirements can be obtained in accordance with standard's Clause 6 by applying a scaling factor equal to the ratio of the flow rates of the non-reference and reference samplers. Accordingly, for a sampler operating at a flow rate of 30 m^3/h, the scaling factor of the filter witnesses is considered to be equal to 30/2.3 (TSE EN 12341, 2014). On the other hand, monitoring of aerosols in workplaces and evaluation of particle concentrations in the air can be done in accordance with the CEN/TR 16013-3:2012. This standard details the use of photometers (aerosol monitors) for the determination of airborne particles of the respirable fraction, their measurement limitations and their possible use in the field of occupational hygiene. All photometer-based direct reading aerosol monitors use the principle of light scattering to determine airborne particle concentration (NSAI, 2012). Studies carried out to estimate PM emission rates resulting from activities in open-pit mining operations and the devices used in measurements are given in Table 2. It has been noted that most studies on PM emissions are conducted on coal mines; whereas, little research has been done on iron, manganese, and copper mines, as well as gypsum and limestone quarries. However, measurements of PM emissions have only been discovered in the aforementioned open-pit mines. Measuring of PM_{10}, $PM_{2.5}$, and TSP emissions was mostly done for routine operations including drilling, loading, and hauling. PM_1 emission levels were the lowest measured. The majority of the indicators measured were meteorological, aside from PM emissions. Thermal comfort and PM emission tests were conducted using various brands and kinds of instruments.

2. Open pit PM emission measurements

It is crucial to estimate PM emissions for comparable activities and to compute the PM emissions from open pit mining operations in a realistic manner in order to regulate air quality. Activity based emissions must be continuously measured and tested with various parameters. Various researchers have used different parameters to estimate PM (TSP, PM_{15}, PM_{10}, $PM_{2.5}$ and PM_1) emission rates resulting from activities during open-pit mining operations. Studies on basic activities such as drilling, blasting, loading and hauling in the mining industry have been compiled. The parameters used by the PM emission estimation equations, handled formations, and particulate matter emission were analyzed in the following sections.

2.1. PM emission from drilling operations

There have been nine studies conducted to estimate PM emissions from drilling operations. The majority of research has focused on TSP estimate (64%) while none has examined PM_{15} estimation (0%) (PM_{10} → 18%, $PM_{2.5}$ → 9% and PM_1 → 9%). Parameters such as moisture and silt content of the drilled formation, wind speed, hole diameter and drilling frequency (Chakraborty et al., 2002; Lal and Tripathy, 2012), moisture and silt content of the drilled material (Nagesha et al., 2016) were employed in the modeling of TSP emission during drilling operations in the overburden layers of open coal mines. Furthermore, during coal drilling, a TSP release rate of 0.1 kg/hole was utilized (USEPA 1998), and during coal pickling, a constant value of 0.59 kg/hole (USEPA 1998; NPI, 2012) was employed. A constant value of 0.31 kg/hole for PM_{10} was utilized in coal mine research (NPI, 2012). On the other hand, air temperature, relative humidity, station pressure, dew point temperature, wind speed (including side and counterwind speeds), silt + clay content of the material, and material moisture were used in TSP, PM_{10}, $PM_{2.5}$, and PM_1 emission modeling that was done in gypsum and limestone quarries (Duran, 2022). Examining the literature, TSP release prediction models considered hole diameter and drilling frequency the least, and the moisture content of the drilled material and wind speed the most. Factors such air temperature, relative humidity, station pressure, dew point temperature, wind speed (including head and side wind speed), silt + clay content of the material, and material moisture were utilized to estimate PM_{10}, $PM_{2.5}$, and PM_1 emissions (Figure 4).

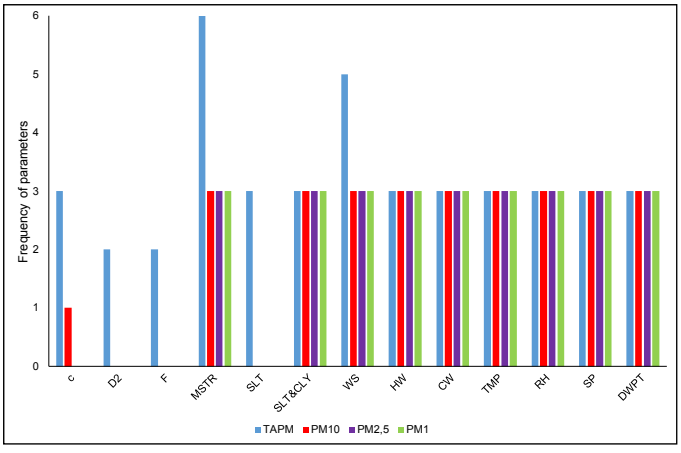

Figure 4. Frequency of parameters used for estimating PM emissions from drilling operations

Table 2. PM release measurements in open mining operations

Author, year	Study area	Remark	Parameter	Instruments
Chakraborty et al., 2002	Drilling, Coal/mineral loading Overburden loading and unloading Haul road and Transport Road Exposed overburden dump Stock yard, Exposed pit surface Coal handling plant Workshop, Overall mine (for TSP)	Coal	TSP Meteorological parameters Particle size (silt content) Moisture content	High volume sampler (HVS) with an average flow rate 1.1 m^3/min (Model: APM 415 Envirotech Instruments Pvt. Ltd) Automatic Digital Weather Monitoring Station, OMNIDATA International, USA Sieve (mesh 4 mm, 2 mm, 125 µm and 75 µm) Oven and electronic balance (Mettler)
Chaulya, 2006	Waste loading and unloading Iron ore loading Haul and Transport Road	Iron	TSP	High volume sampler (HVS) with an average flow rate higher than 1.1 m^3/min (Model: APM 415 Envirotech Instruments, New Delhi, India and measurement by Digital Electronic Balance Mettler, Switzerland)
Lal and Tripathy, 2012	Drilling and Overburden loading Coal handling (Feeder Breaker) Haul road and Transport Road OB unloading and Railway siding Exposed OB Dumps, Coal loading	Coal	TSP Meteorological parameters	Air quality monitoring Meteorological Department
Aneja et al., 2012	Transport road	Coal	PM_{10}	Andersen/GMW Model GUV-16H high volume air samplers
Badu, 2014	Shovel-Loading, Surface Miner Drilling, Wet Haul Road Transportation Road OB Bench (Before blasting) OB Bench (After first blasting) OB Bench (After second blasting)	Coal	PM_{10} PM_4 $PM_{2.5}$ PM_1	DustTrak II Aerosol Monitor (Model No - 8532)
Huertas et al., 2014	Pit, Beltway, Dump and Stock Pit-dump via and Pit-stock via	Coal	TSP Meteorological parameters	Monitoring station Meteorological stations
Kishore, 2015	Surface mine environment	Iron Manganese	TSP, PM_{10} Meteorological parameters	Envirotech APM 460 NL Meteorological stations
Gautam and Patra, 2015	Open-pit mine	Copper	PM_{10}, $PM_{2.5}$ and PM_1 Meteorological parameters	Grimm aerosol spectrometer (Grimm, model 1.108) Portable weather station (Spectrum Technologies, Inc., Model Watchdog 2000)
Gautam et al., 2015	Open-pit mine	Iron	PM_{10}, $PM_{2.5}$ and PM_1 Meteorological parameters	Grimm aerosol spectrometer (Grimm, model 1.108) Portable weather station (Spectrum Technologies, Inc., Model Watchdog 2000)
Lashgari and Kecojevic 2015	Overburden loading by cable shovel Overburden loadind by front-end wheel loader	Coal	TSP, PM_{10}, PM_4, $PM_{2.5}$ and PM_1 Meteorological parameters	TSI DustTrak DRX 8534 real-time aerosol monitoring instrument. Kestrel 4500 Weather Meter
Sastry et al., 2015	Drilling	Coal	PM_{10} $PM_{2.5}$ Meteorological parameters	Personal dust monitors/Dust dosimeter (5 units) Point samplers (2 units) Meteorological monitoring station
Tripathy et al., 2015	Shovel-dumper, Surface miner Drilling, Wet haul road Transportation road Office of colliery manager OB bench (before blasting) OB bench (after blasting 1) OB bench (after blasting 2)	Coal	PM_{10} PM_4 $PM_{2.5}$ PM_1	DustTrakII
Nagesha et al., 2016	Drilling	Coal	PM_{10}	Ambient point samplers

Author, year	Study area	Remark	Parameter	Instruments
			Meteorological parameters Moisture content Particle size (silt content)	Meteorological station
Patra et al., 2016	Open-pit mine	Copper	$PM_{0.23 - 0.3}$, $PM_{0.3 - 0.4}$, $PM_{0.4 - 0.5}$ $PM_{0.5 - 0.65}$, $PM_{0.65 - 0.8}$, $PM_{0.8 - 1.0}$ $PM_{1.0 - 1.6}$	GRIMM aerosol spectrometer (Model 1.108, Grimm)
			Meteorological parameters	Portable weather station (Spectrum Technologies, Inc., Model Watchdog 2000)
Oudwater, 2017	Drilling	Stone quarry	PM_{10}	Turnkey Osiris nephelometer
Wanjun and Qingxiang, 2018	Open-pit mine	Coal	PM_{10} and $PM_{2.5}$	The beta-ray particle monitor
Sahu et al., 2018	Surface coal mine environment	Coal	PM_{10}, $PM_{2.5}$ and PM_1	Grimm aerosol spectrometer (Model 1.108, GRIMM Aerosol Technik GmbH & Co. KG, Germany)
			Meteorological parameters	Portable weather station (Spectrum Technologies, Inc., Model Watchdog 2000)
Richardson et al., 2018	Product stockpile Coal loading, hauling, dumping Topsoil spreading Dragline on overburden Pre-strip Coal preparation plant Dumping into coal hopper Drill Spontaneous combustion Shovel Dozer	Coal	TSP, PM_{10} and PM_2	Optical-Grimm model 1.105
	Mine haul road Product stockpile Background position representing nearest receptor Product stockpile and mine processing area Operating mine as a whole		PM_{10} and $PM_{2.5}$	Gravimetric MiniVol (high-volume sampler)
Tripathy and Dash, 2019	Open-pit mine	Coal	PM_{10} and $PM_{2.5}$	Envirotech APM 460 NL
Richardson et al., 2019	Coal haul road Overburden haul road Drilling, Dragline Overburden loading and dumping Coal loading and dumping	Coal	$PM_{2,5}$	Met-One E-Bam, fitted with US EPA approved reference $PM_{2,5}$ cyclone separator TSI DustTrak model 8530
			Meteorological parameters	Davis weather station for initial stage of sampling. Met-One 034B Windset coupled with a Campbell Scientific CR800 data logger
			Soil moisture and silt content	Calibrated laboratory oven and soil sieve set
Bui et al., 2019	Drilling	Coal	PM_{10}	KANOMAX digital dust monitor model 3442
Luo et al., 2021	Mining area	Coal	TSP, PM_{10} and $PM_{2.5}$ Meteorological parameters	RS-ZSYC-9S-4G multi-parameter monitoring device
Duran, 2022	Drilling Loading Transport road	Gypsum Limestone Quarries	TSP, PM_{10}, $PM_{2.5}$ and PM_1 Particle size (silt content) Moisture content	DustMate environmental monitor Sieve (216 µm, 150 µm, 106 µm and 75 µm) Vibratory Sieve Shaker AS 200 Binder Etuv
			Meteorological parameters	Kestrel 5500 Weather Meter

2.2. PM emission from blasting operations

To quantify PM emissions from blasting activities, nine studies have been undertaken. The majority of research has focused on TSP prediction (43%), whereas no research has targeted on PM_1 prediction (0%) (PM_{15} → 10%, PM_{10} → 33%, $PM_{2.5}$ → 14%). TSP emission during blasting activities in the overburden layers of open coal mines was modeled using factors such as blast area, blast hole length, and moisture of the blasted material (Axetell and Cowherd 1984; USEPA, 1998; NPI, 2001-2012) and blast area alone (USEPA, 1991-1995-1998; NPI, 2001-2012). USEPA (1991-1995-1998) and NPI (2001-2012) multiplied PM_{10} by a fraction (0.52) of TSP in order to model PM_{15} emissions whereas TSP was multiplied by a coefficient of 0.03 to yield $PM_{2.5}$ (Axetell and Cowherd 1984; USEPA, 1998). The blasting area was the most important factor for TSP emission models, whereas the moisture content of the blasted material and the hole size were the least important factors. The blasting area, hole length, and moisture content of the blasted material were all employed in identical numbers for the PM_{15} emission models. Models for PM_{10} and $PM_{2.5}$ emissions were produced by simply multiplying TSP by a certain coefficient (Figure 5).

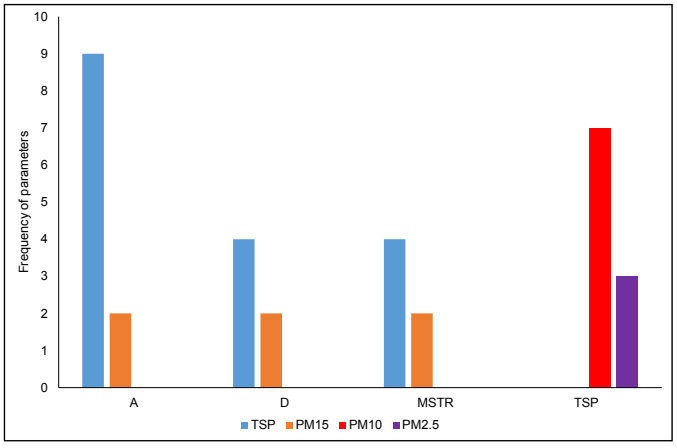

Figure 5. Frequency of parameters used for estimating PM emissions from blasting operations

2.3. PM emission from loading operations

Sixteen research studies have been conducted to estimate PM emissions during loading activities. When the studies on PM estimation are weighted as a percentage, the rate of PM_1 estimation was 3%, whereas the rate of TSP estimation was 44% (PM_{15} → 15%, PM_{10} → 19%, $PM_{2.5}$ → 19%). Parameters like the moisture content of the loaded material (Axetell and Cowherd 1984; USEPA, 1991-1995-1998; NPI, 2012), and the moisture and silt content of the loaded material, material unloading height, wind speed, loading frequency, and loader capacity (Chakraborty et al., 2002; Lal and Tripathy, 2012) were used in the modeling of TSP in loading operations in open coal mines. The modeling of TSP emission during pickling in coal mines took into account moisture and silt content of the loaded material, material unloading height, wind speed, loading frequency and loader capacity (Chakraborty et al., 2002; Lal and Tripathy, 2012) and moisture content and wind speed of the loaded material (NPI, 2012). The TSP generated during ore production and stripping in an open iron mine was modeled using the following factors: wind speed, load frequency, moisture and silt content of the loaded material, material unloading height, loader capacity, and loading frequency (Chaulya, 2006). In aggregate quarries, factors including material moisture content and wind speed (USEPA, 2006) were taken into account in loading operations. Parameters including moisture content of the loaded material (NPI, 2012), moisture content of the loaded material and wind speed during coal pickling (NPI, 2012), and correction factors (0.75*PM15) (USEPA, 1991-1995) were considered while predicting PM_{10} emission in coal production. Similarly, PM10 in aggregate loading was estimated using 0.35*TSP. An equation of 0.053*TSP for aggregate loading (USEPA, 2006) and 0.019*TSP for coal production (Axetell and Cowherd 1984; USEPA, 1991-1995-1998; NPI, 2012) was used for estimating $PM_{2.5}$ emissions. TSP, PM_{10}, $PM_{2.5}$, and PM_1 emissions in gypsum and limestone quarries were predicted using parameters such as air temperature, dew point temperature, station pressure, relative humidity, wind speed (including counter and side wind speed), humidity of the loaded material, and loader bucket volume (Duran, 2022). Based on a review of pertinent literature, the moisture content of the material being loaded, wind speed, loader bucket volume, unloading height, and loading frequency are the main factors used in TSP emission models; at the very least, counter and side wind speeds, air temperature, station pressure, relative humidity, and dew point temperature are considered. Loader bucket volume, material moisture, wind speed (including head and crosswind speeds), air temperature, dew point temperature, relative humidity, and station pressure were all employed in PM1 emission models (Figure 6).

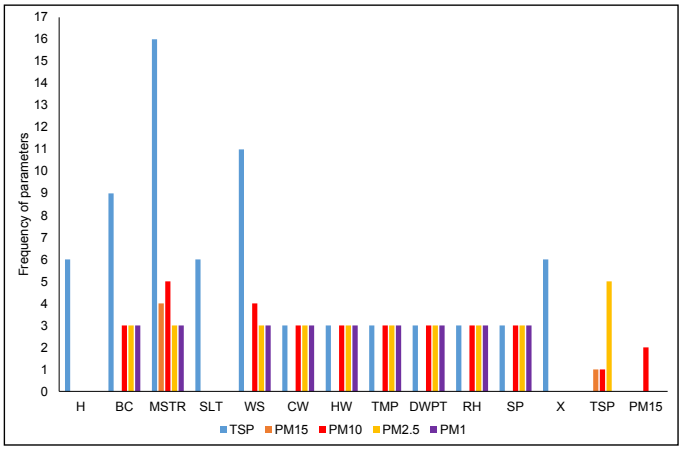

Figure 6. Frequency of parameters used for estimating PM emissions from loading operations

2.4. PM emission from hauling operations

For hauling both within and outside the pit, twelve studies yielded PM emission models. 48% of the research concentrated on TSP estimate and 4% on PM_1 estimation (PM_{15} → 10%, PM_{10} → 21%, $PM_{2.5}$ → 17%). The following parameters were used for TSP emission modeling in open coal mines for in-pit transportation; truck mass and silt content of the road surface (Axetell and Cowherd 1984; USEPA, 1991-1998); silt content, truck mass and moisture content (NPI, 2001); moisture and silt content, wind speed, average truck speed, vehicle cycle frequency and truck capacity (Chakraborty et al., 2002; Lal and Tripathy, 2012); moisture, silt content and average truck speed (NPI, 2012). In the modeling of TSP emission for an open iron mine, Chaulya (2006) profited from moisture and silt content, wind speed, average truck speed, vehicle frequency, and truck capacity. Another method used truck mass and silt content to achieve stabilized road conditions (USEPA, 2006). Furthermore, moisture and silt content, wind speed, average truck speed, and vehicle cycle frequency were employed for TSP emission modeling in hauling operations on the main haul

roads in coal and iron mines (Chakraborty et al., 2002; Lal and Tripathy, 2012; NPI, 2012). For in-pit roads of open coal mines, the formula 0.60*TSP has been suggested for PM_{10} estimation (USEPA, 1991). Modeling of PM_{10} emissions from gravel roads took into account truck mass, moisture, and silt content (NPI, 2001); moisture, silt content, and average vehicle speed (NPI, 2012) and silt content and truck mass (USEPA, 2006). For coal mine main haulage roads silt content and truck mass were considered (NPI, 2012). On a stabilized road, an equation of $0.1*PM_{10}$ is introduced to estimate $PM_{2.5}$ emissions (USEPA, 2006). Air temperature, dew point temperature, station pressure, relative humidity, wind speed (including counter and side wind speed), moisture and silt + clay content of the road material, truck mass, number of wheels, and truck speed were used for TSP, PM_{10}, $PM_{2.5}$, and PM_{1} emission modeling in gypsum and limestone quarries (Duran, 2022). The moisture and silt content of the haul road material, truck mass, and vehicle speed are the most commonly used parameters for TSP emission models, while the counter and side wind speeds, air temperature, station pressure, relative humidity, dew point temperature, number of truck wheels, a specific coefficient, and silt+clay content are the least commonly used ones. Only truck mass was used to build PM15 emission models. For PM_{10} emission models, the highest value was obtained when truck mass and vehicle speed were taken into account, while the lowest value was reached by multiplying TSP with a certain coefficient. Air temperature, dew point temperature, station pressure, relative humidity, wind speed (including head and side wind speed), moisture and silt+clay content of road material, truck mass, number of truck wheels, and vehicle speed were all employed in PM2.5 and PM1 emission models (Figure 7).

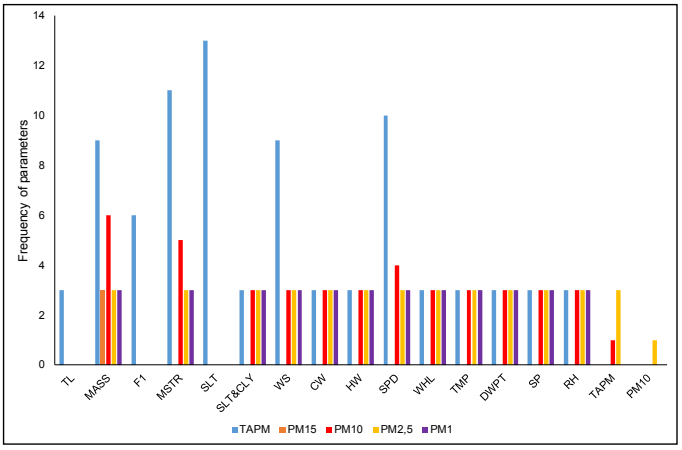

Figure 7. Parameters used in transport activity PM release estimates

3. Conclusions

In this paper, previous research has been compiled on the monitoring and the prediction of PM emissions considering basic open-pit mining activities such as drilling, blasting, loading, and hauling. 69.6% of the research on PM emission measurements and projections were conducted in coal mines, whereas only 30.4% were conducted in iron, manganese, copper mines, and gypsum and limestone quarries. Nevertheless, other than the open-pit mines mentioned above, no measurements of PM emissions have been reported in the literature. This requires that further researches should be carried out in other fields of mining than coal. The majority of the articles reviewed in this field measured PM_{10}, $PM_{2.5}$, and TSP emissions, with PM_{4} emissions being the least. In terms of quantification, 78.26% of the articles had measurements of PM_{10}, 56.52% of $PM_{2.5}$, 39.13% of TSP, 30.43% of PM_{1}, and 13.04% of PM_{4}. Other emission rates were also estimated and the equations developed, primarily utilizing TSP and PM_{10} data. Similar to PM emission, a variety of brands and models of instruments were used to measure meteorological factors. It was found that, even for the same mining activity and for the same location, the equations used for PM emission prediction might create or produce different results. Therefore, it would be appropriate to design or develop prediction models that are unique to the mine in question.

Nomenclature

A	: blasting area (ft^2, m^2)
BC	: Loader bucket volume (m^3)
c	: Constant
CW	: Side wind speed (m/s)
D	: Blasting hole length (ft, m)
DWPT	: Dew point temperature (°C)
D2	: Hole diameter (mm)
F	: Drilling frequency (number of holes/day
F1	: Vehicle frequency (number/hour)
H	: Material unloading height (ft, m)
HW	: Headwind speed (m/s)
MASS	: Truck mass (t)
MSTR	: Moisture content (% mass)
RH	: Relative humidity (%)
SLT	: Silt content (%)
SLT&CLY	: Silt content (%)
SP	: Station pressure (mb)
SPD	: Truck speed (km/h)
TMP	: Air temperature (°C)
TL	: Truck capacity (t)
WHL	: Number of truck wheels (pieces)
WS	: Wind speed (m/s)
X	: Upload frequency (number/hour)

References

Amaral, S.S., Andrade de Carvalho Jr. J., Martins Costa, M. A., Pinheiro, C., 2015. An overview of particulate matter measurement instruments, Atmosphere 6, doi:10.3390/atmos6091327, 1327-1345.

Aneja, P. V., Isherwood, A., Morgan, P., 2012. Characterization of particulate matter (PM10) related to surface coal mining operations in Appalachia. Atmospheric Environment, 54, 496-501.

Axetell, K., Cowherd, C. 1984. Improved emission factors for fugitive dust from western surface coal mining sources. Industrial Environmental Reearch Laboratory, U.S. Environmental Protection Agency, 293p, Cincinnati.

Badu, A., 2014. Dust monitoring, characterization and prediction in an opencast coal mining project, Department of Mining Engineering National Institute Of Technology Rourkela. Erişim adresi: http://ethesis.nitrkl.ac.in/6191/1/110MN0629-11.pdf

Baumann, R., Krzyzanowski, M., Chicherin, S., 2006. Framework plan for the development of monitoring of particulate matter in EECCA, Who European Centre For Environment And Health, Bonn, pp, 40.

Beloconi, A., Chrysoulakisc, N., Lyapustind, A., Jürg Utzinger, J., Vounatsou, P. 2018. Bayesian geostatistical modelling of PM10 and PM2,5 surface level concentrations in Europe using high-resolution satellite-derived products. Environment International, 121, 57-70.

Bui, X-N., Lee, C.W., Nguyen, H., Bui, H-B., Long, N.Q., Le, Q-T., Nguyen, V-D., Ngoc-Bich Nguyen, N-B., Moayedi, H., 2019. Estimating PM_{10} concentration from drilling operations in open-pit mines using an assembly of SVR and PSO. Applied Sciences, 9(14), 1-23. doi:10.3390/app9142806.

Castellani, B., Morini, E., Filipponi, M., Nicolini, A., Palombo, M., Cotana, F., Rossi, F., 2014. Comparative Analysis of Monitoring Devices for Particulate Content in Exhaust Gases, Sustainability, 6, doi:10.3390/su6074287, 4287-4307.

Chakraborty, M.K., Ahmad, M., Singh, R. S., Pal, D., Bandopadhyay, C. and Chaulya, S. K., 2002. Determination of the emission rate from various opencast mines operations. Environmental Modelling & Software. 17 (5), 467–480. doi: https://doi.org/10.1016/S1364-8152(02)00010-5.

Chaulya, S.K., 2006. Emission rate formulae for surface iron ore mining activities. Environmental Modeling Assessment, 11, 361–370. doi: https://doi.org/10.1007/s10666-005-9026-2.

Choudhary, M. P., Garg, V. 2013. Causes, Consequences and Control of Air Pollution, Conference: All India Seminar on Methodologies for Air Pollution Control at: Malaviya National Institute of Technology, Ağustos, 1-10, Jaipur.

Duran, Z., 2022. Particulate matter emission measurement and modeling of variation in some surface mines with meteorological conditions, material and heavy mining equipment properties, Sivas Cumhuriyet University, PhD thesis, 360p, Sivas.

Environment Agency 2011. Technical guidance note (monitoring) m8, monitoring ambient air. Environment Agency, 79p, London.

EPA, 1999. Sampling of ambient air for PM10 concentration using the Rupprecht and Patashnick (R&P) low volume partisol® sampler, U.S. Environmental Protection Agency, 40p, Cincinnati.

EPA, 2008. APTI 435: Atmospheric Sampling Course, Student Manual, https://www.apti-learn.net/LMS/register/my_documents.aspx?-searchText=APTI%20435 pp, 323.

Gautam, S., Patra, A. K., 2015. Dispersion of particulate matter generated at higher depths in opencast mines, Environmental Technology & Innovation 3 11–27, http://dx.doi.org/10.1016/j.eti.2014.11.002.

Gautam, S., Prusty, B. K., Patra, A. K., 2015. Dispersion of respirable particles from the workplace in opencast iron ore mines, Environmental Technology & Innovation 4 137–149, http://dx.doi.org/10.1016/j.eti.2015.06.002.

Giechaskiel, B., Maricq, M., Ntziachristos, L., Dardiotis, C., Wang, X., Axmann, H., Bergmann, A., Schindler, W., 2014. Review of motor vehicle particulate emissions sampling and measurement: From smoke and filter mass to particle number. Journal of Aerosol Science, 67, 48–86.

Grimm, H., Eatough, J.D., 2009. Aerosol Measurement: The Use of Optical Light Scattering for the Determination of Particulate Size Distribution, and Particulate Mass, Including the Semi-Volatile Fraction, Air & Waste Management Association, ISSN:1047-3289, 59, DOI:10.3155/1047-3289.59.1.101, 101–107.

Harrison D., Maggs, R., Booker, J., 2006. UK Equivalence Programme for Monitoring of Particulate Matter, Final Report for: Department for the Environment, Food and Rural Affairs; Welsh Assembly Government; Scottish Executive; Department of Environment for Northern Ireland, Ref: BV/AQ/AD202209/DH/2396, pp, 126.

Hendryx, M., Islam, M.S., Dong, G.H., Paul, G., 2020. Air pollution emissions 2008–2018 from Australian coal mining: Implications for public and occupational health. Int. J. Environ. Res. Public Health, 17, 1570. [Google Scholar] [CrossRef] [PubMed][Green Version].

Huertas, J, I., Huertas, M, E., Cervantes, G., Diaz, J., 2014. Assessment of the natural sources of particulate matter on the opencast mines air quality. Science of the Total Environment, 493, 1047-1055. http://dx.doi.org/10.1016/j.scitotenv.2014.05.111.

Kahraman, M.M., Erkayaoğlu, M., 2021. A data-driven approach to control fugitive dust in mine operations. Min. Metall. Explor, 38, 549–558.

Kamyotra, J.S., 2012. Guidelines for the Measurement of Ambient Air Pollutants Volume-I, Central Pollution Control Board Ministry of Environment & Forests, Parivesh Bhawan, East Arjun Nagar, Delhi,

Kim, K., Ehsanul Kabir, E., Kabir, S. 2015. A review on the human health impact of airborne particulate matter. Environment International, 74, 136-143.

Kishore, K., 2015. Ambient air quality modelling using Aermod and particulate matter characterization in opencast mines. National Institute of Technology Department of Mining Engineering (MTech Thesis), 69p, Rourkela.

Lal, B. and Tripathy, S.S., 2012. Prediction of dust concentration in open cast coal mine using artificial neural network. Atmos. Pollut. Res. 3, 211–218. doi: https://doi.org/10.5094/APR.2012.023.

Lashgari, A. and Kecojevic, V., 2015. Comparative analysis of dust emission of digging and loading equipment in surface coal mining, International Journal of Mining, Reclamation and Environment, 30 (3). 181-196, doi: https://doi.org/10.1080/17480930.2015.1028516.

Li, Q-F., Wang-Li, L., Liu, Z., Heber, A.J., 2012. Field evaluation of particulate matter measurements using tapered element oscillating microbalance in a layer house, Journal of the Air & Waste Management Association, 62:3, DOI: 10.1080/10473289.2011.650316, 322-335.

Luo, H., Zhou, W., Jiskani, I. M., and Wang, Z., 2021. Analyzing characteristics of particulate matter pollution in open-pit coal mines: implications for green mining, Energies, 14, 2680. https://doi.org/10.3390/en14092680.

Mojala, S.K., Prasad, K.M., Sekhar, N.S.S., 2017. Air quality monitoring in iron ore mining site, International Journal for Research in Applied Science & Engineering Technology (IJRASET), ISSN: 2321-9653; Volume 5 Issue VIII, 2177-2182.

Nagesha, K.V., Sastry V.R. and Ram, C. K., 2016. Prediction of dust dispersion during drilling operation in open cast coal mines: A multi regression model, International Journal of Environmental Sciences, 6 (5), 681-696. doi: https://doi.org/10.6088/ijes.6064.

Ngo, N. D., Lee, J., Kim, M-W., Jang, J., 2019. Measurement of PM2.5 Mass Concentration Using an Electrostatic Particle Concentrator-Based Quartz Crystal Microbalance, IEEE Access 7, DOI: 10.1109/ACCESS.2019.2955377, 170640-170647.

Nosratabadi, A. R., Graff, P., Karlsson, H., Ljungman, A. G., Leanderson, P., 2019. Use of TEOM monitors for continuous long-term sampling of ambient particles for analysis of constituents and biological effects, Air Quality, Atmosphere & Health, 12, https://doi.org/10.1007/s11869-018-0638-5, 161–171.

NPI, 2001. Emission estimation technique manual for mining-Version 2.3, Australian Government, 69p, Canberra.

NPI, 2012. Emission estimation technique manual for mining-Version 3.1, Australian Government, 72p, Canberra.

NSAI, 2012. Workplace exposure - guide for the use of direct-reading instruments for aerosol monitoring - Part 3: evaluation of airborne particle concentrations using photometers. National Standards Authority of Ireland, 24p, Dublin.

Nussbaumer, T., Czasch, C., Klippel, N., Johansson, L., Tullin, C. 2008. Particulate emissions from biomass combustion in IEA countries. In Proceeding of the 16th European Biomass Conference and Exhibition, Zurich, Switzerland, 2–6 June; p. 40.

NZG, 2009. Good Practice Guide for Air Quality Monitoring and Data Management 2009, Ministry for the Environment, Manatū Mō Te Taiao PO Box 10362, Wellington 6143, New Zealand, ISBN: 978-0-478-33166-0 (print), 978-0-478-33167-7(electronic), Publication number: ME 933, pp, 105.

O'Connor, S., O'Connor, P. F., Feng, H.A., Ashley, K., 2014. Gravimetric analy-

sis of particulate matter using air samplers housing internal filtration capsules, Gefahrstoffe Reinhaltung der Luft, 74(10): 403–410.

Oudwater, S.A., 2017. Modeling of dust emission in dimension stone quarry, Master's Thesis, European Mining, Minerals and Environmental Programme, 77p.

Patra, A. K., Gautam, S. and Kumar, P., 2016. Emissions and human health impact of particulate matter from surface mining operation - A review, Environmental Technology & Innovation, 5, 233-249. doi: https://doi.org/10.1016/j.eti.2016.04.002

Pfeiffer, R.L., 2005. Sampling for PM10 and PM2.5 Particulates, U.S. Department of Agriculture: Agricultural Research Service, Lincoln, Nebraska, pp, 20.

Pilling, M., ApSimon, H., Carruthers, D., Carslaw, D., Colvile, R., Derwent, D., Dorling, S., Fisher, B., Harrison, R., Heal, M., Laxen, D., Lindley, S., McCrae, I., Stedman, J., 2005. Particulate Matter in the United Kingdom, Department for the Environment, Food and Rural Affairs Nobel House 17 Smith Square, London, Product code PB10580 ISBN 0-85521-143-1, pp, 444.

Richardson, C., Rutherford, S., Agranovski E, I., 2018. Characterization of particulate emissions from Australian open-cut coal mines: Toward improved emission estimates. Journal of the Air & Waste Management Association. VOL. 68, NO. 6, 598–607, https://doi.org/10.1080/10962247.2017.1415236.

Richardson, C., Rutherford, S., Agranovski E, I., 2019. Open cut black coal mining: Empirical verification of PM2.5 air emission estimation techniques. Atmospheric Research, 216, 151-159. https://doi.org/10.1016/j.atmosres.2018.10.008.

Sastry, V.R., Chandar, K. R., Nagesha, K.V., Muralidhar, E., Mohiuddin, M.S., 2015. Prediction and Analysis of Dust Dispersion from Drilling Operation in Opencast Coal Mines, Procedia Earth and Planetary Science 11, 303-311, doi: 10.1016/j.proeps.2015.06.065.

Sahu, S. P., Yadav, M., Rani, N., Das, A. J., 2018. Assessment of occupational health exposure to particulate matter around opencast coal mines, India: a case study. Arabian Journal of, Geosciences, 11(373), 1-11. https://doi.org/10.1007/s12517-018-3631-2.

THHP, 2019. Hava kirliliği ve sağlik etkileri kara rapor. Temiz Hava Hakkı Platformu, 67s, İstanbul.

Tripathy, D. P., Dash, T, R., Badu, A. and Kanungo, R., 2015. Assessment and modelling of dust concentration in an opencast coal mine in India, Global Nest Journal, 17 (4), 825-834. doi: https://doi.org/10.30955/gnj.001611.

Tripathy, D. P. and Dash, T, R., 2019. Measurement of respirable dust concentration and assessment of health risk due to metals around an opencast coal mine of Talcher, Odisha, GEOFIZIKA, 36 (1), 77–106. doi: https://doi.org/10.15233/gfz.2019.36.2.

TSE EN 12341 2014. Ortam havası - askıdaki tanecikli maddenin PM10 veya PM2,5 kütle derişimlerinin tayini için standart gravimetrik ölçme yöntemi. Türk Standartları Enstitüsü, Ankara.

USEPA, 1991. Review of Surface Coal Mining Emissions Factors. U.S. Environmental Protection Agency, Office of Air Quality Planning and Standards, Research Triangle Park, North Carolina, 144 pp.

USEPA, 1995. (United States Environmental Protection Agency), AP-42 Compilation of Air Pollutant Emission Factors, Introduction, North Carolina.

USEPA, 1998. Revision of emission factors for AP-42 Section 11.9 Western surface coal mining. Revised final report, MRI Project No. 4604-02; Emission Factor and Inventory Group, Office of Air Quality Planning and Standards, US Environmental Protection Agency, pp, 350.

USEPA, 2006. Revision of Emission Factors for AP-42. Chapter 13: Miscellaneous Source. Section 13.2.4: Aggregate Handling and Storage Piles, 6 pp.

Vincent, J.H., 2007. Aerosol Sampling: Science, Standards, Instrumentation and Applications; JohnWiley & Sons: Hoboken, NJ, USA.

Wanjun, T., Qingxiang, C., 2018. Dust distribution in open-pit mines based on monitoring data and fluent simulation, Environ Monit Assess, 190: 632 https://doi.org/10.1007/s10661-018-7004-9.

Whalley, J., Zandi, S., 2016. Particulate Matter Sampling Techniques and Data Modelling Methods, Chapter 2, http://dx.doi.org/10.5772/65054, pp, 27.

Winkel, A., Demeyer, P., Feilberg, A., Jørgensen, M., Puterflam, J., Engel, P., 2014. Measurement of particulate matter: recommendations for the VERA test protocol on air cleaning Technologies, Livestock Research Report 797, pp, 38.

Url-1 <https://www.thermofisher.com/tr/en/home/industrial/environmental/environmental-learning-center/air-quality-analysis-information/teom-technology-particulate-matter-measurement.html> acessed on: 21.11.2023.

Url-2 <https://en.wikipedia.org/wiki/Tapered_element_oscillating_microbalance> acessed on: 21.11.2023.

Url-3 <https://metone.com/products/bam-1020/> acessed on: 23.11.2023.

Url-4 <https://en.wikipedia.org/wiki/Beta_attenuation_monitoring> acessed on: 23.11.2023.

Url-5 <https://infostore.saiglobal.com/preview/98705579385.pdf?sku=857774_SAIG_NSAI_NSAI_2040554> acessed on: 23.11.2023.

Madencilik - Mining, 2024, 63(1), 31-40

BİLİMSEL MADENCİLİK DERGİSİ
SCIENTIFIC MINING JOURNAL

TMMOB Maden Mühendisleri Odası Yayını / The Publication of the Chamber of Mining Engineers of Turkey

www.mining.org.tr

Original Research

Role of Inorganic Materials on Oil Agglomeration of Zonguldak Bituminous Coal Dust

Kemal Şahbudak[a,*], Yakup Cebeci[b,*]

[a] *Sivas Cumhuriyet University, Department of Metallurgical and Materials Engineering, Sivas, TÜRKİYE*
[b] *Sivas Cumhuriyet University, Department of Chemical Engineering, Sivas, TÜRKİYE*

Received: 6 July 2023 • Accepted: 28 January 2024

A B S T R A C T

This study investigates the oil agglomeration method which has significant importance for achieving high recovery and cost-effectiveness in utilizing energy resources. This method is particularly relevant for resources that pose environmental challenges due to their fine particle size or low quality, such as oxidized coal with large reserves. This research examines the effects of various factors, i.e. type of inorganic pretreatment material, proportion of bridging liquid, duration of agglomeration and mixing speed, on the efficiency of oil agglomeration in the beneficiation of Zonguldak coal dust, which has a low ash content of 2.23%. In the experiments, kerosene serves as the bridging liquid, and various inorganic pretreatment materials, including NaCl, $FeCl_2$, $Fe_2(SO_4)_3$ and $Al_2(SO_4)_3$, are tested. The experiments revealed that when inorganic pretreatment materials were combined with kerosene, the maximum agglomeration recovery of 81.6% was achieved at kerosene concentration of 15%, mixing speed of 800 rpm, and agglomeration time of 10 minutes. The agglomeration recovery was found to be 71.5% when using only kerosene under suitable conditions, but it varied between 78.3% and 81.6% when pretreatment materials were combined with kerosene. Among the inorganic pretreatment materials, the highest recovery was obtained with the use of 50 mg/L $Fe_2(SO_4)_3$ in combination with kerosene. Furthermore, the optimum agglomeration recovery obtained with only kerosene could be achieved in a shorter agglomeration time when inorganic pretreatment materials were used together with kerosene.

Keywords: *Bituminous coal. Bridging liquid. Coal dust. Kerosene. Oil agglomeration.*

Introduction

Today, the recovery of coal dust through cleaning and increasing the quality of coal becomes imperative along with developing technology due to both economic reasons and environmental issues. Excessive fragmentation of Zonguldak coals due to their brittle structure and applied production methods significantly increases plant losses in the fine size fractions. Of the raw coal produced in the basin, according to the enterprises, 15-30% constitutes 1 mm size coals, which can be referred to as fine coal. For this reason, the significance of fine coal enrichment increases significantly (Hacıfazlıoğlu, 2013).

The beneficiation of fine coal in coal washing plants is performed with the help of some new technology devices such as coal spirals, flotation machines, feldspar jigs, shaking tables, water cyclones, multi-gravity separators, teetered-bed separators and reflux classifiers. Heavy media beneficiation method, which is based on the density difference between coal and mineral matter, is one of the most widely used methods in coal beneficiation plants (Abbott and Miles, 1991; Aktaş, 1993; Özbayoğlu and Mamurekli, 1994; Aktaş and Woodburn, 1995; Aktaş et al., 1998; Çelik, 2002; Çelik, 2006; Yüce et al., 2009). The ash content in the floating part of the coal obtained in the beneficiation process performed with heavy media separation is equivalent to the maximum amount of mineral matter that can be removed (Flynn and Woodburn, 1987; Stockton, 1989; Aktaş, 1993; Aktaş et al., 1998; Ünal et al., 2000). On the other hand, in the heavy media beneficiation method, the recovery decreases at fine sizes, and especially the recovery of coals at sizes finer than 0.5 mm becomes quite difficult (Kemal and Arslan, 2000).

Due to the inadequacy of traditional gravity methods for fine coal beneficiation, methods like flotation, selective flotation, and oil agglomeration, which leverage the physicochemical surface properties of mineral grains, are becoming increasingly important (Cebeci and Sönmez, 2002). Flotation is a beneficiation method that is widely used in cleaning coal dust and is performed by utilizing the differences in surface properties of organic and inorganic components of coal. However, in the flotation process of oxidized coals under 0.074 mm size and coal dusts with high clay content, various technical and economic problems arise, such as high moisture in the clean coal filter cake, low recovery and poor selectivity (Aktaş, 2002).

* Corresponding author: ksahbudak@cumhuriyet.edu.tr • https://orcid.org/ 0000-0003-4853-6843
** ycebeci@cumhuriyet.edu.tr • https://orcid.org/0000-0001-5344-8392

https://doi.org/10.30797/madencilik.1404703

In the field of beneficiation studies; the flocculation method, which is used to regulate the distribution of very fine-sized coal particles (<0.15 mm) in suspension, is not economically viable (Hacıfazlıoğlu, 2013; Şahinoğlu, 2006) and the oil agglomeration method holds significant importance in terms of high recovery and low cost, particularly for the utilization of our energy resources that pose environmental challenges due to their fine particle size or for our low-quality oxidized coal resources with substantial reserves. The oil agglomeration method is a beneficiation technique capable of selective separation by exploiting differences in the surface properties of minerals associated with raw coal (-0.5 mm) or finely ground (<0.074 mm) intermediate products. Furthermore, oil agglomeration is an efficient process that can replace flotation in certain contexts, as it can reduce coal moisture in the form of oil agglomerates without the need for thermal drying, filtration or thermal dewatering. It also enables the cleaning of oxidized coals and the recovery of coal from coal washery residues (Nicol and Swanson, 1980; Guerra et al., 1986; Hazra et al., 1986; Hoşten and Uçbaş, 1989; Cebeci et al., 2002).

However, the major drawback of the oil agglomeration method is its high oil consumption (Kılınç, 2000). To mitigate this issue, recent studies have focused on optimizing the usage of oil and exploring alternative, more sustainable agglomerants that could potentially lower costs and reduce the environmental impact associated with oil agglomeration. The oil agglomeration method represents a critical advancement in coal beneficiation technologies, offering a promising approach for enhancing the utilization of coal as an energy resource. Its ability to address the specific challenges posed by fine and oxidized coals, combined with ongoing research aimed at improving its economic and environmental performance, underscores its potential as a key strategy in the sustainable management and utilization of coal reserves.

Oil agglomeration is a beneficiation method in which selective separation is performed by making use of the differences in the surface properties of coal and accompanying minerals (Kılınç, 2000). Coal consists of organic contents, inorganic compounds constituting ash and other mineral substances. Factors such as the carbon content percentage in coal, the presence of inorganic materials, and the level of carbonization influence the surface characteristics of coal, which in turn impacts its beneficiation process (Laskowski and Parfitt, 1988; Şahinoğlu, 2006; Gülsuna, 2007).

In the oil agglomeration method, fine hydrophobic coal particles are agglomerated with an oil containing hydrocarbons, and the obtained dispersion resistant agglomerates are taken from the liquid phase with a mechanical method. Hydrophilic mineral substances, on the other hand, remain in suspension in a dispersed state (Mehrotra et al., 1983; Capes and Darcovich, 1984; Capes, 1991). The separation of coal from the accompanying inorganic substances depends on the fact that both coal particles show sufficient natural hydrophobic characteristics and the oil selectively wets coal surfaces in appropriate conditions and forms spherical agglomerates by bridging particles (Capes and Germain, 1982; Slaghuis and Ferreira, 1987; Steedman and Krishnan, 1987; Petela, 1991; Shrauti and Arnold, 1995; Garcia et al., 1998; Laskowski and Yu, 2000; Düzyol, 2015).

The amount of bridging liquid strongly affects agglomerate structure, recovery of agglomerates and selectivity (Capes and Germain, 1982; Capes and Darcovich, 1984; Steedman and Krishnan, 1987; Petela, 1991), while also determining the size and appearance of agglomerates (Darcovich et al., 1989; Petela, 1991; Garcia et al., 1995; Alonso et al., 2002; Cebeci and Sönmez, 2002; Chary and Dastidar, 2010; Cebeci, 2003; Gence, 2006; Cebeci and Sönmez, 2006; Chary and Dastidar, 2013; Düzyol, 2015; Kumar et al., 2015). Agglomerants form smaller, rounder and more compact agglomerates in low concentrations, whereas larger, irregular and looser agglomerates are formed at higher concentrations (Cebeci, 2003).

Although oil agglomeration processes have been used since 1920, microscopic coal-oil-water interactions are still yet to be completely understood. This originates from the heterogeneous structure of coal, which consists of hydrophilic and hydrophobic regions (Keller and Burry, 1987; Özer et al., 2017). Coal agglomeration processes are based on the wettability difference between clean coal particles and mineral substance when coal is treated with an agglomerant or bridging agent such as light and heavy hydrocarbons or non-hydrocarbon oils. In fact, agglomeration is only possible when coal particles are hydrophobic enough to allow selective wetting with oil in place of water. Agglomeration is strongly dependent on petrography, structure, type, sequence and surface oxidation of coal in addition to agglomerant type and concentration. If the coal particle hydrophobicity is not sufficient, surface modification agents are usually added to the coal-water-oil slurry to enhance the agglomeration of clean coal particles. Besides, in some circumstances, surface active agents can be incorporated into the slurry to reduce the amount of agglomerant and oil needed in the process (Özer et al., 2017).

In the agglomeration experiments, kerosene was used as the bridging liquid because Zonguldak hard coal is bituminous coal. On the other hand, heavy oils are used in the agglomeration of coals such as sub-bituminous and lignite. Heavy oils characteristically comprise polar hydrophilic functional groups, such as nitrogen, oxygen and sulfur, and these groups promote adsorption on the relatively hydrophilic surfaces of coals to create agglomerates, whereas light oils with low density and viscosity are used in the agglomeration of bituminous coal (Capes, 1976). Light oils increase the probability of particle-oil droplets collision as they can be easily dispersed in the pulp through mixing (Capes, 1991; Ünal et al., 2000; Chary and Dastidar, 2010).

There are many studies in the literature regarding the effect of different processing factors, such as coal recovery, ash content, coal petrography and composition of agglomerates, coal particle size, pulp density, type and concentration of bridging liquid and mixing speed, on agglomeration performance in beneficiation by oil agglomeration (Capes and Germain, 1982; Mehrotra et al., 1983; Capes and Darcovich, 1984; Slaghuis and Ferreira, 1987; Steedman and Krishnan, 1987; Darcovich et al., 1989; Hoşten and Uçbaş, 1989; Capes, 1991; Petela, 1991; Yamık et al., 1994; Garcia et al., 1995; Shrauti and Arnold, 1995; Garcia et al., 1998; Kılınç, 2000; Laskowski and Yu, 2000; Ünal et al., 2000; Alonso et al., 2002; Cebeci and Sönmez, 2002; Cebeci, 2003; Cebeci and Sönmez, 2006; Gence, 2006; Ünal and Erşan, 2007; Chary and Dastidar, 2010; Kılınç Aksay et al., 2010; Uslu and Şahinoğlu, 2010; Düzyol et al., 2012; Chary and Dastidar, 2013; Düzyol, 2015; Kumar et al., 2015). The biggest disadvantage of oil agglomeration is high oil consumption. There exist a limited number of studies towards the use of surface active agents, which improve the hydrophobicity of coal and assist the oil to disperse in water, to reduce oil consumption and to obtain agglomerates with high quality in the agglomeration of dust coals (Kılınç Aksay et al., 2010).

This study involves the use of the floating part obtained from the beneficiation of hard coal from the Zonguldak-Kozlu region through heavy medium separation in oil agglomeration experiments. This research investigates the effects of variables such as bridging liquid concentration, agglomeration time, mixing speed, and the use of various inorganic pretreatment materials on recovery. This study presents significant methodological differences from similar works in the literature by emphasizing the importance of optimizing kerosene concentration and adjusting mixing speed and agglomeration time. Particularly, the maximum recovery (81.6%) achieved at 15% kerosene concentration and 800 rpm mixing speed demonstrates the critical impact of mixing speed on agglomeration efficiency. Additionally, the use of cleaned coal resulting in a homogeneous coal structure and low ash content has led to different outcomes compared to previous studies using raw

coal. These differences highlight that the efficiency of the agglomeration process can vary depending on the quality of the coal used and the processing conditions.

1. Materials and Methods

1.1. Materials

In the beneficiation studies using oil agglomeration method, the samples taken from the coal mine belonging to the Turkish Hard Coal Institution, Kozlu Hard Coal Enterprise were used. Raw coal was subjected to a float-sink operation in a heavy medium, formed from $ZnCl_2$ solution, at a density of 1.3 g/cm^3. The size reduction process was applied to the floating part using a jaw crusher and a ball mill. The sample obtained from the size reduction process was sieved with a 0.5 mm sieve, and the oversize was stored, while the undersize was used in oil agglomeration experiments. The flowchart followed in sample preparation is shown in Figure 1.

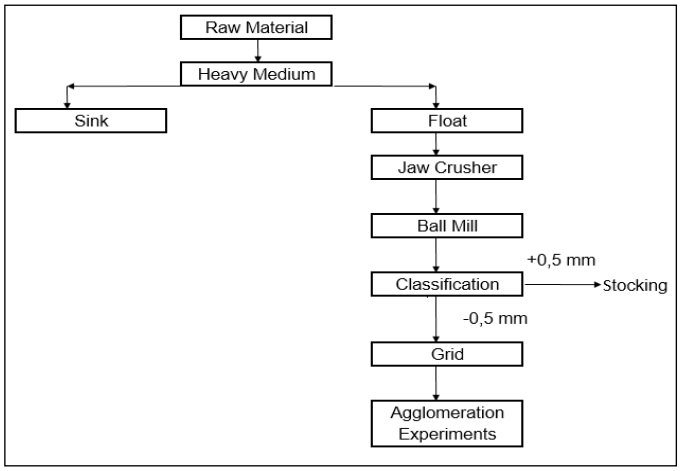

Figure 1. Sample Preparation Flowchart

Particle size analysis was performed on the coal sample prepared for agglomeration experiments. The particle size distribution curve of the coal used in the agglomeration experiments is given in Figure 2.

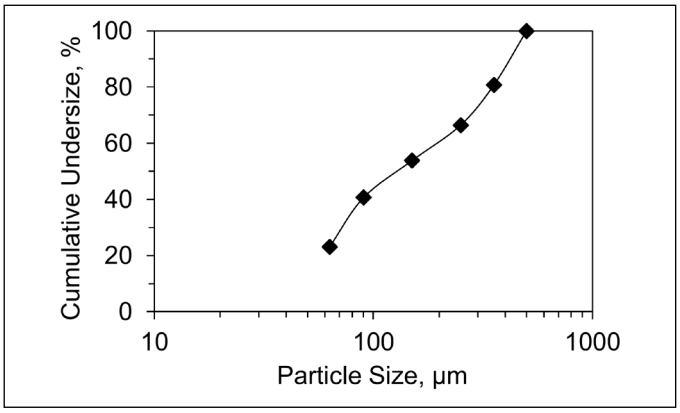

Figure 2. Particle Size Distribution of the Coal Sample

The chemical analyses of the coal used in the experimental studies were carried out using an IKA-Mag branded ash furnace for ash analysis, an IKA 4000 device for total calorific value analysis, and a LECO branded sulfur-carbon test device for sulfur analysis. The results of these analyses are given in Table 1.

Table 1. Chemical Analysis Results of the Coal Sample

Property	Value
Gross calorific value, cal/g	7790
Sulfur, %	0.30
Ash, %	2.23

In oil agglomeration experiments, kerosene (Sigma) with a density of 0.78 g/cm^3, viscosity of 1.5 cSt and 99% purity was used as the bridging liquid. The selection of inorganic pretreatment materials, NaCl, $FeCl_2$, $Fe_2(SO_4)_3$ and $Al_2(SO_4)_3$, all from Merck, was based on a literature-based evaluation of their effects on surface properties of coal particles and how these properties influence the oil agglomeration process. The inorganic pretreatment materials were chosen to enhance the hydrophobic properties of coal particles and to facilitate more effective agglomeration during the process. NaCl and $FeCl_2$ can interfere with the agglomeration process by affecting the electrical charge distribution on coal surfaces, whereas $Fe_2(SO_4)_3$ and $Al_2(SO_4)_3$ promote the formation of hydrophobic areas on the surface, easing the interaction between oil droplets and coal particles. These inorganic pretreatment materials were selected with the aim of better understanding the mechanisms behind coal agglomeration and enhancing the effectiveness of the oil agglomeration method in coal beneficiation technologies.

1.2. Methods

Agglomeration experiments were carried out in a 50 mL beaker in which three 2 cm wide plates were present. In addition, an IKA RW-20 stirrer was used for mixing, and the mixing was ensured by a propeller with four blades having 5 cm diameter and 1 cm width, and held 1 cm above bottom of the beaker.

The experiments were conducted using 10 g coal at 10% solids ratio. A conditioning time of 5 minutes was allowed in all experiments before adding the bridging liquid. The sample obtained at the end of the experiments was sieved with a 0.710 mm sieve, and the oversize fraction was taken as the agglomerate. The agglomerates obtained were dried in an oven at 105 °C after being subjected to the cleaning process. The agglomeration recovery was determined as the ratio of the mass of agglomerate to the mass of coal fed. This recovery was employed in the evaluation of experimental results.

In the experiments in which only kerosene was used, the bridging liquid in the ratios of 2, 4, 8, 12, 15, 20, 30, and 40% were used. In the experiments carried out with only inorganic pretreatment materials, 25, 50, 250, 500, and 1000 mg/L pretreatment materials were added to the system. The agglomeration time of 10 min was given in the these experiments.

In the experiments conducted with only kerosene; when the effect of agglomeration time on the recovery was examined, the bridging liquid in the ratios of 5, 10 and 15% were incorporated to the system, and the agglomeration times of 1, 5, 10 and 15 min were applied for each ratio; in investigating the effect of mixing speed on the recovery, kerosene in the ratios of 5, 10 and 15% was added at the mixing speeds of 300, 600 and 1200 rpm, and 10 minutes of agglomeration time was allowed.

In the experiments in which inorganic pretreatment materials and kerosene were used together, a conditioning time of 5 min was given after the addition of the pretreatment materials to the system, then kerosene in the ratio of 15% was incorporated, and the agglomeration time of 10 min was applied. In these experiments, when the effect of agglomeration time on the recovery was investigated, after the addition of 5, 50 and 150 mg/L NaCl and $Fe_2(SO_4)_3$ as the pretreatment material, 5 min conditioning time was used, afterwards the bridging liquid in the ratio of 15% was incorporated to the system, and the agglomeration times of 1, 5,

10 and 15 min were given for each amount of the pretreatment materials.

In the preliminary agglomeration experiments conducted at various pH levels (3, 5, 7, 8, 10, 12) using only coal and kerosene, the effect of pH on agglomeration recovery was investigated. The highest agglomeration recovery was observed between pH 7.3 and pH 8, with recovery decreasing as the pH increased. In this study, the optimal pH value was determined to be 7.7. This represents the pH range that optimizes interaction in the agglomeration process, thereby achieving maximum recovery.

2. Results and Discussion

2.1. Agglomeration Experiments Conducted with Only Kerosene

2.1.1. Effect of Kerosene Concentration on Recovery

In the experiments in which only kerosene was used, the bridging liquid in the concentration of 2, 4, 8, 12, 15, 20, 30 and 40% were used, and the agglomeration time of 10 min was given. The recovery values obtained in the agglomeration experiments conducted with the use of kerosene only are illustrated in Figure 3.

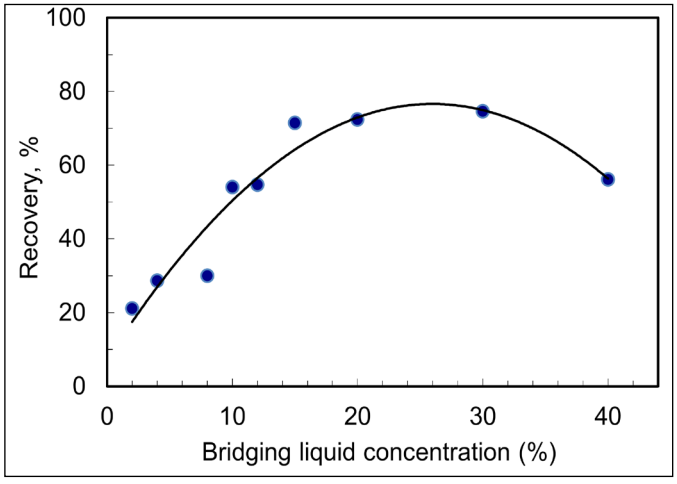

Figure 3. Recovery Variation Depending on the Bridging Liquid Concentration

The investigation of experimental data presented in Figure 3 reveals a complex interplay between the concentration of the bridging liquid and its impact on the efficiency of coal recovery via agglomeration. It was observed that recovery rates progressively increased with the concentration of bridging liquid up to 25% and beyond this point, a significant reduction in recovery was noted. This reduction at higher concentrations primarily results from spherical agglomerates transforming into less coherent, paste-like structures. These structures tend to form bulkier clusters, which diminish their structural integrity under mechanical stress (Capes and Jonasson, 1988; Hacıfazlıoğlu, 2008; Aslan and Ünal, 2011). Sub-optimal concentrations resulted in the formation of loose flocs due to insufficient oil coverage around the coal particles. This led to an increased presence of water within the agglomerates, making them prone to easy breakdown during operations, such as sieving or washing (Nicol and Swanson, 1980; Cebeci and Sönmez, 2006). Crucially, optimal agglomeration efficacy is achieved with a careful application of oil, typically maintained between 10% and 50% of the mass of coal (Hacıfazlıoğlu, 2008). Excessive application of oil was found to be detrimental to recovery, leading to the conversion of agglomerates into oil sludge and causing coal particles to form non-cohesive, paste-like flocs in an oil-rich environment (Özer et al., 2017).

Additionally, insights from experiments utilizing only kerosene have revealed that although a 25% concentration of the bridging liquid facilitated high recovery rates, the formed agglomerates exhibited irregularities and compromised durability against mechanical forces. Conversely, a 15% concentration produced denser, more spherically shaped agglomerates with superior resistance to breakage. This emphasizes the necessity of finely tuning the concentration of the bridging liquid to foster the formation of agglomerates with optimal physical characteristics and stability, highlighting the intricate balance essential in the agglomeration process to maximize coal recovery efficiency.

The findings of the study reveal that the agglomeration process achieves its highest recovery (71.5%) at a kerosene concentration of 15%, and the recovery decreases when this concentration is exceeded. Using clean coal resulted in a more homogeneous coal structure and lower ash content, differing from the results obtained with raw coal used in the study by Cebeci et al. (2002). These differences indicate that the impact of kerosene concentration on agglomeration recovery can vary depending on the quality of the coal used.

2.1.2. Effect of Agglomeration Time on Recovery

In the experiments that used only kerosene to investigate the effect of agglomeration time on recovery, bridging liquid concentrations of 5%, 10%, and 15% were added to the system. Agglomeration times of 1, 5, 10, and 15 minutes were applied for each concentration.The effect of agglomeration time on the recovery in different kerosene concentrations is shown in Figure 4.

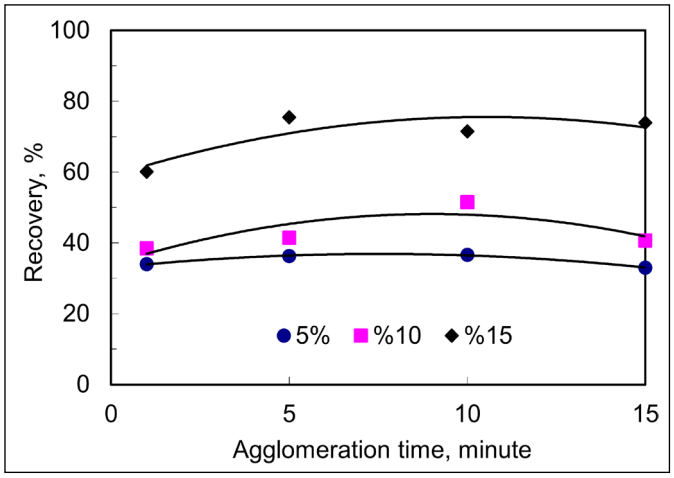

Figure 4. Effect of Agglomeration Time on Recovery at Kerosene Concentrations of 5, 10 and 15%

As shown in Figure 4, with a 15% concentration of the bridging liquid, the recovery increased from 60% to 71.5% as a result of mixing for 1 and 10 minutes, respectively. This increase in recovery was attributed to the increased likelihood of particle-oil, particle-particle and particle-microagglomerate contacts, resulting in agglomerates that were more stable, contained less water, and were more spherical.The maximum recovery (71.5%) was reached at the end of the 10 min mixing time. A slight downward trend in recovery was observed when the mixing time increased from 10 to 15 minutes. This decrease in recovery may be attributed to the agglomerates, having reached a certain size, being partially fragmented by rubbing against each other and the beaker wall. Furthermore, it was observed that the agglomerates had a looser structure, as particle-oil contacts and attachments were reduced at shorter mixing times. Similar results were reported by Osborne (1988), Uçbaş et al. (1997), Hacıfazlıoğlu (2008), Şahino-

glu and Uslu (2008), Chary and Dastidar (2010) and Shukla and Venugopal (2019). Analysis of Figure 4 indicated that the optimal agglomeration time was 10 minutes.

The results of this study, compared to those of Cebeci et al. (2002), highlight significant differences in the effect of agglomeration time. Experiments conducted with clean coal achieved the highest agglomeration recovery at a kerosene concentration of 15%, with increases in this concentration negatively affecting the recovery. The maximum recovery value (71.5%) was reached within a mixing time of 10 minutes, whereas in the study of Cebeci et al. (2002) using raw coal, this duration was determined to be 15 minutes. This difference demonstrates that the efficiency of the agglomeration process varies depending on the quality of the coal used and the processing conditions. The use of clean coal, resulting in a more homogeneous and lower ash content structure, has led to different outcomes compared to previous studies that utilized raw coal.

2.1.3. Effect of Mixing Speed on Recovery

To investigate the effect of mixing speed on recovery, kerosene at different concentrations (5%, 10%, and 15%) was added to the system at mixing speeds of 300, 600, and 1200 rpm, with an agglomeration time of 10 minutes for each. The impact of mixing speed on recovery, in experiments utilizing only kerosene, is illustrated in Figure 5.

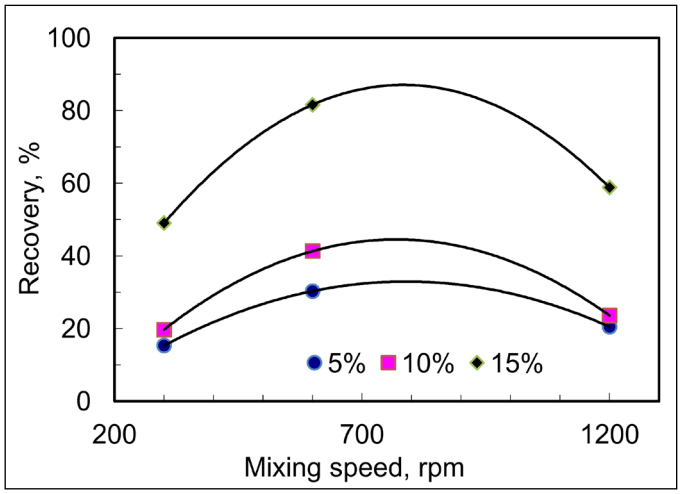

Figure 5. Recovery Variation with Mixing Speed at Kerosene Concentrations of 5, 10 and 15%

Analysis of Figure 5 shows that at a 15% bridging liquid concentration, increasing the mixing speed from 300 rpm to 800 rpm raised the recovery rate from 49% to 81.6%. However, further increasing the speed to 1200 rpm reduced the recovery to 58.8%. The diminished recovery at lower speeds is attributed to the inadequate dispersion of oil in the pulp and reduced collisions among oil-coated particles (Bhattacharyya et al., 1977; Coleman et al., 1995; Aslan and Ünal, 2011). As the mixing speed increases, the bridging liquid more effectively coats particle surfaces, enhancing the likelihood of collisions between oil-coated particles and thus improving recovery. The decline in recovery beyond a critical mixing speed is due to high shear and turbulence (Yu, 1998), uneven distribution of oil droplets (Capes and Germain, 1982; Coleman et al., 1995), and collisions of coal-oil agglomerates with each other and the beaker walls at high speeds (Cebeci and Sönmez, 2002; Kumar et al., 2015). The literature indicated that agglomeration recovery increases with mixing speed up to a critical point, beyond which it decreases (Cebeci and Sönmez, 2006; Gence, 2006; Şahinoğlu and Uslu, 2008; Aslan and Ünal, 2011; Duzyol, 2015; Özer et al., 2017). Upon reviewing Figure 5, the optimal mixing speed was identified as 800 rpm.

2.2. Agglomeration Experiments Conducted with Only Inorganic Pretreatment Materials

The agglomeration recovery values obtained from agglomeration experiments conducted using only inorganic pretreatment materials indicated that, in the absence of kerosene as a bridging liquid, the effectiveness of all tested inorganic pretreatment materials in coal agglomeration was negligible, with agglomeration efficiencies being less than 1%. This outcome underscores the critical role of bridging liquids in facilitating agglomeration, as inorganic pretreatment materials alone, without the presence of a bridging agent, fail to achieve significant dispersion on particle surfaces or to exhibit bridging properties.

2.3. Agglomeration Experiments Conducted with Inorganic Pretreatment Materials and Kerosene

In the experiments in which inorganic pretreatment materials and kerosene were used together, after the addition of the pretreatment material, a conditioning time of 5 min was allowed, then kerosene in the concentration of 15% was added to the system and 10 min agglomeration time was given.

2.3.1. Agglomeration Experiments Conducted with $Al_2(SO_4)_3$ and Kerosene

The recovery values obtained as a result of the oil agglomeration experiments conducted with $Al_2(SO_4)_3$ were given Figure 6. An increase in $Al_2(SO_4)_3$ concentration to 50 mg/L led to an enhanced recovery, after which a slight decrease was observed. The initial recovery improvement at lower concentrations can be attributed to electrostatic attractions facilitating better cohesion among coal particles and their interaction with oil droplets. In contrast, at higher concentrations, electrostatic repulsion may have impeded effective agglomeration due to the partial surface coating of coal particles with $Al(OH)_3$, thereby preventing direct contact between oil droplets and coal surfaces.

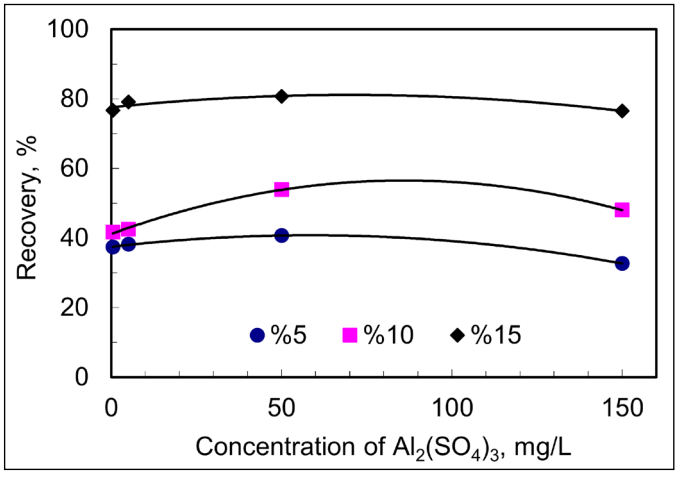

Figure 6. Recovery Variation with respect to $Al_2(SO_4)_3$ Concentration (Kerosene concentration: 5, 10 and 15%; pH=7.5)

These observations align with previous research indicating that $Al_2(SO_4)_3$, among other salts, influences the electrokinetic properties of coal and oil droplets, affecting their interactions and, ultimately, the efficiency of the agglomeration process. Notably, this study observed a 12.9% increase in recovery with 50 mg/L $Al_2(SO_4)_3$ at a 15% bridging liquid concentration, highlighting the

nuanced role of inorganic pretreatment materials in optimizing the agglomeration process.

Furthermore, salts such as $Al_2(SO_4)_3$, $CaCl_2$, NaCl, and $FeSO_4$ have been shown to impact the zeta potential of oil droplets (Wen and Sun, 1981; Gurses et al., 1997). The ions $Al(OH)_2^+$ and $Al(OH)_4^-$ are found to affect the electrokinetic potential of coal particles and oil droplets (Özbayoglu, 1980; Cebeci et al., 2002), contributing directly to the agglomeration process's efficiency. This study underscores the importance and potential effects of using inorganic pretreatment materials in the agglomeration process, providing detailed insights into their contribution to the field of coal beneficiation technologies.

In this study, the use of clean coal resulted in an increase in agglomeration recovery with the increase of $Al_2(SO_4)_3$ concentration up to 50 mg/L, followed by a subsequent decrease. This indicates that electrostatic attractions facilitated better cohesion among coal particles and their interaction with oil droplets. In contrast, the study by Cebeci et al. (2002), which used raw coal, reported a decrease in combustible recovery with the increase of $Al_2(SO_4)_3$ concentration up to 75 mg/L, but then observed a partial increase. This difference highlights the effects of the type of coal used (clean coal vs. raw coal) on the agglomeration process and the role of inorganic pretreatment materials. Both studies underscore the complexity of $Al_2(SO_4)_3$'s impact on the agglomeration process and the significance of the coal type used.

2.3.2. Agglomeration Experiments Conducted with $Fe_2(SO_4)_3$ and Kerosene

The recovery values obtained as a result of the oil agglomeration experiments in which $Fe_2(SO_4)_3$ was used as the inorganic premateriał are illustrated in Figure 7. As seen in Figure 7, similar to the trend observed in $Al_2(SO_4)_3$ experiments, an increase in recovery was noted with the concentration of $Fe_2(SO_4)_3$ up to 50 mg/L, followed by a slight decrease. The increase in recovery at low concentrations can be attributed to the enhanced hydrophobicity of coal particles due to the adsorption of Fe^{3+} ions on their surface. Conversely, the decrease in recovery at high concentrations may be linked to the obstruction of oil droplets contact with coal particles, presumably because the $Fe(OH)_3$ compound, believed to be present in the medium, partially coats the coal particle surface. Similar findings have been reported in studies by Butler (1964), Özbayoğlu (1987) and Cebeci et al. (2002). Evaluating the results from agglomeration experiments with $Fe_2(SO_4)_3$, it was observed that 50 mg/L of $Fe_2(SO_4)_3$ increased the recovery by 14.1% at the bridging liquid concentration of 15%.

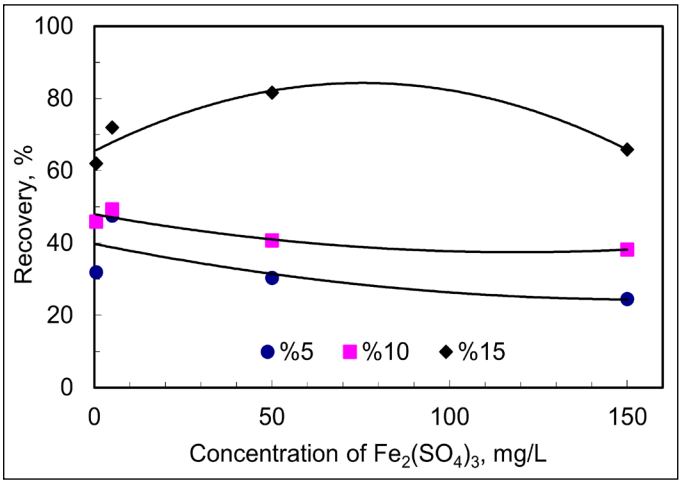

Figure 7. Recovery Variation with respect to $Fe_2(SO_4)_3$ Concentration (Kerosene concentration: 5, 10 and 15%; pH=7.8)

In this study, the increase in recovery at low concentrations has been linked to the adsorption of Fe^{3+} ions on the surface of coal particles. The adsorption of Fe^{3+} ions enhances the hydrophobicity of coal surfaces by forming complex bonds with oxygen-containing functional groups, such as carboxyl (-COOH) and hydroxyl (-OH), present on the coal surface. These complex bonds reduce the interaction potential of the coal surface with water molecules, thereby giving the surface a more hydrophobic character. This, in turn, facilitates easier coalescence of coal particles with oil droplets during the oil agglomeration process, leading to an increase in agglomeration efficiency. Research conducted by Arbiter (1985), Wen and Sun (1981), and Langmuir (1969) has shown that the adsorption of Fe^{3+} ions significantly enhances the hydrophobicity of coal surfaces, thereby improving the efficiency of oil agglomeration.

2.3.3. Agglomeration Experiments Conducted with $FeCl_2$ and Kerosene

The recovery results obtained from the oil agglomeration experiments conducted with $FeCl_2$ are shown in Figure 8. As seen in Figure 8, the recovery slightly decreased with an increase in the concentration of $FeCl_2$. This decrease in recovery was attributed to the fact that Fe^{2+} and $Fe(OH)^+$ cations, which are believed to be present in the medium, render the surfaces of coal particles and oil droplets more hydrophilic by altering their surface charge (Frederick, 1964; Langmuir, 1969; Wagman, 1969; Fuerstenau et al., 1983; Gutierrez-Rodriguez and Aplan, 1984; Arbiter, 1985; Özbayoğlu, 1987; Laskowski and Parfitt, 1988). Additionally, the $Fe(OH)_2$ compound, also presumed to exist in the medium albeit in smaller quantities, prevents coal particles from contacting the bridging liquid (Butler, 1964; Fuerstenau and Palmer, 1976; Özbayoglu, 1980; Wen and Sun, 1981; Gurses et al., 1997). The results from the experiments showed that 50 mg/L $FeCl_2$ increased the recovery by 11.1% at a bridging liquid concentration of 15%.

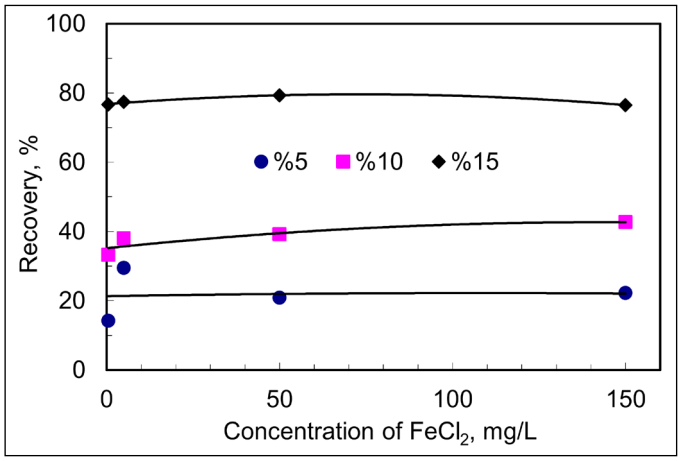

Figure 8. Recovery Variation with respect to $FeCl_2$ Concentration (Kerosene concentration: 5, 10 and 15%; pH=7.3)

2.3.4. Agglomeration Experiments Conducted with NaCl and Kerosene

The recovery values obtained from the oil agglomeration experiments conducted with NaCl are presented in Figure 9. As seen in Figure 9, the evaluation of experimental results showed that adding 50 mg/L NaCl increased recovery by 9.5% at a 15% bridging liquid concentration. The increase in recovery with rising sodium chloride concentration in oil agglomeration is attributed to the reduced thickness of the electrical double layer between coal particles and oil droplets (Özbayoglu, 1980; Wen and Sun, 1981; Cebeci et al., 2002). Fan et al. (1988) explored the impact of NaCl on the oil agglomeration recovery of coals with varying hydrophobicity levels. They discovered that as NaCl concentration in-

creased, agglomeration recovery improved in highly hydrophobic coals but decreased in less hydrophobic ones. Yang et al. (1987) demonstrated that recovery slightly increases in oil agglomeration as NaCl concentration rises, attributing this improvement to the compression of the electrical double layer between coal particles and oil droplets. The analysis of experimental data confirmed that 50 mg/L NaCl enhanced recovery by 9.5% at a 15% bridging liquid concentration.

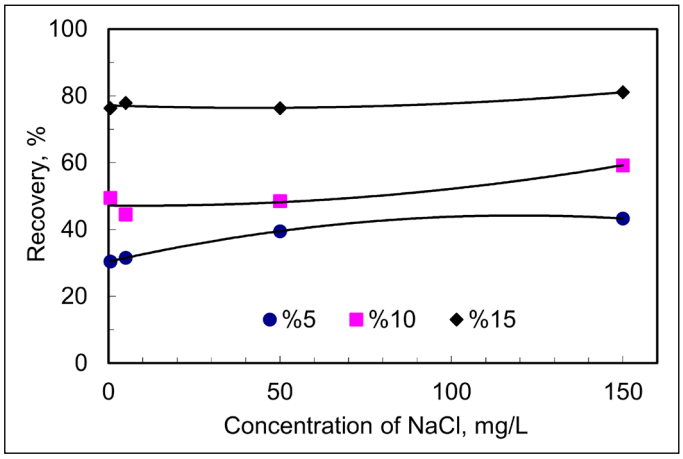

Figure 9. Recovery Variation with respect to NaCl Concentration (Kerosene concentration: 5, 10 and 15%; pH=7.7)

In this study, the results showed that adding NaCl to a mixture with a 15% kerosene concentration and using clean coal led to a 9.5% increase in recovery. These findings align with those of Cebeci et al. (2002), who used raw coal, highlighting NaCl's influence on the agglomeration process. However, the substitution of raw coal with cleaned coal altered the process's efficiency, yielding a more uniform coal structure with lower ash content and, consequently, different outcomes.

2.4. Comparison of the Results of Experiments Conducted with Different Inorganic Pretreatment Materials at Different Agglomeration Times

In the experiments where the effect of agglomeration time on recovery was investigated using different inorganic pretreatment materials and kerosene, after the addition of 50 mg/L of NaCl, $FeCl_2$, $Al_2(SO_4)_3$ and $Fe_2(SO_4)_3$ as pretreatment materials to the suspension, a conditioning time of 5 minutes was allowed. Then, the bridging liquid at a concentration of 15% was added, and agglomeration times 1, 5, 10 and 15 minutes were applied for each concentration. To determine the effect of mixing time on agglomeration, four different mixing times were tested at the mixing speed of 800 rpm. The results obtained from these experiments are shown in Figure 10.

As can be seen from Figure 10, the recovery was found to be low when the agglomeration time was 1 minute. The particle-oil contacts and particle-oil attachments were low at short mixing times (Bhattacharyya et al., 1977; Osborne, 1988; Coleman et al., 1995; Hacıfazlıoğlu, 2008; Şahinoğlu and Uslu, 2008; Aslan and Ünal, 2011; Shukla and Venugopal, 2019). When the agglomeration time was increased from 1 to 5 min, recovery increased due to increased contact of oil coated particles (Capes and Germain, 1982; Kumar et al., 2015; Özer et al., 2017). From 10 to 15 min, a slight downward trend was observed in recovery. This decrease may be due to the fact that, at longer mixing times, agglomerates reaching a certain size were partially fragmented by rubbing against each other and the wall of the beaker (Coleman et al., 1995; Yu, 1998; Cebeci and Sönmez, 2002; Özer et al., 2017). In experiments conducted with only kerosene, the maximum recovery was 71.5% when the agglomeration time was 10 min. In experiments where different pretreatment materials were used (NaCl, $FeCl_2$, $Al_2(SO_4)_3$ and $Fe_2(SO_4)_3$) with kerosene, the recovery values were found to be 9.5%, 11.2%, %12.9% and 14.1%, respectively, when the agglomeration time was 5 minutes.

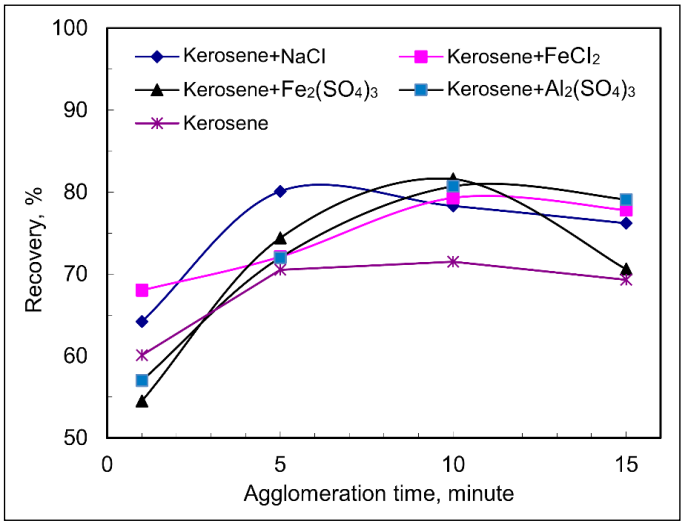

Figure 10. Recovery Variation with respect to Agglomeration Time (Pretreatment material: 50 mg/L; Kerosene: 15%)

3. Conclusions

The results of the agglomeration experiments conducted only with kerosene indicated that recovery increased up to a bridging liquid concentration of 25%, and then decreased beyond this concentration. Diminished recovery at lower bridging liquid concentrations resulted from inadequate coverage of the coal surface, whereas the decline at higher concentrations occurred because the agglomerates formed had lower resistance to mechanical forces.

In the experiments where the effect of agglomeration time on recovery was investigated using only kerosene, it was determined that the optimal time for agglomeration of hard coal was 10 minutes.

Coal could not be agglomerated using only pretreatment materials without a bridging liquid.

Using inorganic pretreatment materials led to specific increases in recovery rates, ranging from 9% to 15%, at a 15% bridging liquid concentration. This variation in recovery rates, is dependent on the specific type of pretreatment material used. Notably, the employment of $Fe_2(SO_4)_3$ and $Al_2(SO_4)_3$ resulted in significant recovery improvements, with increases of 14.1% and 12.9%, respectively. These findings imply that such materials potentially augment the hydrophobic qualities of coal particles, thereby promoting agglomeration and consequently elevating recovery rates. Conversely, the utilization of $FeCl_2$ and NaCl was associated with more modest recovery increments, 11.2% and 9.5% respectively, suggesting that these substances may restrict agglomeration efficiency. This limitation appears to stem from modifications in surface charges induced by these materials, which in turn adversely impact the agglomeration process.

Recovery levels achieved in 10 minutes with only kerosene were reached in just 5 minutes when pretreatment materials were added. This indicates that inorganic pretreatment materials can shorten the agglomeration time, thereby increasing process efficiency.

Experiments showed that maximum recovery occurred at a mixing speed of 800 rpm. This finding demonstrates the significance of mixing speed as a parameter in the agglomeration process and suggests that selecting an optimal speed can maximize recovery efficiency.

References

Abbott, J., & Miles, N.J. (1991). Smoothing and interpolation of float/sink data for coals. Minerals Engineering, 4(3/4), 511-524. https://doi.org/10.1016/0892-6875(91)90152-L

Aktaş, Z. (1993). The absorption behavior of non-ionic reagent on two low rank British coals and their influence on the froth structure and flotation performance. [Doctoral dissertation, Victoria University of Manchester].

Aktaş, Z. (2002). Some factors affecting spherical oil agglomeration performance of coal fines. International Journal of Mineral Processing, 65, 177–190. https://doi.org/10.1016/S0301-7516(01)00074-6

Aktaş, Z., & Woodburn, E.T. (1995). The effect of non-ionic reagent adsorption on the froth structure and flotation performance of two low rank British coals. Powder Technology, 83, 149-158. https://doi.org/10.1016/0032-5910(94)02950-S

Aktaş, Z., Karacan, F., & Olcay, A. (1998). Centrifugal float-sink separation of fine Turkish coals in dense media. Fuel Processing Technology, 55, 235-250. https://doi.org/10.1016/S0378-3820(98)00053-8

Alonso, M., Valdés, A., Martınez-Tarazona, R., & Garcia, A. (2002). Coal recovery from fines cleaning wastes by agglomeration with colza oil: A contribution to the environment and energy preservation. Fuel Processing Technology, 75, 85–95. https://doi.org/10.1016/S0378-3820(01)00233-8

Arbiter, N. (Ed.). (1985). SME Mineral Processing Handbook Section 5, Flotation. New York: AIME.

Aslan, N., & Ünal, İ. (2011). Multi-response optimization of oil agglomeration with multiple performance characteristics. Fuel Processing Technology, 92, 1157–1163. https://doi.org/10.1016/j.fuproc.2010.05.029

Bhattacharyya, R., Moza, A., & Sarkar, G. (1977). Role of operating variables in oil-agglomeration of coal. In K.V.S. Sastry (Ed.), Agglomeration 77 (pp. 931–938), Vol. 77. New York: American Institute of Mining, Metallurgical, and Petroleum Engineers.

Butler, J.N. (1964). Ionic Equilibrium. Reading: Addison-Wesley, p.173.

Capes, C. (1976). Basic research in particle technology and some novel applications. The Canadian Journal of Chemical Engineering, 54, 3–12. https://doi.org/10.1002/cjce.5450540102

Capes, C. (1991). Oil agglomeration process principles and commercial application for fine coal cleaning. Coal Preparation, 4, 1021–1029.

Capes, C. E., & Jonasson, K. A. (1988). Application of Oil-Water of Coals in Beneficiation, Interfacial Phenomena in Coal Technology, Surfactant Science Series, v.32.

Capes, C., & Germain, R. (1982). Selective oil agglomeration in fine coal beneficiation. In Y.A. Liu (Ed.), Physical cleaning of coal (pp. 293–351). New York: Marcel Decker.

Capes, C.E., & Darcovich, K. (1984). A survey of oil agglomeration in wet fine coal processing. Powder Technology, 40, 43–52. https://doi.org/10.1016/0032-5910(84)85054-8

Cebeci, Y. (2003). Investigation of kinetics of agglomerate growth in oil agglomeration process. Fuel, 82, 1645–1651. https://doi.org/10.1016/S0016-2361(03)00095-4

Cebeci, Y., & Sönmez, İ. (2002). The investigation of coal–pyrite/lignite concentration and their separation in the artificial mixture by oil agglomeration. Fuel, 81, 1139–1146. https://doi.org/10.1016/S0016-2361(02)00028-5

Cebeci, Y., & Sönmez, İ. (2006). Application of the Box-Wilson experimental design method for the spherical oil agglomeration of coal. Fuel, 85, 289–297. https://doi.org/10.1016/j.fuel.2005.07.017

Cebeci, Y., Ulusoy, U., & Şimşek, S. (2002). Investigation of the effect of agglomeration time, pH and various salts on the cleaning of Zonguldak bituminous coal by oil agglomeration. Fuel, 81, 1131-1137. https://doi.org/10.1016/S0016-2361(02)00030-3

Chary, G., & Dastidar, M. (2010). Optimization of experimental conditions for recovery of coking coal fines by oil agglomeration technique. Fuel, 89, 2317–2322. https://doi.org/10.1016/j.fuel.2009.12.016

Chary, G., & Dastidar, M. (2013). Comprehensive study of process parameters affecting oil agglomeration using vegetable oils. Fuel, 106, 285–292. https://doi.org/10.1016/j.fuel.2012.12.002

Coleman, R.D., Sparks, B.D., Majid, A., & Toll, F.N. (1995). Agglomeration-flotation: Recovery of hydrophobic components from oil sands fine tailings. Fuel, 74, 1156–1161. https://doi.org/10.1016/0016-2361(95)00067-F

Çelik, H. (2002). İnce Kömürlerin Temizlenmesinde Köpük Flotasyonu ve Ağır Ortam Siklonlarının Entegrasyonu. [Doctoral dissertation, Dokuz Eylül Üniversitesi].

Çelik, H. (2006). İnce Kömürlerin Temizlenmesinde Köpük Flotasyonu ve Ağır Ortam Siklonlarının Entegrasyonu. Dokuz Eylül Üniversitesi Mühendislik Fakültesi Fen ve Mühendislik Dergisi, 8(2), 93-106.

Darcovich, K., Capes, C.E., & Talbot, F.D.F. (1989). Surface characteristics of coal-oil agglomerates in the floc regime. Energy & Fuels, 3, 64–70. https://doi.org/10.1021/ef00013a011

Duzyol, S. (2015). Investigation of oil agglomeration behaviour of Tuncbilek clean coal and separation of artificial mixture of coal-clay by oil agglomeration. Powder Technology, 274, 1-4. https://doi.org/10.1016/j.powtec.2015.01.011

Duzyol, S., Ozkan, A., & Yekeler, M. (2012). Critical Oil–Liquid Interfacial Tension for Some Oil Assisted Fine Particle Processing Methods, Colloids and Surfaces A: Physicochemical and Engineering Aspects, 398, 3236.

Fan, C., Markuszewski, R., & Wheelock, T. (1988). Oil agglomeration of coal in salt solutions: Effects of hydrophobicity and other parameters on coal recovery. Environmental Science, Chemistry.

Flynn, S.A., & Woodburn, E.T. (1987). A froth ultra-fine model for the selective separation of coal from mineral in a dispersed air flotation cell. Powder Technology, 49, 127-142. https://doi.org/10.1016/0032-5910(87)80055-4

Frederick, M.F. (1964). Contact angle, wettability, and adhesion, Vol. 43. Washington, DC: American Chemical Society.

Fuerstenau, D.W., Rosenbaum, J.M., & Laskowski, J. (1983). Effect of surface functional groups on the flotation of coal. Coll Surf, 8, 153–174. https://doi.org/10.1016/0166-6622(83)80082-1

Fuerstenau, M.C., & Palmer, B.R. (1976). Flotation of oxides and silicates. In A.M. Gaudin (Ed.), Flotation, A.M. Gaudin Memorial Volume, I. New York: AIME, p. 148.

Garcia, A.B., Martinez-Tarazona, M.R., Vega, J.G., & Wheelock, T.D. (1998). On the role of oil wetting in the cleaning of high rank coals by agglomeration. Fuel, 77, 387–392. https://doi.org/10.1016/S0016-2361(98)80028-8

Garcia, A.B., Vega, J.G., & Martinez-Tarazona, M.R. (1995). Effects of oil concentration and particle size on the cleaning of Spanish high-rank coals by agglomeration with n-heptane. Fuel, 74, 1692–1697. https://doi.org/10.1016/0016-2361(95)00149-Y

Gence, N. (2006). Coal recovery from bituminous coal by aggloflotation with petroleum oils. Fuel, 85, 1138–1142. https://doi.org/10.1016/j.fuel.2005.11.001

Guerra, E.A., Rubio, J., & Solari, J.A. (1986). A Comparative Study Of Oil Based Beneficiation Processes Of Ultrafine Brazilian Coals, 10.International Coal Preparation Congress,105-120.

Gurses A, Doymus¸ K., & Bayrakceken S. (1997). Evaluation of response of brown coal to selective oil agglomeration by zeta potential measurements of the agglomerates. Fuel, 76, 1439–44.

Gutierrez-Rodriguez, J., & Aplan, F. (1984). The effect of oxygen on the hydrophobicity and floatability of coal. Colloids and Surfaces, 12, 27–51. https://doi.org/10.1016/0166-6622(84)80087-6

Gülsuna, G. (2007). Linyit Kömürü Ara Ürününün Flotasyon İle Zenginleştirmesinin Araştırılması. [Master's thesis, Çukurova Üniversitesi].

Hacıfazlıoğlu, H. (2008). Azdavay Kömürünün Yağ Aglomerasyonu ve Bazı Önemli Çalışma Parametrelerinin Etkilerinin Belirlenmesi. Madencilik, 47(4), 3-11.

Hacıfazlıoğlu, H. (2013). İnce Kömür Zenginleştirme Teknolojisindeki Yenilikler ve Çift Tamburlu Ayırıcı (ÇTA)'nın Endüstriyel Uygulaması. Nevşehir Bilim ve Teknoloji Dergisi, 2(2), 109-119. https://doi.org/10.17100/nevbiltek.210863

Hazra, S.K., Rao, T.C., & Sarkar, G.G. (1986). Studies on the Performance of an Oil Agglomeration Process Evaluated From Bench-scale Batch and Continuous Operations with Critical Variables. CIM 10.Int. Coal Prep. Congr., Edmonton, Canada, pp. 163-177.

Hoşten, Ç., & Uçbaş, Y. (1989). Zonguldak Taşkömürleri Üzerinde Yağ Aglomerasyonu Çalışmaları. Türkiye Madencilik Bilimsel ve Teknik 11.Kongresi, ss. 355-364.

Keller, D.V., Jr., & Burry, W. (1987). An investigation of a separation process involving liquid–water–coal systems. Colloids and Surfaces, 22, 37–50. https://doi.org/10.1016/0166-6622(87)80004-5

Kemal, M., & Arslan, V. (2000). Toz Kömürlerin Değerlendirilmesinde Yeni Teknolojiler. V.Kömür Teknolojisi Ve Kullanım Semineri.

Kılınç Aksay, E., Arslan, V., & Polat, H. (2010). Toz Kömürlerin Zenginleştirilmesinde Yağ Aglomerasyonu Yöntemi ve Yenilikler. İstanbul Yerbilimleri Dergisi, 23(2), 97–108.

Kılınç, E. (2000). Toz Kömürlerin Yağ Aglomerasyonu ile Zenginleştirilmesi. [Master's thesis, Dokuz Eylül Üniversitesi].

Kumar, S., Chary, G., & Dastidar, M. (2015). Optimization studies on coal–oil agglomeration using Taguchi (L16) experimental design. Fuel, 141, 9–16. https://doi.org/10.1016/j.fuel.2014.09.119

Langmuir, D. (1969). Professional paper. US Geol Surv 650-B:181.

Laskowski, J., & Parfitt, G. (1989). Electrokinetics of coal-water suspensions. In G.D. Botsaris & Y.M. Glazman (Eds.), Interfacial Phenomena in Coal Technology (pp. 279–327). New York: Marcel Decker Inc.

Laskowski, J.S., & Parfitt, G.D. (1988). Interfacial Phenomena in Coal Technology, Vol.32 (pp.280-323).

Laskowski, S.J., & Yu, Z.M. (2000). Oil Agglomeration and Its Effect on Beneficiation and Filtration of Low-Rank/Oxidized Coals. International Journal of Mineral Processing, 58, 237-252. https://doi.org/10.1016/S0301-7516(99)90040-6

Mehrotra, V., Sastry, K., & Morey, B. (1983). Review of oil agglomeration techniques for processing of fine coals. International Journal of Mineral Processing, 11, 175–201. https://doi.org/10.1016/0301-7516(83)90025-X

Nicol, S.K., & Swanson, A.R. (1980). Oil in water emulsion for agglomeration of coal fines. Patent US4209301 A. File date May 8, 1978, Issue date June 24, 1980.

Osborne, D. (1988). Flotation, agglomeration and selective flocculation. Coal Preparation Technology, 1, 415–477.

Özbayoglu, G. (1980). The electrokinetic properties of Zonguldak coal seams. Second Turkish Coal Congress. Zonguldak. 12–16 May, 1980. P. 443–51

Özbayoğlu, G. (1987) Coal flotation. In: Yarar B., Doğan Z.M., editors. Mineral Processing Design, NATO ASI series. The Hague: Martinus Nijhoff, 1987. p. 76–105.

Özbayoğlu, G., & Mamurekli, M. (1994). Super-clean coal production from Turkish bituminous coal. Fuel, 73, 1221-1223. https://doi.org/10.1016/0016-2361(94)90263-1

Özer, M., Basha, O.M., & Morsi, B. (2017). Coal-Agglomeration Processes: A Review. International Journal of Coal Preparation and Utilization, 37(3), 131-167. https://doi.org/10.1080/19392699.2016.1142443

Petela, R. (1991). Prediction of the product size in the agglomeration of coal particles in a water-oil emulsion. Fuel, 70, 509–517. https://doi.org/10.1016/0016-2361(91)90029-A

Shrauti, S.M., & Arnold, D.W. (1995). Recovery of waste fine coal by oil agglomeration. Fuel, 74, 459–465. https://doi.org/10.1016/0016-2361(95)93483-T

Shukla, D., & Venugopal, R. (2019). Optimization of the process parameters for fine coal–oil agglomeration process using waste mustard oil. Powder Technology, 346, 316-325. https://doi.org/10.1016/j.powtec.2019.02.001

Slaghuis, J.H., & Ferreira, L.C. (1987). Selective spherical agglomeration of coal: An amended mechanism of agglomerate formation and growth and its effect on product quality. Fuel, 66, 1427–1430. https://doi.org/10.1016/0016-2361(87)90191-8

Steedman, W.G., & Krishnan, S.V. (1987). Oil agglomeration process for the treatment of fine coal. In Fine Coal Processing (pp. 179–204). Park Ridge, NJ: Noyes Publications.

Stockton, J.B. (1989). The effect of froth structures on flotation kinetics and selectivity. [Doctoral dissertation, Victoria University of Manchester (UMIST, Chem. Eng. Dep.)], Manchester, UK.

Şahinoğlu, E., & Uslu, T. (2008). Amenability of Muzret Bituminous Coal to Oil Agglomeration. Energy Conversion and Management, 49(12), 3684-3690. https://doi.org/10.1016/j.enconman.2008.06.026

Şahinoğlu, E., 2006. Müzret (Yusufeli – Artvin) Kömürünün Yağ Aglomerasyonu ile Temizlenmesi, Yüksek Lisans Tezi, K.T.Ü., Fen Bilimleri Enstitüsü, Trabzon.

Uçbaş, Y., Öteyaka, B., & Özdağ, H. (1997). Manyezit Cevherinin Yağ Aglomerasyonu İle Zenginleştirilmesinde Bazı Proses Değişkenlerinin Aglomerat Boyutu ve Proses Verimi Üzerine Etkisi. Türkiye 15. Madencilik Kongresi, Ankara, 383-388.

Uslu, T., & Şahinoğlu, E. (2010). Atık Yağların Kömürün Temizlenmesinde Kullanımı ve Türkiye'deki Potansiyel. Madencilik Türkiye (Madencilik ve Yer Bilimleri Dergisi), cilt.1, sa.5, ss.30-34.

Ünal, İ., & Erşan, G.M. (2007). Factors Affecting The Oil Agglomeration of Sivas-Divriği-Uluçayır Lignite. Energy Sources, 29, Part A, 983–993. https://doi.org/10.1080/00908310500430992

Ünal, İ., Aktaş, Z., & Olcay, A. (2000). Bitümlü Kömür ve Linyitin Yağ Aglomerasyonu. Türkiye 12. Kömür Kongresi Bildiriler Kitabı, Zonguldak.

Wagman, D.D. (1969). NBS Technical Note 270-4.

Wen, W.W., & Sun, S.C. (1981). An electrokinetic study on the oil flotation of oxidized coal. Separation Science and Technology, 16, 1491–1521. https://doi.org/10.1080/01496398108058313

Yamık, A., Tosun, Y.İ., & Güneş, N. (1994). Kömürden Külün ve Kükürdün Arındırılması. Türkiye 9. Kömür Kongresi, Zonguldak, 201-210.

Yang, G.C.C., Markuszewski, R., & Wheelock, T.D. (1987). Oil Agglomeration of Coal in Inorganic Salt Solutions. Separation Science and Technology, 22, 133-146. https://doi.org/10.1080/07349348808945562

Yu, Z. (1998). Flocculation, hydrophobic agglomeration and filtration of ultrafine coal. Vancouver, Canada: University of British Columbia.

Yüce, S., Alp, İ., Sarı, S., Arabacı, R., & Karagöz, H. (2009). Cause of medium loss in coal washing plants - Analysis of Eski Çeltek coal washing plants. 21.Uluslararası Madencilik Kongresi ve Sergisi, Antalya.

BİLİMSEL MADENCİLİK DERGİSİ
SCIENTIFIC MINING JOURNAL
TMMOB Maden Mühendisleri Odası Yayını / The Publication of the Chamber of Mining Engineers of Turkey
www.mining.org.tr

Original Research

Research and Application of Sealed coring Technology in In-situ Coal Seam of Directional Long-boreholein Coal mine

Dayong Tang[1,*], Wenbing Wu[2], Yi Tang[3], Zhengyong Duan[1], Xiaolong He[1], Shubo Zhou[1], Linlong Ni[1]

[1] *The School of Mechanical and Electrical Engineering, Chongqing University of Arts and Sciences, Chongqing Yongchuan, 402160, CHİNA*
[2] *Chongqing Research Institute Co., Ltd, China Coal Technology Engineering Group, Chongqing, 400039, CHİNA*
[3] *School of Mechanical and Electrical Engineering, XipuCampus, Southwest Jiaotong University, Emei, Sichuan, 614202, CHİNA*

Received: 26 September 2024 • Accepted: 26 December 2024

A B S T R A C T

To accurately obtain the gas content of in-situ coal seams in coal mines, a sealed coring technology for in-situ coal seams in coal mines is proposed. Utilizing the pressure difference generated by high-pressure water at both ends of the piston, the piston is driven to cut off the positioning pin. This in turn drives the ball valve in the coring device to rotate, cut off and seal the in-situ coal core. Performance tests were conducted on the sealing pressure of the coring device by opening the water holes on the piston and using suspension pins of different materials. This verifies the working parameters of the piston opening amount and suspension pins made of different materials, providing basic data for subsequent industrial underground tests. Finally, during the industrial test underground, it was found that the gas content in the coal seam measured by closed sampling was 1.9-2.5 times higher than that of the coal seam sampled by the hole. This verifies the successful design of the closed sampling device.

Keywords: *Directional long-borehole; In-situ coal seam; Sealed coring; Pressure difference; Cutting mechanism.*

Introduction

Coalbed methane(CBM) content is an important technical parameter to characterize the characteristics of underground coal reservoirs, and is the main basis for the development and utilization of CBM resources and comprehensive gas control (Chen et al., 2017).The coal-bed gas resources are rich in China, with up to 29.8 trillion cubic meters (Tao et al., 2019).However, due to complex geological conditions as well as difficult exploration and development technology, the main method is the underground gas drainage drilling methods (Sang et al., 2024). CBM is usually stored in coal seams or rock fractures with the characteristics of flammability and explosiveness. During the construction of underground gas drainage drilling, if the samples and the gas content parameters of in-situ coal seam cannot be accurately obtained, it is difficult to formulate effective and reasonable gas control measures, posing a serious safety hazard to coal mine production (Van et al., 2020).

Coal seam borehole sampling and testing technology is an important means to obtain original geological information such as coal seam gas content. It is the most basic technical work for underground gas disaster control and comprehensive utilization of coalbed methane (Long et al., 2022; Karacan et al., 2021). The detection parameters of coal seam gas content mainly include gas content, desorption amount and residual amount (Li et al., 2020; Szlązak et al., 2021; Akdaş et al., 2023). The desorption amount and residual amount can be accurately measured, while the gas content can only be estimated based on the initial desorption law of the coal sample taken. The estimated value is related to sampling time, and coal sample exposure time. The longer the coal sample exposure time, the more inaccurate the estimated value will be (Zhao et al., 2023; Guo et al., 2023). Therefore, how to ensure the in-situ information of coal samples is closely related to the sampling method of coal samples. There are two methods to determine the gas content of coal seam: the orifice sampling method and the coal sample tube method. Due to the prolonged exposure time of the coal seam during the process of returning to the borehole, not all coal samples are immediately drilled from the borehole. Therefore, the coal sample data obtained through this method is far from the data of the on-site coal seam. However, the coal sample tube method also has some problems, such as long exposure time of samples, ands serious deterioration of coal

* Corresponding author: e7917252tangf@126.com • https://orcid.org/0009-0009-82364070

https://doi.org/10.30797/madencilik.1426095

samples due to grinding and heating. Therefore, the coal sample data obtained using the orifice sampling method and coal sample tube method have serious distortion problems, which cannot meet the accurate formulation and implementation of gas control measures. To obtain accurate coal samples of underground coal seams, many researches on adopting in-situ coal seam coal samples have been conducted.

To accurately obtain deep oil and gas resources, Guo et al. (2023a, b, 2024) and Xie et al. (2021) proposed a design scheme for a new in-situ pressure-preserved coring (IPP-Coring) tool. This scheme is used to complete performance tests and on-site industrial tests to obtain stable sealed samples. In response to the current situation of shallow sampling depth and low accuracy, Li et al. (2017) proposed a long-distance fixed-point pressure sealed coal seam gas content measurement sampling technology underground. It can improve the coal sample collection rate and sampling depth, and improve the accuracy of coal sample collection to a certain extent. With the development of the resource exploration and environmental science drilling, Yu et al. (2020) proposed an in-situ core drilling method to obtain fidelity rock samples from deep rocks. To avoid distortion in the evaluation of deep oil and gas reserves, Wu et al. (2023) studied a pressure intelligent control coring device and innovatively proposed the theory and method of deep intelligent temperature pressure coupling control. To obtain high-condition preserved core samples, Yang et al. (2023) proposed a development strategy for a high toughness and high barrier sealing film based on molecular structure design and filler synergistic enhancement. To solve the problem of low core recovery rate during drilling, Wang et al. (2022a) discussed the flow field characteristics of the closed device valve core under different working conditions.

In terms of coal mine soft rock coring, Zhao et al. (2023) developed the Pressure Maintaining Continuous Coring Technology (PHCCT) and equipment and achieved high coring quality. To improve the sampling rate of fragmented soft coal seams, Chu et al.(2022) studied the "mechanical+hydraulic" multi branch hole sampling drilling technology combined sampling technology with directional branch hole drilling technology. This provides a new method for sampling and gas parameter determination of fragmented soft coal seams in coal mines. To avoid the influence of cutting and friction of the drilling bit for coal core quality, Wang et al. (2022b) established a thermodynamic model of the coring drilling bit and coring tube during the coring process. They studied the main influencing factors during the coring process through numerical simulation. To accurately obtain deep coal cores in coal mines, Huang et al. (2023) developed a low disturbance pressure maintaining coring sampler for sampling tests and analysis of coalbed methane content. To determine the methane content in hard coal seams, Szlązak et al. (2021) studied the gas loss during the sampling process to estimate the consistency between the core and drill cuttings samples. To measure the gas content of coal samples, Hua et al. (2022) used different sampling methods to obtain in-situ coal seams, measured the gas content and compared and analyzed the data. To solve the problem of inaccurate estimation of coalbed methane loss, Chen et al. (2017) proposed a testing device for sealed coring of coal seam, and improved the CBM sealed coring drilling process. Based on the characteristics of conventional coring and closed coring, combined with underground directional drilling in coal mines, an in-situ coal seam closed sampling device for long directional drilling in coal seams is studied. Many performance tests and field tests are conducted to improve the in-situ coal sampling rate and sealing effect. The results can provide reliable in-situ coal seam data for gas detection in coal mines.

1. Design of coal seam closed core-taking device

1.1. Technical development ideas

Since the depth of directional drilling long hole in coal mines is deeper, generally more than 300m, the coal samples obtained by conventional coring drilling technology will be exposed to the air for a long time during coring and drilling. A large number of gas adsorbed in the coal seam will be rapidly desorbed and dissipated. As a result, the gas loss estimated by the method ("Coal Seam Gas Content Underground Direct Determination Method" or the power function method) is quite different from the actual loss. The coal seam gas content cannot be accurately measured. Therefore, according to the technical requirements for measuring coal mine gas content, an in-situ coal seam sealed sampling and testing device is developed. That is, when coring drilling, the coring drilling time and the contact time between coal samples and air are reduced as much as possible. After sampling drilling, the coal samples are quickly sealed in the core tube by using relevant mechanisms to avoid exposure to the air for escaping of gas. Then, the sealed coal sample is analyzed on site with special sampling. After recording the analytical data, the coal sample is loaded into the coal sample tank and sent to the laboratory for other data detection. Compared with conventional sampling techniques, the coal sample taken by this device can greatly reduce the exposure time of the coal sample in the air. It can preserve the original occurrence of the coal seam, greatly improve the accuracy of data testing such as the original coal seam gas content, and provide accurate coal seam data for coal mine gas control.

1. 2. Structural design and working principle of the in-situ sealed core-taking device

The in-situ sealed coring device is mainly composed of outer tube, piston, suspension pin, intermediate tube, rear inner joint, coring inner tube, rear outer joint and coring bit, as shown in Fig. 1. The device adopts a three-tube single-acting structure, wherein an outer tube is connected with a drill rod through a rear outer joint. The front end of the outer tube is provided with a coring bit that has the functions of power transmission and movement. The middle tube is a drive tube, which is connected with the rear inner joint through a suspension pin. Under the action of hydraulic pressure difference, the suspension pin can be cut off, and the piston pushes the drive tube to move forward. At the same time, the drive tube drives the gear fixedly connected with the ball valve to rotate 90 degrees through its own rack mechanism, to complete the cutting and sealing of the coal sample. The coring inner tube can accommodate and resolve the coal sample.

During coring drilling, the coring device is sent to the bottom of the hole. When it touches the coal wall, the coring device is slowly drilled with a small bit pressure and a small pump volume. When the coring is 3-5 m, the drilling is suspended, and the bit pressure is increased. The connecting pin between the outer bit and the inner bit for coring is cut off, and then the coring drilling is carried out. Under the action of the coal core, the inner bit and the coal core are pushed into the inner tube for coring. After the sampling is completed, the pump pressure is increased. The pressure difference between the two ends of the piston is also increased. The suspension pin between the middle tube and the rear inner joint is cut off. The middle tube moves rightward under the action of the piston, and drives the gear rack mechanism to act. In this way, the ball valve cuts off the coal core and seals the coal core in the coring inner tube, and the coal sample drilling is completed.

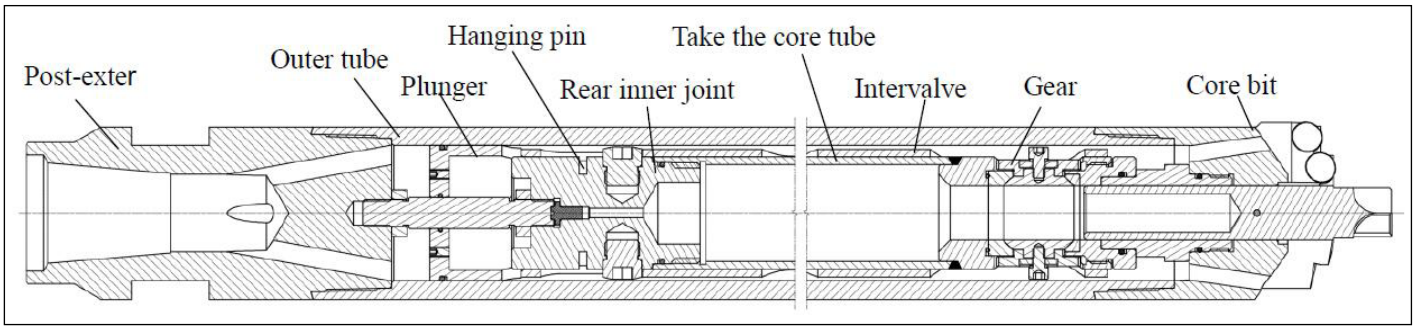

Figure 1. Structural design of the in-situ sealed core device

1.3. Calculation of the cutting force of the suspension pin

The drive pipe and the rear inner connector are fixed by the suspension pin (as shown in Fig. 2). As the pressure difference between the piston sides gradually increases, the allowable shear stress of the suspension pin is exceeded. According to the assembly structure, the shear force of the suspension pin under the differential pressure of both sides of the piston is as follows:

$$F = 2\,A \bullet \tau \tag{1}$$

where, F is the actual shear force of the piston on the suspension pin, N; A is the shear area of the suspension pin, m^2, as shown in Fig.2, and τ is the shear stress on the suspension pin, MPa.

To ensure that the piston thrust can cut the suspension pin, the actual shear force should be greater than the allowable shear stress of the material τ. That is, the actual shear force of the hanging pin in the upper type should be greater than the maximum shear stress that the material can withstand under the allowable shear stress state, namely:

$$F \geq 2\,A \bullet [\tau] \tag{2}$$

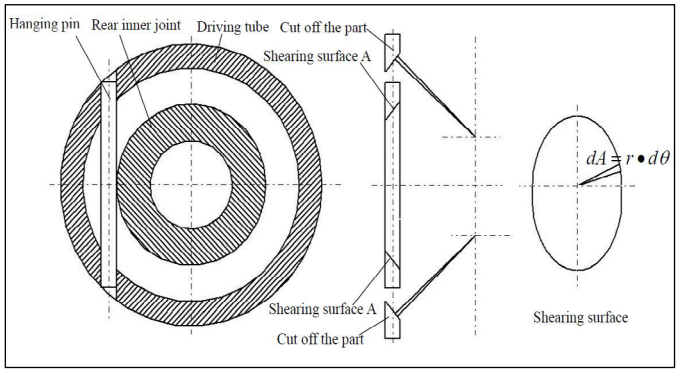

Figure 2. Assembly structure and force analysis of the hanging pin

1.4. Calculation of the pressure difference between both ends of the piston

According to the fluid dynamic knowledge, the flow rate and pressure difference characteristics at both ends of the piston are as follows (Ding, 2022):

$$Q = K \bullet A_0 \bullet \Delta p^m \tag{3}$$

where, K is the coefficient of throttling, decided by the shape of the throttle orifice, and fluid properties. $K = d^2 / (32v \bullet L)$, where d and L are the diameter and length of the throttle orifice, respectively. v is the dynamic viscosity of the fluid; A_0 is the flow area of the throttle hole, mm^2; Δp is the pressure difference between the two ends of the piston, MPa.

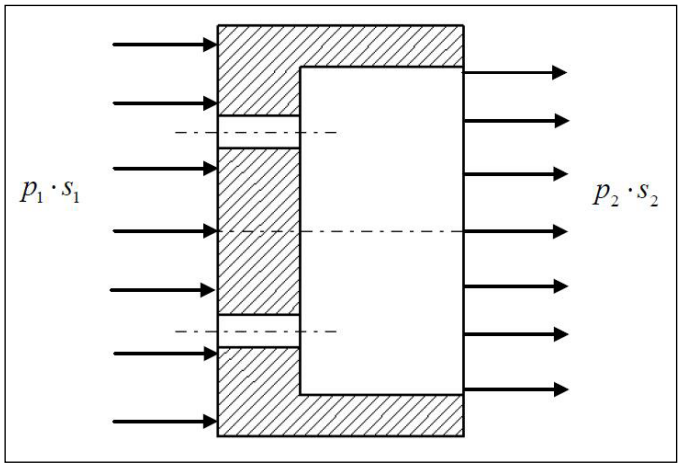

Figure 3. Flow and pressure difference characteristics on both sides of the piston

Through calculating the pressure difference and flow characteristics on both sides of the piston, the thrust force of the fluid on the piston can be calculated as $F = p_1 s_1 - p_2 s_2$ (s_1 and s_2 represent the area on both side of the piston, respectively). From the force analysis of the suspension pin, we have $F = F \geq 2\,A \bullet [\tau]$. Thus, the relationship between the flow rate and the shape and quantity of the piston throttle mouth can be obtained.

1.5. Calculation of the core cut force

When the pressure difference on the piston is large enough, the suspension pin is cut off and the high pressure water pushes the piston to the right. At the same time, the end surface on the right side of the piston acts on the left side of the drive pipe. The gear rack on the drive pipe pushes the gear fixed on the cut-off valve core to rotate. When the driving force is sufficient, the core is cut and sealed.

According to the engagement of the gear and the drive pipe, the tangential force and torque on the gear are as follows:

$$F_t = F' / 2 = p_1 s_1 - p_2 s_2 \tag{4}$$

$$T_c = F_t \cdot \frac{d}{2} \tag{5}$$

where, F_t is the tangential force of the gear, which is equal to the thrust of the piston on the drive pipe. Due to the double teeth, the tangential force is half of the force on the driving pipe; T_c is the rotation torque of the gear, acting on the indexing circle; d is the diameter of the gear indexing circle, mm.

The gear is connected to the ball valve through a hexagonal connection, as shown in Fig. 4. Therefore, the shear torque of the

ball valve subjected to the coal core should be equal to the rotating torque on the gear:

$$T_c = F_{\text{shear}} \cdot d_1 \quad (6)$$

where, F_{shear} is the ball valve is subjected to a shear force derived from the coal core, N; d_1 is ball valve diameter, mm.

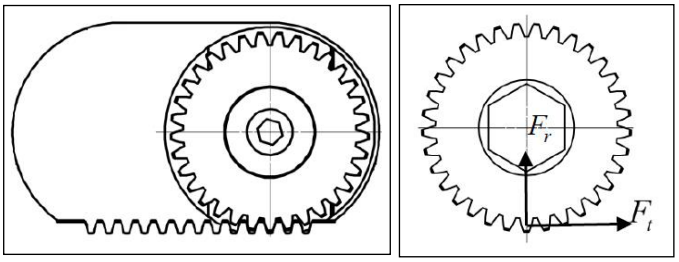

a) Figure of the gear and rack engagement *b) gear*

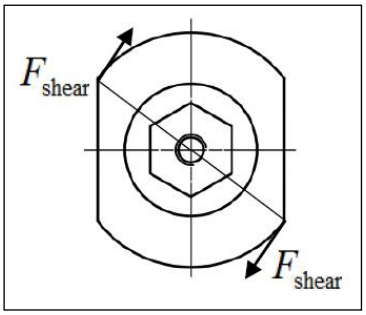

c) ball valve

Figure 4. Force analysis of the gear and the ball valve

2. Testing of closed coring devices

2.1. Performance test

The device was tested on an FMC mud pump to test the closing pressure of the closed core device ball valve and the number of upward pressure holes on the piston. The rated working pressure of the FMC mud pump is 10.3 MPa, and the flow rate is 80-284 L/min. The schematic diagram of the test connection and the pressure regulation performance test are shown in Fig. 5 and Fig. 6, respectively.

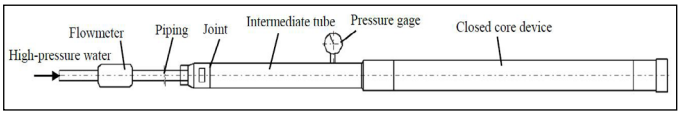

Figure 5. Schematic diagram of performance test connection for closed core device

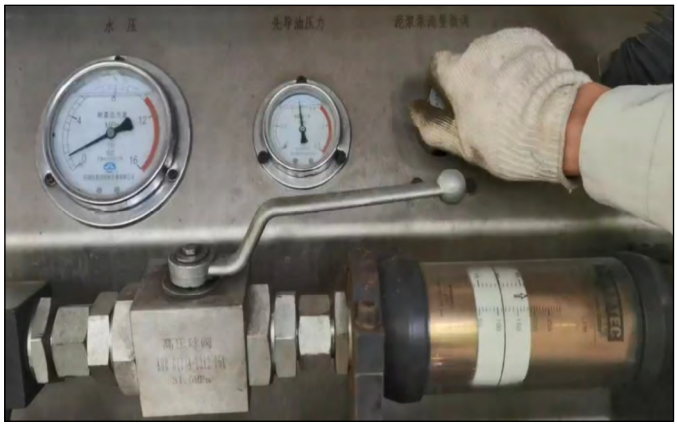

Figure 6. Pressure performance test diagram

During the test, 6061 aluminum alloy rod and 35 steel rod were used as cutting pins. The coal core was replaced by carrot, cucumber and cement block respectively. The pressure regulating holes on the piston were tested according to the number of 2, 3 and 4 openings respectively. During the test, the pump volume is slowly adjusted to slowly increase the pump pressure. When the pressure gauge has a large swing arc and the suspension pin shear sound is heard in the closed corer, the test is stopped. The test of carrot and cucumber as coal core is shown in Table 1, and the situation after the "coal core" is cut off is shown in Fig.7.

Table 1 Performance test of the sealed core device

Serial number	Number of the piston regulator openings	Pump pressure /MPa	Pump volume /L/min	Material of the suspension pin	Whether the hanging pin and the "coal core" are cut off	Conclosed condition of the ball valve
1	2	1.5	100	6061	yes	obturation
		4	150	35	yes	obturation
2	3	2.5	150	6061	yes	obturation
		6.0	200	35	yes	obturation
3	4	4	200	6061	yes	obturation
		8.5	280	35	yes	obturation

Note: In the cement block test, due to its high hardness, the pump volume and pump pressure increased appropriately, in which the pump pressure increased by 1MPa compared with the carrot and cucumber. However, due to the damage of the front and rear gaskets after the shear test, it was stopped only after two tests.

Figure 7. The cutting-off "coal core"

From the test, as the regulating holes increase, the pump pressure and pump volume required for the suspension pin and the "coal core" are gradually increased, and the ball valve can be well closed and sealed. When the suspension pin is made of 6061 aluminum alloy, the pump pressure and pump volume when it is cut off are only about 40% of the 35 steel. It shows that the sealed core sampling is feasible, and it will be sent to the underground for industrial test.

2.2. Industrial testing

1) The general situation of the test mine

The designed annual production capacity of Zhaogu No. 2 Mine of Henan Coking Coal Group is 1.8 million tons; the construction period is 45.3 months, and the service life is 55.5 years. The mine geological reserves are 339 million tons, and the designed recoverable reserves are 140 million tons.

The main coal seam is No. 1 coal seam of Permian, whose inclination Angle is generally 2°-6°.Its average thickness is 6.16m, belonging to a nearly horizontal and stable thick coal seam. The coal quality is high quality anthracite with medium ash, low sulfur, high calorific value, high ash melting point and high yield of lump coal, and the calorific value can reach 30.03 MJ/ kg. The construction of the mine was officially started on January 9, 2007, and completed and put into operation on April 23, 2011. After full operation, the annual sales revenue is 1.6 billion yuan, and the profit and tax are 600 million yuan.

2) Main test equipment

In this test, the deep hole fixed point sealing core device is used to close the coal seam of different depths of underground coal seam, and the gas content is measured. The closed core drilling equipment is ZYD6000-type directional drill and NB-300 mud pump of Xi'an Research Institute of China Coal Science and Industry Group. The drill pipe adopts Φ73 groove spiral drill rod of Xi'an Research Institute.

3) Analysis of the test results

The gas content of coal samples is determined according to GB/T23250-2009 "Underground Direct Determination Method of Gas Content in Coal Mines". A total of 9 test holes in the test were carried out, and coal samples were connected to the holes using a coal sample tank for comparative measurement of the same gas parameters. The test results are shown in Table 2.

Table 2 Comparison of CBM gas content for different core-extraction methods

Hole number	Sampling method	Sampling depth/m	Shear pressure of Cut-off pin(ball valve closing pressure) /MPa	Mud pump flow/L/min	The CBM gas content/(m^3/t)		Hanging pin material
					The amount of the hole	obturation	
1#	Closed core	80	6	190	2.33	5.85	35
2#	Closed core	130	6	190	2.85	6.23	35
3#	Closed core	180	6.2	200	3.04	6.30	35
4#	Closed core	230	6.2	200	3.15	6.50	35
5#	Closed core	280	6.4	220	3.42	6.80	35
6#	Closed core	330	6.5	220	3.78	7.35	35
7#	Closed core	380	6.5	230	3.75	7.45	35
8#	Closed core	430	6.8	230	3.93	7.86	35
9#	Closed core	480	7	240	4.20	8.01	35

According to Table 2, at the same depth, the CBM content measured by the sealed core sampling method is 1.9-2.5 times that of the CBM content measured by coal sampling of orifice. It shows that the closed core device can meet the sealed sampling of in situ coal seam, and effectively avoiding the escape of sampling gas from coal connecting orifice. The main reason for the low CBM content measured by coal seam sampling of orifice is that the coal samples are already exposed to the air when the coal seam returns to the orifice from the bottom of the hole. However, the sealed coring is only exposed to air for a short time, and the CBM escapes less, which can measure the true content of in-situ coal seam gas more accurately.

3. Conclusion

From the experimental process of the closed core device, it can be concluded that:

1) The developed "three tube single action" sealed coring device can effectively drill coal samples from the original coal seams of the mine. This provides an effective guarantee for coal mines to obtain data on the gas content of the in-situ coal seams.

2) The developed pressure differential piston sampling structure can improve the utilization rate of mud pump pressure and effectively increased the success rate of in-situ coal core extraction in underground coal seams.

3) A 20 day industrial underground test was conducted using a sealed coring device at Zhaogu No. 2 Mine of Henan Coking Coal Group. The test results showed that the gas content of coal samples obtained by the sealed coring method was increased by 90% to 150% compared to the gas content obtained by coal sampling of orifice.

Acknowledgements

The authors gratefully acknowledge the support of the key project of Science and Technology Plan of Chongqing Municipal Education Commission (Grant No.KJZD-K202401303), the Planning Project of Chongqing Education Commission (Grant No.24SKGH260), the general project of Natural Science Foundation of Chongqing (Grant No.CSTB2023TFII-OFX0011), the Banan District Natural Science Foundation Project (Grant No. 7), the Yongchuan District Natural Science Foundation Project (Grant No. Ycstc, 2019nb0801).

References

Akdaş, S. B., Fişne, A. 2023. A data-driven approach for the prediction of coal seam gas content using machine learning techniques. *Applied Energy*, 347, 121499. Doi: 10.1016/j.apenergy.2023.121499

Chen, S., Tang, D., Tao, S., Xu, H., Li, S., Zhao, J., Fu, H. 2017. In-situ stress measurements and stress distribution characteristics of coal reservoirs in major coalfields in China: Implication for coalbed methane (CBM) development. *International Journal of Coal Geology*, 182, 66-84. DOI: 10.1016/j.coal.2017.09.009

Ding, Z.R. *Engineering Fluid Mechanics* [M].Beijing: Higher Education Press, 2022.

Guo, D., Chen, L., Zhou, Z., Wang, D., Zhang, Y., Yang, X., Xie, H. 2023b. Development of a pressure coring system for the investigation of deep underground exploration. *International Journal of Mining Science and Technology*, 33(11), 1351 -1364.DOI:10.1016/j.ijmst.2023.10.001

Guo, D., Xie, H. P., Chen, L., Zhou, Z. Y., Lu, H. P., Dai, L., Gao, M. Z. 2023a. In-situ pressure-preserved coring for deep exploration: Insight into the rotation behavior of the valve cover of a pressure controller. *Petroleum Science*, 20(4), 2386-2398.DOI: 10.1016/ j.petsci.2023.02.020

Guo, D., Xie, H., Gao, M., Li, J., He, Z., Chen, L., Dai, L. 2024. In-situ pressure-preserved coring for deep oil and gas exploration: Design scheme for a coring tool and research on the in-situ pressure-preserving mechanism. *Energy*, 286, 129519. DOI: 10.1016/j.energy.2023.129519

Hua, C., Wang, Z., Su, E., Dong, J., Yue, J., Cui, Y., & Zhang, K. 2022. In situ volume recovery method for non-seal gas pressure measurement technology: a comparative study. *ACS Omega*, 7(45), 41341-41352. DOI:10.1021/acsomega.2c05120

Huang, W., Li, J., Liu, Z., Yang, M., You, Z., & Xie, H. 2023.Study of a low-disturbance pressure-preserving corer and its coring performance in deep coal mining conditions. *International Journal of Mining Science and Technology*, 33(11), 1397-1410. DOI: 10.1016/j.ijmst.2023.07.003

Karacan, C. Ö., Martín-Fernández, J. A., Ruppert, L. F., & Olea, R. A. 2021. Insights on the characteristics and sources of gas from an underground coal mine using compositional data analysis. *International Journal of Coal Geology*, 241, 103767.DOI:10.1016/j.coal.2021.103767

Long, W.C., Sun, S.Q., Chen, J. 2022.Study on long-distance fixed-point sealed coring technology in broken-soft coal seam. *Coal Geology & Exploration*, 50(8), 93-98. DOI:10.12363/issn.1001-1986.21.12.0882

Sang, S., Li, R., Liu, S., Zhou, X., Wei, B., Han, S., Zhou, Z. 2024. Research progress and breakthrough directions of the key technical fields for large scale and efficient exploration and development of coalbed methane in Xinjiang. Journal of China Coal Society, 49(1), 563-585. Doi: 10.13225/j.cnki.jccs.YH23.1313

Szlązak, N., Korzec, M., & Piergies, K. 2021. The determination of the methane content of coal seams based on drill cutting and core samples from coal mine roadway. *Energies*, 15(1), 178.DOI:10.3390/en15010178

Szlązak, N., Obracaj, D., &Korzec, M. 2021. Estimation of gas loss in methodology for determining methane content of coal seams. *Energies*, 14(4), 982.Doi: 10.3390/en14040982

Tao, S., Pan, Z., Tang, S., & Chen, S. 2019. Current status and geological conditions for the applicability of CBM drilling technologies in China: A review. *International Journal of Coal Geology*, 202, 95-108. Doi: 10.1016/j.coal.2018.11.020

Van Dyke, M., Klemetti, T., & Wickline, J. 2020. Geologic data collection and assessment techniques in coal mining for ground control. *International Journal of Mining Science and Technology,* 30(1), 131-139.Doi: 10.1016/j.ijmst.2019.12.003

Wang, J., Yu, M., Qian, D., Wan, B., Sun, Y., Chen, C., Tang, Y. 2022a. Optimisation of drainage performance of the thin-walled core barrel sealing technology for pressure preservation sampling. *Ocean Engineering*, 250, 110996.DOI: 10.1016/j.oceaneng.2022.110996

Wang, Q., Wang, Z., Yue, J., An, F., Dong, J., & Ke, W. 2022b. Temperature of the Core Tube Wall during Coring in Coal Seam: Experiment and Modeling. *ACS Omega*, 7(9), 7901-7911. DOI:10.1021/acsomega.1c06746

Wu, N. H., Gao, M. Z., Zhu, L. Y., Li, J. N., Fan, D., You, B., Zhu, G. D. 2023. Pressure control method and device innovative design for deep oil in-situ exploration and coring. *Petroleum Science*, 20(2), 1169-1182. DOI:10.1016/j.petsci.2022. 10.011

Xie, H. P., Liu, T., Gao, M. Z., Chen, L., Zhou, H. W., Ju, Y., Zhao, Z. Y. 2021. Research on in-situ condition preserved coring and testing systems. *Petroleum Science*, 18(6), 1840-1859. DOI:10.1016/j.petsci.2021.11.003

Yang, D., Zhao, Z., Wu, Y., Zhu, L., Lu, J., Liu, T., & Xie, H. 2023. A graphene-enhanced high-barrier and fast-curing film for deep in situ condition preserved coring in coal seams. *International Journal of Mining Science and Technology*, 33(11), 1365-1376. DOI:10.1016/j.ijmst.2023.08.005

Yu, B., Xie, H., Chen, L., Zhao, W., & He, Z. 2020.Exploration of digital twin design mechanism of the deep in situ rock insulation coring device. *Geofluids*, 2020, 8835085. DOI: 10.1155/2020/8835085

Zhao, F.J., Deng, Q.G., Hao, F.C., Zuo, W.Q. 2023. A new method of coring in coal mine: pressure-holding and continuous coring technology. *Bulletin of Engineering Geology and the Environment*, 82(1), 17. DOI: 10.1007/s10064-022-03038-7

Madencilik - Mining, 2024, 63(1), 47-52

BİLİMSEL MADENCİLİK DERGİSİ
SCIENTIFIC MINING JOURNAL

TMMOB Maden Mühendisleri Odası Yayını / The Publication of the Chamber of Mining Engineers of Turkey

www.mining.org.tr

Original Research

Economic Evaluation of Thermal and Mechanical Activation Energies in Plaster Production

Muhammed Şener[a,*], Turan Uysal[b,**], Murat Erdemoğlu[c,***]

[a] Turgut Özal University, Hekimhan Vocational School, Department of Civil, Malatya, TÜRKIYE
[b] Gümüşhane University, Faculty of Engineering and Natural Sciences, Department of Mining Engineering, Gümüşhane, TÜRKIYE
[c] İnönü University, Faculty of Engineering, Department of Mining Engineering, Malatya, TÜRKIYE

Received: 2023 • Accepted: 2024

A B S T R A C T

Plaster is among the most needed raw materials in the world. In this study, thermal activation provided by calcination and mechanical activation methods provided by intensive milling in the plaster production process were evaluated in terms of activation energy. In this context, the energies of laboratory-scale thermal and mechanical activation processes were calculated and these activation methods were evaluated economically and the ideal activation methods were determined. Although the mechanical activation method creates additional investment and operating costs, it reduces the calcination temperature by 13 °C, thus provides lower energy costs. Addition of a mechanical activator mill before thermal activation in plaster production as a more economical and more environmentally friendly method was proposed.

Keywords: *Plaster, Thermal Activation, Mechanical Activation, Energy Cost.*

Introduction

Gypsum ($CaSO_4.2H_2O$) is a naturally occurring calcium sulphate mineral containing two moles of water in its crystal structure. When pure, it contains 79.1% calcium sulphate and 20.9% water. According to the mineralogical formula $CaSO_4.2H_2O$, when gypsum, which contains approximately 21% water, is heated, 15% of this water is removed (Eq. 1). Thus, hemihydrate ($CaSO_4.1/2H_2O$), also known as plaster, containing 0.5 moles of water is obtained. If the hemihydrate continues to be heated, it loses all the water in its structure and turns into anhydrite (Eq. 2).

$$CaSO_4.2H_2O(\text{Gypsum}) \xrightarrow{\text{Calcination (160-170°C)}} CaSO_4.{}^1/_2\,H_2O(\text{Plaster}) + {}^3/_2\,H_2O \quad (1)$$

$$CaSO_4.{}^1/_2\,H_2O\,(Plaster) \xrightarrow{\text{Calcination (250°C)}} CaSO_4(Anhydrite) + {}^1/_2\,H_2O \quad (2)$$

Depending on the properties of gypsum ore (pure gypsum, natural gypsum, gypsum grade, component type, etc.) and calcination conditions, the calcination temperature varies. The conversion temperatures of gypsum to hemihydrate are in the range of 100-120 °C, which is the temperature at which gypsum starts to lose mass; 160-180 °C, which is the temperature at which the transition from hemihydrate to anhydrite starts, and 180-250 °C, which is the temperature at which it no longer loses mass (Putnis et al., 1990; Hudson-Lamb et al., 1996). The production of plaster used in the construction sector is generally carried out by rotary kiln or vertical kiln. The flow chart of the process including a rotary kiln is given in Figure 1. Simply, plaster is obtained by heating in such a way that 15% of the water contained in the gypsum is evaporated and milling the plaster before packaging.

Mechanical activation (MA) is defined as an "increase" in the reactivity of a solid whose chemical structure remains unchanged throughout the milling process, during which mechanical energy transfer takes place. During MA, the particle size of the mineral is reduced by milling, while defects in the crystal structure are formed depending on the mechanical energy density (Baláž and Achimovičová, 2006). Thus, fresh, clean surfaces and semi-stable species are formed (Boldyrev, 1986; Sekulic et al., 1999). In the case of mechanical activation, the mineral will then behave more actively during a metallurgical process such as calcination (Uysal

* Corresponding author: muhammed.sener@ozal.edu.tr • https://orcid.org/0000-0002-7567-4654
** turanuysal@gumushane.edu.tr • https://orcid.org/0000-0003-1643-6725
*** murat.erdemoglu@inonu.edu.tr • https://orcid.org/0000-0003-2922-7965

https://doi.org/10.30797/madencilik.1440130

et al., 2016; Erdemoğlu et al., 2020; Aydoğmuş et al., 2023) sintering (Uysal et al., 2015; Birinci et al., 2017; Alyousif et al., 2023a) or leaching (Erdemoğlu et al., 2017; Uysal, 2018), which will reduce the temperature or increase the speed of the process. Recovery as a result of this mechanical activation can be realized at lower energy costs than thermal activation (Alyousif et al., 2023b). Even if thermal activation (TA) can be achieved at lower temperatures, it may result in less energy costs in the calcination process. It is also known that in the plants where mechanical activation is applied, reactions take place in shorter times, using simpler and cheaper reactors or furnaces (Erdemoğlu et al., 2018; Barry et al., 2019). The only modification to the present plant is the installation of a high-energy transfer mill before the kiln.

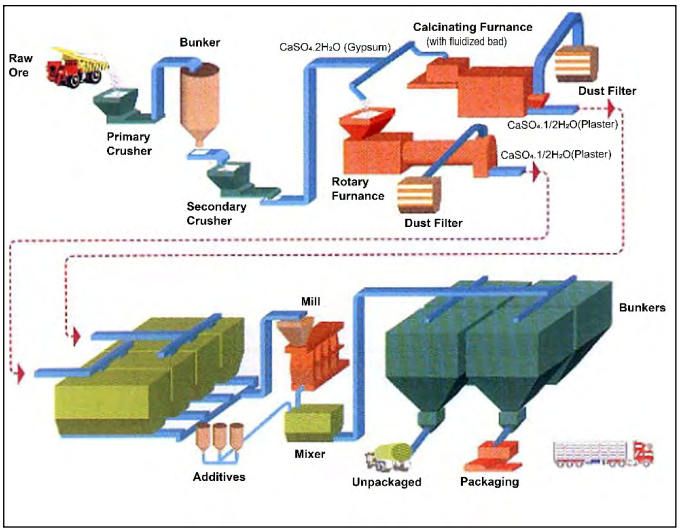

Figure 1. General flow chart of plaster production

Although there are many studies on plaster production, there is not enough work in the literature on the activation energy calculation, which has a significant effect on the economics of the production process. In this study, thermal and mechanical activation energy calculation was carried out in order to contribute to the research on plaster production with lower costs. With MA, gypsum formation temperature decreases and energy cost decreases. With this reduced energy cost, it was calculated how many years the initial investment cost required for MA can be amortised and evaluated economically. The activation energy spent per unit quantity was evaluated and the appropriate activation method was determined.

2. Materials and Methods

2.1. Material

The gypsum used for the experimental studies was obtained from Arslanlı Alçı A.Ş. (Elazığ, Türkiye) plaster plant. The ore used in the experiments is a massive natural alabaster gypsum ore with a CaO content of 32.45%. The chemical analysis results of this gypsum ore are given in Table 1 and XRD analysis results are given in Figure 2. According to the CaO and loss on fire values in Table 1, the $CaSO_4.2H_2O$ content of the ore was determined to be approximately 99.0%. According to XRD results, the ore consists of gypsum and anhydrite.

Table 1. Chemical content of the gypsum ore sample (Şener, 2012)

CaO	SO_3	SiO_2	MgO	Cl	LOI*
32.45	44.49	0.2	0.004	0.41	20.63

**LOI: Loss on ignition (1000 °C)*

2.2. Method

Representative samples of ore with an average particle size of 20 cm were taken from the plant stockpile by sampling. The samples were crushed in a jaw crusher and then ground to a particle size of -2 mm in a ceramic ball mill. This milling was performed under dry conditions. Samples (1 kg) were ground in the ceramic mill at 200 rpm for 5 min. The ore with -2 mm particle size was intensively milled to provide mechanical activation. Intensive milling operations were carried out using Fritsch Pulverisette 6 mono mill model planetary ball mill. In the air-cooled mill, a 250 cm^3 bowl made of hard metal tungsten carbide (WC) and and 10 mm diameter 50 pieces balls made of the same material with the bowl were used. Protherm PLF120/5 model muffle furnace and 15 ml porcelain crucibles were used for calcination of the intensively milled samples. A Setaram LabSys 60 model TG-DSC device was used to observe the thermal behavior of the intensive milled gypsum. The measurements were carried out in an argon atmosphere at a heating rate of 10 °C/min in a platinum crucible. The crystal structures of the powders subjected to intensive milling were examined by X-ray diffraction analysis performed using a Rigaku brand RadB model device in a Cu-Kα (λ = 1.5405 Å) radiation environment at a scanning speed of 2 min^{-1} and at diffraction angles varying between 5-80°.

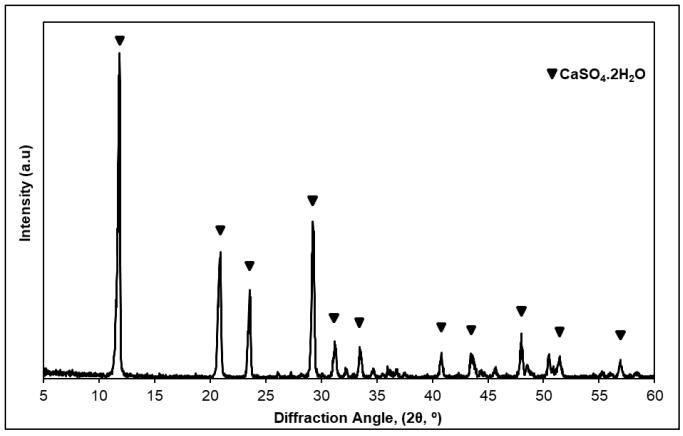

Figure 2. XRD pattern of the gypsum ore sample

The ball-to-ore ratio by weight was 10 and the mill rotation speed was 300 rpm, as recommended by Şener (2014). In the calculation of activation energies, the specific milling energy per unit amount of ore was calculated using Eq. 3 (Pourghahramani and Forssberg, 2007; Balăz, 2008) and the specific heat energy was calculated using Eq. 4.

$$SE = (m_B/m_S) * a * n * t_M * D \quad (3)$$

Where, m_B is mass of milling media (balls) (kg), m_S is mass of ore to be milled (kg), a is theoretical acceleration of the balls (26.41 m/s^2 for the planetary mill used), n is mill rotation speed (1/s), t_M is milling time (s) and D is mill diameter (m). In this formula, the specific energy unit is kJ/kg and kWh is converted (1 kJ: $2{,}78*10^{-4}$ kWh).

$$Q = m * C_p * \Delta T \quad (4)$$

Where m is the mass in kg, Cp is the heat capacity at constant pressure and ΔT is the difference between the initial ambient and final temperature. The Cp of gypsum was calculated as the sum of the specific heat and mass fraction of each of the chemical elements of gypsum and estimated as 1.090 kJ/kg.K (Engineering toolbox, 2003; Evans, 2016). In both activation methods, sample masses were taken as 1 kg due to the close feed amounts.

3. Results and Discussion

3.1. Particle Size Distribution

Table 2 shows variations of selected cut point particle size values with increasing milling time. Milling, as expected, not only decreased the particle size, but also increased the amount of fine particles in the powders. Milling up to 15 min significantly shifted the size distribution to finer sizes, however milling for longer times as much as 18 and 20 min shifted the distribution relatively coarse sizes again. The particle size of unmilled gypsum is minus 2 mm, milling 15 min decreased the cut point d_{90} from 710.29 µm to 38.56 µm. But, prolonged milling for 18 and 20 min increased it to 52.81 and 75.90 µm, respectively. Some coarse particles of long milled powders are not primary but formed by coating of secondary fines or aggregation.

Table 2. Variation of cut point particle size with increasing milling time.

Milling time (minute)	Particle Size (µm)		
	d_{90}	d_{50}	d_{10}
0	710.29	250.27	53.46
5	104.31	34.19	2.45
10	63.02	9.16	1.48
15	38.56	5.74	1.34
18	52.81	5.38	1.08
20	75.90	15.04	1.51

3.2. Energy Consumption

The thermal behaviour of gypsum samples was investigated by thermal analysis methods and the thermal analysis (TG) curve is given in Figure 3. TG and DTA curves of the 15 minutes milled sample are given in Figure 4.

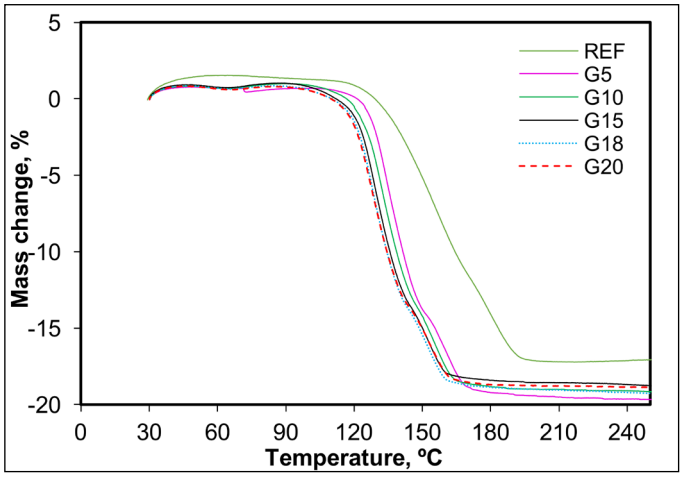

Figure 3. TG curves of unmilled (REF) and prolonged milled gypsum samples (G5: 5 minutes, G10: 10 minutes, G15: 15 minutes, G18: 18 minutes, G20: 20 minutes) (Şener and Erdemoğlu, 2014)

According to the results showed in Figure 3, with the increase in milling time, the conversion temperatures of gypsum to hemihydrate and hemihydrate to anhydrite decreased. It was observed that the transformations shifted to lower temperature regions. In thermal analysis, one reason for the shift of the mass loss temperature value to lower temperature regions is the reduction of the particle size of the gypsum exposed to calcination. However, since the gypsum sample was also prepared by milling for thermal analysis, it was assumed that the effect of particle size on the decrease in conversion temperatures can be neglected. Results similar to these results obtained as a result of thermal analyses were also determined by various researchers. In a study by Lou et al. (2011), the dehydration behaviour of artificially produced gypsum was investigated with the help of TG and DSC analyses. In this study, the temperature at which gypsum starts to lose mass is shown in the range of 110-115 °C; the temperature at which the transition from hemihydrate to anhydride starts is 160-165 °C and the temperature at which it starts not to lose mass is 175-185 °C.

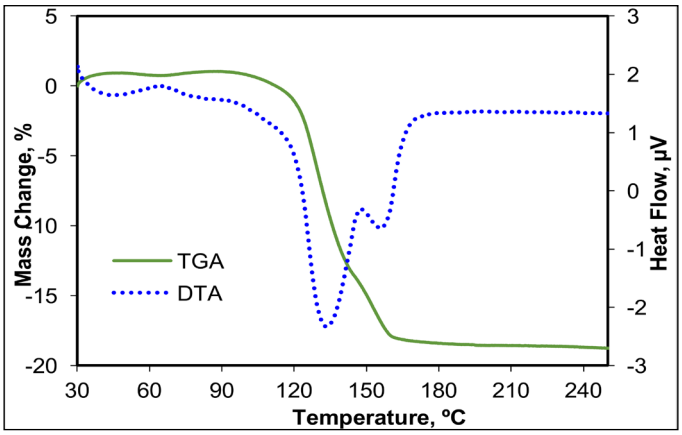

Figure 4. TG and DTA curves of the sample milled for 15 minutes

When the curves in Figure 4 are analyzed, it was determined that the initial temperature of conversion of the sample milled for 15 minutes to hemihydrate was 99.1 ºC, the initial temperature of conversion from hemihydrate to anhydrite was 140.9 ºC and the mass loss ended at 157.4 ºC. When the specific milling and heat energy values were evaluated together, the optimum milling time was determined as 15 minutes (Figure 5). Therefore, the TG and DTA curves of the sample milled for 15 minutes were taken into consideration and the specific milling and heat energy changes depending on the milling time are given in Figure 5. The initial temperature values of conversion of gypsum milled and calcined at different times to gypsum and anhydrite are given in Table 3, and the specific milling, heat energy values and costs are given in Table 4. The specific heat energy (kWh/ton) value was calculated depending on the temperature required for gypsum conversion.

Table 3. Initial temperature values for conversion of gypsum milled and calcined at different times to plaster and anhydrite

Milling time, minute	0	5	10	15	18	20
Initial temperature for conversion to plaster, °C	112.8	109.2	107.3	99.7	100.2	103.4
Initial temperature for conversion to anhydrite, °C	166.6	145.9	144.1	140.9	140.1	137.9

In Table 3, it was observed that the initial temperature of gypsum to plaster transformation decreases until 15 minutes of milling time and increases slightly after 15 minutes. The increase after 15 minutes of milling was thought to be due to the decrease in intensive milling efficiency with agglomeration. This was also observed in the specific heat energy value given in Figure 5. When these two data were evaluated together, the optimum milling time was determined as 15 minutes as indicated by the dashed line in

Figure 5. With 15 minutes of milling, the initial temperature of conversion from gypsum to plaster decreased by 13.15 ºC and the initial temperature of conversion to anhydrite decreased by 25.7 ºC.

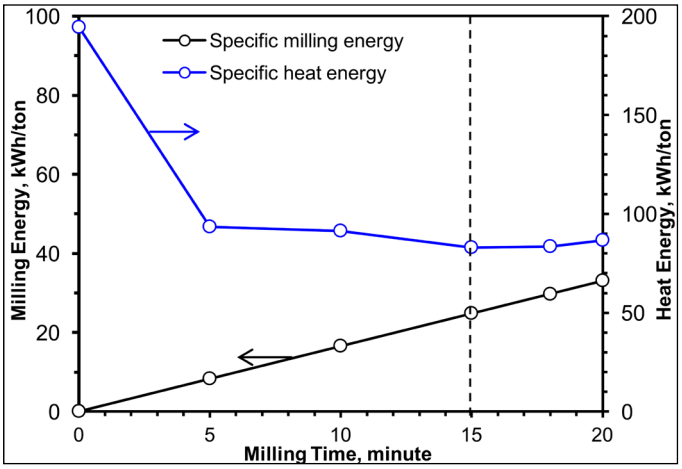

Figure 5. Variation of specific milling energy and heat energy with respect to milling time

Table 4. *Specific milling and heat energy value and costs of samples milled at different times*

Milling time, minute	0	5	10	15	18	20
Specific milling energy (kWh/ton)	-	8,26	16,52	24,78	29,74	33,04
Specific heat energy, (kWh/ton)	194,24	93,43	91,36	82,86	83,47	86,58
Milling energy cost, TL	-	33,33	66,66	99,99	120,00	133,32
Heat energy cost, TL	783,77	376,97	368,64	334,33	336,80	349,34

The average electricity consumption cost per kWh of the enterprises located in Türkiye in January 2024 is 4.035 Turkish Liras (Energy Agency, 2024) and this price was taken as a source in the calculations. While the initial temperature of conversion of unmilled gypsum to plaster is 112.8 ºC, the calcination temperature decreases as the milling time increases (Table 3). The initial temperature of conversion to plaster decreased by 13 ºC with 15 minutes milling and the initial temperature of conversion to anhydrite decreased by 25.7 ºC. When the energy consumption and energy cost values per ton were analyzed, 194.24 kwh/ton energy is required for complete calcination of unmilled gypsum, while this energy requirement is 107.64 kwh/ton with 15 minutes milling, which was the sum of milling energy and heat energy (Table 5). For more than 15 minutes of milling, specific energy values largely decreased.

Table 5. *Energy consumption and energy cost values per ton of gypsum*

Cost	TA	MA + TA
Energy Consumption, kWh/ton	194.20	107.64
Energy Cost, Turkish Liras	783.77	434.32

With the addition of the mechanical activator mill before calcination in plaster production per ton, the calcination temperature required for plaster production was lowered by 13.15 °C. The energy saving resulting from this temperature reduction was 349.45 TL per ton.

4. Conclusions

In this study, TA and MA circuits used in the production of plaster, which has an intensive use today, were evaluated economically. From the economic analysis, it was determined that the MA circuit is generally efficient and the addition of mechanical activator mills to the plaster production circuit before calcination as suggested in Figure 6 is a more economical and environmentally friendly method with less energy consumption. Considering the global energy crisis in recent years, it was evaluated that the MA+TA circuit will be a more profitable investment. Since it is thought that the correlation of the data obtained with the equipment used in the laboratory scale with the data to be obtained in industrial plants will be very low, no evaluation has been made regarding how long the initial investment cost of the mechanical activator mill will be covered during the calculations. This study was a reference in terms of energy efficiency and cost analysis stages, which are the most important steps of feasibility studies to be carried out for a gypsum production plant to be established on an industrial scale.

The need for ultrafine materials in the industry will continue to grow in the future. Consequently, the use of mechanical activator mills in industry is expected to continue to grow. The use of mechanical activator mills in many different processes on an industrial scale is already available in literature. When evaluating plaster production, it is predicted that activator mills will be used in this sector in the near future because they are economical and environmentally friendly.

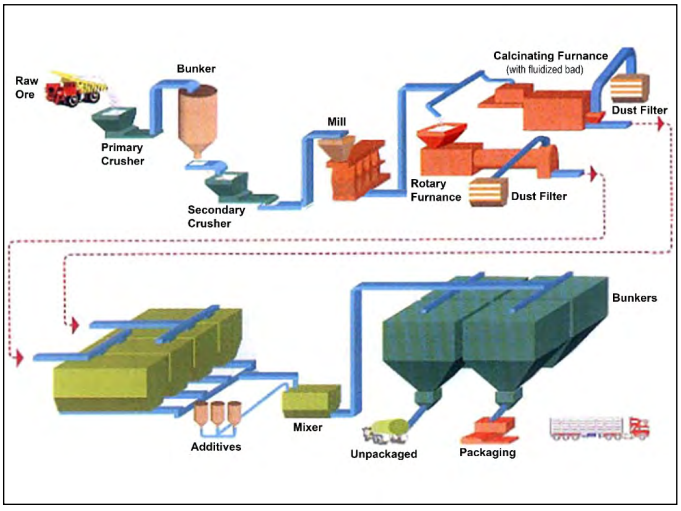

Figure 6. Proposed flow chart for plaster production

Acknowledgement

The ore samples used in this study were obtained from Arslanlı Alçı A.Ş. (Elazığ-Türkiye). Financial supports of TÜBİTAK (Project No: 111M028) and İnönü University (BAPB Project No: 2011/108) are gratefully acknowledged.

References

Alyousif, B., Uysal, T., Erdemoğlu, M. 2023a..Potassium chloride recovery from mechanically activated microcline through the chlorination roasting and leaching route. Physicochem. Probl. Mineral Processing. 59, 5,167500.

Alyousif, B., Uysal, T., Aydemir, M.K., Erdemoğlu, M. 2023b. Contribution of Mechanical Activation for Obtaining Potassium Chloride from Microcline. Mining, Metallurgy & Exploration. 40, 4, 1311 - 1319.

Aydoğmuş, R, Erdemoğlu, M, Uysal, T. 2023. Aluminum recovery from pyrophyllite: Effects of various enrichment and activation methods. Mining, Metallurgy & Exploration. 40, 4, 1333 - 1343.

Balăz P. 2008. Mechanochemistry in nanoscience and minerals engineering. Springer, Berlin.

Baláž, P., Achimovičová, M., 2006. Mechano-chemical leaching in hydrometallurgy of complex sulphides. Hydrometallurgy. 84, 60-68.

Barry, T.S., Uysal, T., Erdemoğlu, M., Birinci, M. 2019. Thermal and mechanical activation in acid leaching processes of non-bauxite ores available for alumina production-review. Min Metall Exp Mining, Metallurgy & Exploration. 36:557–569.

Birinci, M., Uysal, T., Erdemoğlu, M., Porgalı, E., Barry, T.S. 2017. Acidic Leaching of Thermally Activated Pyrophyllite Ore from Pütürge (Malatya-Turkey) Deposit. 17. Balkan Mineral Processing Congress, Antalya.

Boldyrev, V.V. 1986. Mechanochemistry of inorganic solids. Proc. Indian Nat. Sci. Acad., 52, 400-417.

Energy Agency, 2024. https://enerjiajansi.com.tr/elektrik-birim-fiyatlari/ (Access Date: 17.11.2023).

Erdemoğlu, M., Birinci, M., Uysal, T., Porgalı, E., Barry, T.S., 2017. Acid leaching performance of mechanically activated pyrophyllite ore for Al_2O_3 extraction. 9th International Conference on Mechanochemistry and Mechanical Alloying, Kosice-Slovakia.

Erdemoğlu, M., Birinci, M., Uysal, T. 2018. Alumina production from clay minerals: current reviews. Journal of Polytechnic. 21, 387-396.

Erdemoğlu, M., Birinci, M., Uysal, T. 2020. Thermal behavior of pyrophyllite ore during calcination for thermal activation for aluminum extraction by acid leaching. Clays and Clay Minerals. 68(2):89–99.

Evans, 2016. Specific heat capacity of materials. https://theengineeringmindset.com/specific-heat-capacity-of-materials/ (Access Date: 17.11.2023).

Hudson-Lamb, D.L., Strydom, C.A., Potgieter, J.H. 1996. The thermal dehydration of natural gypsum and pure calcium sulphate dihidrate (gypsum), Thermochimica Acta. 282-283, 483-492.

Lou, W., Guan, B., Wu, Z., 2011. Dehydration behavior of FGD gypsum by simultaneous TG and DSC analysis, Journal of Thermal Analysis and Calorimetry. 104, 661-669.

Pourghahramani P, Forssberg E (2007) Effects of mechanical activation on the reduction behavior of hematite concentrate. Int J Miner Process 82:96–105.

Putnis, A., Winkler, B., Fernandezdiaz, L., 1990. Insitu spectroscopic and thermagravimetric study of the dehydration of gypsum. Mineralogical Magazine, 54(374), 123-128.

Sekulić, Z., Popov, S., Đuričić, M., Rosić, A. 1999. Mechanical activation of cement with addition of fly ash. Materials Letters. 39, 115-121.

Şener, M. 2012. The effect of mechanical activation on the thermal behaviour of gypsum. Master's Thesis, Inonu University Institute of Science and Technology, Malatya, Türkiye.

Şener, M. Erdemoğlu, M. 2014. Effect Of Mechanical Activation on Thermal Behavior of Gypsum. Scientific Mining Journal, Volume: 53 Issue: 4, 19-26.

The Engineering ToolBox. 2003. Solids - Specific Heats. https://www.engineeringtoolbox.com/specific-heat-solids-d_154.html (Access Date: 17.11.2023).

Uysal, T., Mutlu, H.S., Erdemoğlu, M. 2016. Effects of mechanical activation of colemanite ($Ca_2B_6O_{11}5H_2O$) on its thermal transformations. International Journal of Mineral Processing. 151:51–58.

Uysal, T. 2018. Investigation of activation conditions in alumina production from pyrophyllite ore by acid leaching method, PhD Thesis, İnönü University Institute of Science and Technology, Malatya, Türkiye.

Uysal, T., Mutlu, S., Erdemoğlu, M. 2015. Investigations for Innovative Ceramic Wall Tiles: Synergistic Effects of Pyrophyllite and Colemanite. XVI Balkan Mineral Processing Congresses, Belgrad-Sırbistan.